THE UNIVERSITY *of* EDINBURGH

Exploring the importance of axial identity in transplantation studies using neural progenitors of specific anteroposterior identity

---

Aaron Alonso Torrens

THE UNIVERSITY *of* EDINBURGH

Doctor of Philosophy

MRC Centre for Regenerative Medicine

University of Edinburgh

2023

Declaration.

I declare that this thesis is of my own composition. The work presented in this thesis is my own, unless otherwise stated, and has not been presented for any other degree or professional qualification.

Aaron Alonso Torrens.

Acknowledgements.

And here I am, writing my acknowledgements at the very end, mainly because I can't even begin to start counting the number of people that have been part of such a journey. I started my PhD without much confidence in myself and feeling that I had to prove myself all the time. I would compare myself, my work, and my ideas to others and always felt they were never good enough. However, this PhD has completely changed that for me and for that, I thank Professor Val Wilson for giving me the opportunity to work with her while also allowing me the freedom to take on different opportunities in and outside of academia which has allowed me to grow as a scientist. I would like to also thank Emma, for being my companion through hurdles and struggles, and the other members of the lab, especially Alessandra, for her incredible help and support, always having an answer to the many questions I have thrown her way and always checking on me and making sure I was doing okay. I would also like to thank the Lowell lab for their amazing help and advice, especially during the first years of my PhD. To all the facility members and many other scientists at the University of Edinburgh who have also helped and guided me in the moments I needed it.

I would also like to thank the many wonderful people I met during my time at SCRM from all over the world who have become very important people in my life. Daniel, a friend who keeps reminding me every day how far I have come and cheering me up when I am feeling down. To Telma Ventura, one of the greatest and most precious friends I have found, who for good and for worse, in sickness and in health, when thick or thin has always been there for me, always with a hug and snack in hand when I needed it most. And to Claudio Casti for his amazing care, support, patience, positivity, and unwavering belief that I could complete this hug milestone. Thank you.

And now, of course, my family, I would like to thank my auntie Gogi who took care of me during my first years abroad and always reminded me that everything would be ok. Alongside my cousin Julie and little cousin Finn, they always believed in me and made sure to make me feel loved and at home, even abroad.

And the biggest thanks goes to my mum and dad, who really are the most supportive and caring parents I could have ever asked for, and words could never describe how thankful I am to them. Their extreme patience, love, care and support, always listening when an experiment has gone wrong, picking me back up when I fall, and always offering a helping hand even from afar is what has allowed me to always push forwards and get to where I am today.

To all of you, from the bottom of my heart

Thank you.

Abstract.

After an injury, axons in the mammalian spinal cord fail to regenerate, and the spinal cord cannot repair itself. A promising approach to improving recovery after spinal cord injury (SCI) is the transplantation of neural stem or progenitor cells (NPCs) derived from pluripotent cells into the injury site. However, there are significant challenges to this potential therapeutic approach. Grafted NPCs must survive, differentiate, grow neurites, and integrate appropriately into the host. One reported cause of the failure of integration is a mismatch between the anteroposterior identity of the grafted cells and the host site. The differentiation of pluripotent cells in vitro to posterior NPCs corresponding to a thoracic/lumbosacral spinal cord identity has been achieved by using neuromesodermal progenitors (NMP) as an intermediate. Cells of the most caudal/sacral identity have not been produced.

I first tested several conditions for generating NPC of defined identities and characterised the cells produced. I confirmed that the generation of NMPs is an essential step to generate NPCs of a posterior identity and that the addition of RA in NMP cultures is not sufficient to induce the expression of the most posterior Hox genes. GDF11 is reported to posteriorize differentiating human ESC towards a sacral identity. I tested the effects of this protein in an established NMP culture protocol. I showed that timing of GDF11 treatment during NMP differentiation is critical for the optimal expression of sacral/caudal Hox genes and the overall cellular phenotype acquired. The addition of GDF11 early during NMP differentiation factors results in cells acquiring an endoderm fate. In contrast, GDF11 added to established NMP populations in culture results in cells developing a neural identity capable of expressing the late paralog groups (PGs), including PG13.

To determine functional integration, survival, neurite outgrowth and pathfinding of cells after grafting, I differentiated Epiblast stem cells (EpiSCs) towards NPCs of anterior (NA), hindbrain (NH) and posterior thoracic spinal cord identity (NS) and grafted them into E10.5 mouse embryos at homotopic and heterotopic locations. Since the culture period of whole embryos is limited, I also grafted cells of defined axial identities into dissected spinal cord slices and allowed these to grow in culture for five days. Grafted NPCs survive and integrate into the host while retaining their neural and anteroposterior axial identity when grafted into the neural tube. In addition, we show

that cells grafted in isotopic sites show higher rates of proliferation and integration into the tissue. Overall, this suggests that cells' axial identity is fixed in the grafted NPCs and contributes to successful integration, highlighting the importance of axial identity in cellular therapies.

Lay summary.

The vertebrate central nervous system (CNS) consists of anterior (forebrain, midbrain and hindbrain) and posterior (spinal cord) regions. During development, the CNS is formed by a process known as axial elongation, which results in the formation of the anterior-posterior (head to tail) axis. The posterior CNS forms from a group of progenitors known as neuromesodermal progenitors (NMPs). These progenitors reside at the posterior end of the embryo, producing first cells of the neck, then the trunk and finally the tail. This temporal sequence of axis elongation can be measured by the expression of a group of genes known as Hox genes. These are arranged in four clusters (HOXA-D). The position of each of the 13 paralogous group members (PG 1-13) reflects both the time at which they become active and the anterior limit of their expression. PG1 is expressed most anteriorly, while PG13 is expressed at the most posterior site. This spatial expression is important to define anteroposterior identity. Several studies suggest that the transplantation of progenitors in the spinal cord may be optimal only when they are matched to the correct anteroposterior level. However, making cells of some axial levels in vitro remains challenging. Previous studies have shown that it is possible to produce neural precursor cells (NPCs) and motor neurons of a posterior identity (indicated by expression of posterior Hox genes) by adding an NMP differentiation step to an ESC neural differentiation protocol. However, in this protocol, the cells produced had heterogeneous axial identities, and motor neurons expressing the most posterior markers (HOX PG 11-13) were not produced. Therefore, the aim in this project is to optimize ways to produce cells of specific axial identity, including NPCs of tail identity, and determine whether they show differences in functional integration, including survival, neurite outgrowth and pathfinding upon being grafted into different axial levels of the posterior CNS. The experiments summarised in this thesis shows that addition of signalling molecule GDF11 at the appropriate time in an NMP differentiation protocol can generate NPCs expressing the most posterior PG genes, including PG13. In addition, experimental work that transplantation of NPCs to regions of the spinals cord with matching axial identity results in higher levels of engraftment.

List of tables.

List of figures.

Table of Contents

List of abbreviations.

ActRI	activin receptor I
ActRII	activin receptor II
AP	anterior-posterior
AVE	Anterior Visceral Endoderm
BMP	bone morphogenic protein
BMP11	bone morphogenic protein 11
CLE	caudal lateral epiblast
CNH	chordoneural hinge
CNS	central nervous system
cyp26a1	Cytochrome P450 hydroxylase A1
EB	Embryoid bodies
EC	embryonal carcinoma
EpiSCs	Epiblast stem cells
ESC	embryonic stem cells
FCS	foetal calf serum
FGF	fibroblast growth factor
GDF11	Growth differentiation factor
HAG	Human-specific Shh agonist
hf	Headfold
hPSCs	human pluripotent stem cells
ICC	Immunocytochemistry
ICM	inner cell mass
LIF	Leukaemia Inhibiting factor
LS	Late Streak
LSD	lysine-rhodamine-dextran
MEFs	mouse embryonic fibroblasts
MNs	motor neurons
NA	Neural Anterior
NCC	Neural Crest Cells
NH	Neural Hindbrain
NMJ	neuromuscular junctions

NMP	neuromesodermal progenitors
NPCs	Neural Progenitor Cells
NS	Neural Spinal Cord
NSB	node-streak border
NT	Neural tube
PE	primitive endoderm
PG	paralog groups
PS	primitive streak
PUR	purmorphamine
R-smad	receptor-Smad
RA	Retinoic acid
RALDH	Retinaldehyde dehydrogenase
RAR	retinoic acid receptor
ROCK	Rho-associated protein kinase
ROI	Region of interest
RXR	retinoic acid receptor
SAG	Smoothened Agonist
SCI	spinal cord injury
Shh	Sonic hedgehog
TB	tail bud
Tbra	Brachyury
TE	trophectoderm
TF	transcription factors
TGF-β	transforming growth factor-β
Wnt	Wingless-related integration site

Chapter 1. Introduction.

1.1. Early embryonic development in the mouse.

The formation of the embryonic body is the result of multiple interactions between several progenitor types, which determine its specification, regionalization and morphogenesis. This process initiates after fertilization generating a single totipotent cell or zygote with the ability to give rise to embryonic and extraembryonic lineages (Tarkowski and Wróblewska, 1967). In mammals, subsequent division of this cell eventually leads to the formation of the blastocyst, in which two distinct substructures exist, the trophectoderm (TE) and the inner cell mass (ICM) (reviewed in Saiz and Plusa, 2013). In mouse embryos on embryonic day (E)4.0 of development, the ICM forms the primitive endoderm (PE) and the preimplantation epiblast, which produces the entire embryo, including all three embryonic germ layers (ectoderm, mesoderm, and endoderm) (Lawson & Wilson, 2016). At E5.0, the embryo implants in the uterus and starts to elongate along the proximal-distal axis. Anterior and posterior identities are then determined by specific interactions between different transcription factors (TFs) and signalling pathways such as Wnt, Nodal and bone morphogenic protein (BMP) (Reviewed in by Arkell and Tam, 2012).

At E6.5, gastrulation begins with the initiation of the primitive streak (PS) in the most proximal posterior midline epiblast. The PS is present continuously throughout gastrulation and early organogenesis and consists of cells undergoing epithelial-to-mesenchymal transition to ingress between the epiblast and the endoderm to form the extraembryonic and embryonic mesoderm. From early to late streak stages (E6.5-E7.5), the PS extends distally and caudally, growing in length by progressive incorporation of descendants of cells from the lateral and more anterior regions of the expanding epiblast, eventually reaching the distal tip of the embryo. The most posterior cells of the epiblast that pass through the PS initiate the formation of the amniochorionic fold by inserting between the posterior extraembryonic ectoderm and the extraembryonic visceral endoderm. This will later become the yolk sac cavity. The PS continues to grow until it reaches the distal tip of the embryo. The cells which pass through the PS travelling anteriorly will form the lateral, intermediate mesoderm and paraxial mesoderm. The lateral and intermediate mesoderm is formed from the

posterior primitive streak, while the anterior sites of the primitive streak form the paraxial mesoderm. In the same manner, the most anterior end of the PS (the node) contributes to the formation of the axial mesoderm, which includes the notochord. The remaining epiblast will contribute to the development of the surface ectoderm and neural ectoderm (neural plate forming the neural tube) (Tam & Loebel, 2007; reviewed in Lawson & Wilson., 2016). At this stage of development, the proximal region of the ectoderm becomes restricted to a surface ectoderm fate, while the distal part of the epiblast in the gastrulation stage embryo will form neuroectoderm. Anteriorly, this forms the brain, and posteriorly it will form the spinal cord (Tam, 1989; Tam and Quinlan, 1996).

E7.5 marks the end of gastrulation and the formation of the three primary germ layers. It also indicates the start of the early head fold stage, where the primitive streak ceases to grow, and new cells are added to the axis from cells in the primitive streak from E8.0. This stage also marks the beginning of organogenesis, and the anterior-posterior (AP) axis begins to extend and produce somites and the spinal cord from E8.5- E13.5.

1.2. Neural induction in mammals.

In the mouse, neural induction initiates around E7.5. This results in morphological changes consisting of a thickening of the anterior ectoderm, located opposite the PS, which eventually results in the formation of the neural plate. As development continues, cells continue to proliferate, eventually forming neural folds and grooves. When the neural folds contact each other and fuse in the dorsal midline, the neural tube is formed. The neural tube eventually loses its connection with the surface ectoderm, which results in the formation of the epidermis. The formation of the spinal cord results from the enclosure of the neural tube by the emerging vertebrae resulting in the formation of the vertebral canal (Aaku-saraste et al., 1996; reviewed in Henrique et al., 2015).

Understanding how neural induction occurs has been a question of much debate resulting in several theories being proposed. Embryological studies in amphibians over the past century have allowed us to gain an understanding of the molecules and signalling pathways involved in this process. One of the most well-known experiments

is the one carried out by Spemann and Mangold., 1924. Spemann and Mangold transplanted the dorsal blastopore lip of the early gastrula of one salamander into the ventral side of another early gastrula of a different species of salamander. This resulted in the development of conjoined twins attached through their belly. They determined that the bulk of the secondary embryo arose from the host embryo, given their species-specific phenotypical differences, while the grafted tissue gave rise to the notochord and few somitic cells. This showed that the dorsal blastopore tip, currently known as the organiser, can induce a secondary body axis and trigger neural development in the ectoderm when transplanted to the ventral side of a host embryo. Work later carried out by Wilson and Hemmati-Brivanlou, 1995, identified BMP4 as one of the main signals involved in the formation of neural tissue, where inhibition of BMP4 has shown to be capable of inhibiting neural fate in Xenopus. This suggests that the organiser releases BMP inhibitors to induce the formation of neural tissue, leading to what is known as the 'default' model of neural induction. Peter Niewkoops activation-transformation model further elaborates on this model, mentioning that inhibition of ventral BMP at the gastrula stage induces neural tissue (activation) of anterior identity. Neural tissue will then be posteriorized (transformation) by signals later released from the chordamesoderm giving rise to the more posterior tissues midbrain, hindbrain, and spinal cord tissue (Nieuwkoop & Nigtevecht, 1954).

In mammals, it has been proposed that the node, located at the distal tip of the embryo (Reviewed in Beddington and Robertson, 1999), is the molecular equivalent of the organiser found in amphibians. This claim is based on experiments where the node can firstly induce anterior markers in ectoderm explants, as shown in Klingensmith et al., 1999, and secondly, produce signalling factors shown to be required for neural induction such as BMP antagonist, chordin, and noggin (Bachiller et al., 2000 & Beddington, 1994). However, the fact that the node does not form until after neural induction has started questioning the validity of this claim (Streit et al., 2000, reviewed in Martinez Arias and Steventon, 2018). Therefore, the predecessor of the node is a more likely candidate responsible for inducing neural tissue, as it appears prior to neural induction and produces the signal required for this process (Kinder et al., 2001). This suggests that the early gastrula organiser can induce neural tissue by inhibiting BMP signalling, a balance which is later maintained by the anterior visceral endoderm (AVE) (Levine and Brivanlou, 2007), further supporting the evidence of a "default" model of neural induction.

However, the “default model” is challenged by experimental work carried out in chick embryos, where they showed that inhibition of BMP signalling by Chordin is not sufficient to induce neural tissue in ectodermal explants (Streit et al., 1998) and that FGF signalling may play an important role in neural induction (Streit et al., 2000; reviewed in Stern et al., 2006). These studies suggest the inclusion of a stabilization step to Niewkoops model, therefore suggesting the “activation-stabilisation-transformation” model (Nieuwkoop & Nigtevecht, 1954). This model states that the default anterior fate requires to be actively maintained by protection from posteriorizing signals such BMP, Fgf, Wnt and RA. On the other hand, several studies in mouse embryos continue to support the default model. Knockout of type I BMP receptor, Bmpr1a in mice promotes expression of neural markers throughout the epiblast at E6.5 and suppresses mesoderm, further supporting the idea from the default model that BMP inhibition promotes neural fate. Inhibition of FGF signalling between stages E5.5 and E7.5 results in ectopic expression of neural marker Hesx1, contrasting previous studies and suggesting that FGF does not act as a direct neural inducer in the mouse embryo (Di-Gregorio et al., 2007). In fact, it suggests that FGF activity is required during the early stages of neural induction to specify a post-implantation epiblast-like gene expression pattern (Kunath et al., 2007, Di-Gregorio et al., 2007), providing a possible explanation for the differing results in chick and Xenopus.

The default model is further supported by a similar set of experiments to those conducted by Wilson and Hemmati-Brivanlou., 1995, which also examined the time during which cells were competent for neural induction. In this study, mouse anterior ectodermal explants at stages E6.0, E7.0 and E7.5 were bisected into anterior and posterior portions, followed by 5 days of culture in serum-free N2B27 medium in the presence or absence of BMP4. Explants treated in the absence of BMP4 became neural, whilst those treated with BMP4 produced surface ectoderm, mesoderm, and endoderm at E6.5. At E7.0, untreated explants generated neural ectoderm, with the posterior bisected portion expressing lower levels of neural markers than the anterior portion. Anterior portions treated with BMP4 gave rise to surface ectoderm, whilst the posterior portion formed mesoderm and endoderm. At E7.5, BMP4 no longer inhibited neural expression in anterior explants, indicating that at this stage, cells have committed to the neural lineage (Li et al., 2013).

1.3. Axial elongation and establishment of anteroposterior identity.

1.3.1. Neuromesodermal progenitors (NMPs) and axial elongation.

As briefly mentioned, E7.5-E8.0 marks the end of gastrulation and the initial formation of the three primary germ layers. This stage also marks the beginning of organogenesis, and the anterior-posterior (AP) axis begins to extend and produce somites and the spinal cord from E8.5- E13.5 by a process known as axial elongation. Neuromesodermal progenitors (NMPs) are a transient population of cells that arise at E7.5 and contribute to axis elongation until E13.5 (Reviewed in Henrique et al., 2015, Wymeersch et al., 2019).

The first evidence of the presence of a group of multipotent cells which can give rise to neural and mesodermal lineages came from lysine-rhodamine-dextran (LRD) fate map experiments in the node region in chick, where cells were found to contribute to more than one tissue (Selleck and Stern, 1991). Similar cell labelling experiments in mouse embryos further supported these findings. Cells labelled in the epiblast at the prospective organiser region were able to contribute to multiple lineages, as well as to cells remaining in the node region (Lawson et al., 1991). In addition, single labelled cells at the node in late streak and headfold (hf) stage embryos contributed to mesodermal and neural lineages. However, labelled cells anterior to the node only showed a contribution to neuroectodermal tissues (Forlani et al., 2003). The fate of cells in the node and the PS at E8.25-E8.5 was further investigated in the mouse by labelling cells in specific locations with DiI (Wilson and Beddington, 1996). Results showed that labelled cells from the ventral node contributed towards a notochordal fate, while labelled cells from the dorsal node contributed towards neuroectoderm and paraxial mesoderm. Further distinctions were also found through different regions of the streak, with the rostral streak contributing to paraxial mesoderm and the caudal region contributing towards lateral mesoderm (Wilson and Beddington, 1996).

The specific location of NMPs was further detailed with fate map experiments using homotopic grafts of GFP-expressing cells from the node and primitive streak regions, including epiblast lateral to it (Cambray and Wilson, 2007). The node-streak border (NSB) and caudal lateral epiblast (CLE) were the only regions that contributed to both neural and paraxial mesoderm, as well as the tail bud (TB) (Cambray and Wilson., 2007; Wymeersch et al., 2016). Interestingly, two different fates were found in the CLE,

where cells from the most rostral site contributed to paraxial mesoderm and neural tube, whilst the caudal site mainly contributed only to paraxial mesoderm.

Labelled cells from homotopic grafts of the NSB were also found in a specific area of the tail bud known as the chordoneural hinge (CNH) (Cambray and Wilson, 2002, 2007). The grafting of CNH regions derived from E10.5-E12.5 embryos into E8.25 NSB resulted in a contribution to neural and mesodermal tissue, as well as the CNH itself (Cambray and Wilson, 2002). Serially transplanting cells from the CNH of an E10.5 stage mouse embryo into the NSB of an E8.5 stage mouse embryo showed contribution to the axis and CNH after each grafting step, further indicating that the CNH of E10.5-E12.5 embryos and the NSB contain cells with the equivalent potential to contribute to the axis (Cambray and Wilson, 2002). This shows that NMPs can adapt to temporally unmatched environments. Work carried out by Wymeersch et al., 2019 shows that over time the transcriptome of NMPs also changes over time. Together with heterochronic transplantation studies by McGrew et al., 2008 of tail bud progenitors to the node region of gastrula-stage chicken embryos showed that the anteroposterior identity of cells can be reset, therefore indicating that cells can change their transcriptome upon grafting. Together this suggests that extrinsic signals may play a big role in defining the temporal NMP transcriptional state. Nevertheless, throughout these different grafting experiments, the efficiency of integration was observed to be lower in heterochronic grafts when compared to cells grafted isochronally, regardless of location along the axis.

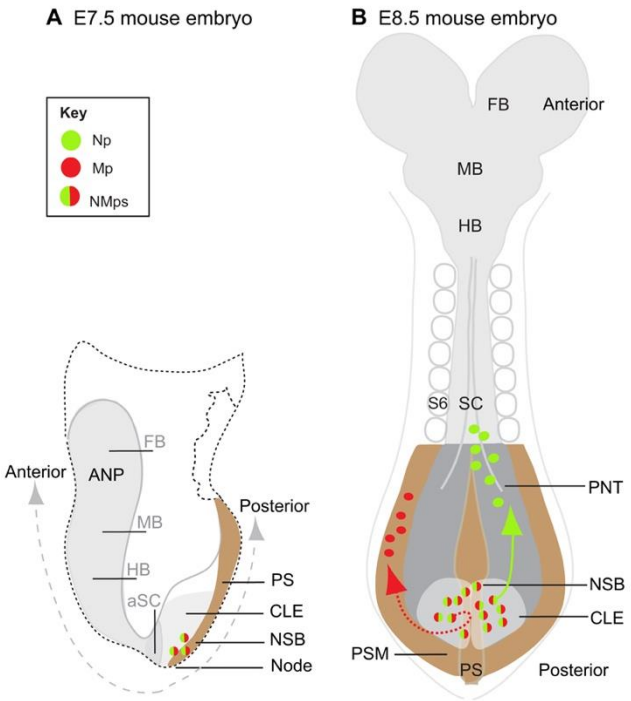

Figure 1.1. Locations of NMP populations in the developing embryo.

Schematics of E7.5 (A) and E8.5 (B) mouse embryos indicating cell populations that give rise to the CNS. At E8.5 NMPs transition through the PNT to form spinal cord or through the presomitic mesoderm to form somites. Reproduced from Henrique et al., 2015. Abbreviations: Caudal Lateral Epiblast (CLE), Primitive Streak (PS), Presomitic mesoderm (PSM). Node Streak Border (NSB), Preneural Tube (PNT), Spinal Cord (SC), Forebrain (FB), Midbrain (MB), Hindbrain (HB).

1.3.2. Axial elongation.

Axial elongation is a highly coordinated process that results in forming the anterior-posterior axis. At each anteroposterior level, cells express a specific combination of Hox genes, also known as the "Hox code", which defines that axial position. Hox genes are homeodomain-containing transcription factors which in vertebrates are organised into four clusters (HoxA-D). Each Hox gene in any one cluster is subtly divergent, and because the clusters arose through a putative genome tetraploidization, the genes in each cluster can be aligned to form thirteen paralogous groups (PG1-13) (reviewed in Wymeersch, Wilson and Tsakiridis., 2021. The position of a given gene along the chromosome is reflected in both the anterior limit of their expression, with PG1 expressed most anteriorly and PG13 most posteriorly (spatial collinearity) and their time of activation, with PG1 expressed earliest and PG13 latest (temporal collinearity). The concept of collinearity between the spatial activity of genes and their position along the axis was suggested by Lewis (1978) following his analysis of homeotic mutations in the Bithorax complex in Drosophila. Lewis suggested that the observed

organization could form a combinatorial code that facilitates axial diversity and segment identity. Using explants from gastrulation stage embryos Forlani et al., 2003 describes that expression of 3' and 5' Hox genes develop sequentially in the primitive streak region, from posterior to anterior as the streak extends. In addition, she describes expression of 3' Hox genes spreading towards an anterior boundary. This suggests that tissues are primed to express Hox genes early in gastrulation, and that Hox gene inducibility is transferred by cell-to-cell signalling. However, Hox expression can change. Hoxb9 in situ hybridizations carried out on transverse sections of mouse from six different stages shows that at the earliest stages, labelled cells showed a uniform distribution. However, at later stages, expression of Hoxb9 becomes restricted to dorsal sensory regions before reappearing in the ventral regions. This suggests that despite a common set of CNS-specific genes defining neural identity, the temporal changes in the pattern of expression in the CNS show a difference between the PGs (Gaunt et al., 1990, Graham., et al., 1991).

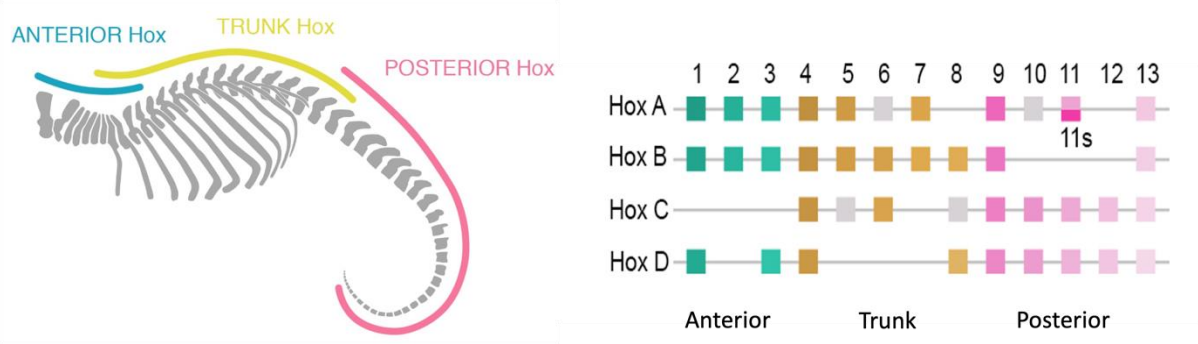

Figure 1. 1. Schematic representation of the hox gene clusters and their organization in the genome.
Diagram adapted from Wymeersch et al., 2019.

1.3.3. Genes and signals driving axial progenitor cell fate decisions.

Despite the extensive transcriptomic analysis across vertebrate embryos at a single-cell and bulk population level, no unique markers have been found for NMPs. To date, the best readout for NMPs is the co-expression of neural and mesodermal genes, such as transcription factors Sox2 and Brachyury (Tbra) (Tsakiridis et al., 2014; Wymeersch et al., 2016). Cells that subsequently differentiate into neural lineages downregulate Tbra but maintain Sox2 expression (Gouti et al., 2014; Gouti et al., 2015; Tsakiridis and Wilson, 2015), while those committing to mesoderm downregulate Sox2 but

upregulate Tbra, as well as Msgn1 and Tbx6 (Chalamalasetty et al., 2014; Gouti et al., 2017).

In addition to Sox2 and Tbra, transcriptome analysis and lineage-tracing experiments have revealed several other transcription factors, such as Nkx1-2, Cdx2, Tbx6, Epha1 and Hox family members, which are expressed in the posterior CNS and help identify NMP populations in the mouse (Garriock et al., 2015, Rodrigo Albors et al., 2018). Loss-of-function studies have identified key regulators of NMP ontogeny, as the absence of specific components of these signalling pathways has a direct impact on mesoderm production and progenitor maintenance which can result in embryo truncation.

Takada et al., 1994 identified Wnt3a as a signalling molecule being extensively expressed in cells fated to give rise to embryonic mesoderm. Subsequent generation of Wnt-3a mutants showed mice embryos with a lack of caudal somites, disrupted notochord and inability to form tail bud resulting in tail truncation. Using mice mutant embryos for Wnt3a and T-box-containing transcriptions factors, Yamaguchi et al., 1999 showed that Wnt3a acts as a direct inducer of Tbra, and that the absence of Tbra and Tbx6 results in impaired paraxial mesoderm formation. Tail truncations were also observed in Tbra and Cdx2 mutants generated by Amin et al., 2016. He further describes that the simultaneous loss of function of these two genes disrupts axial elongation to a much greater extent than each single mutation alone. The importance of Cdx2 is further shown in chromatin accessibility changes during NMP differentiation where cells lacking all Cdx genes showed a profound effect on the response to WNT signalling in comparison to the wild-type cells (Metzis et al., 2018). Furthermore, embryo work by Olivera-Martinez et al., 2012 shows a correlation between Tbra expression and FGF signalling, where loss of Tbra from the CNH and the mesoderm progenitor domain directly correlates with a decrease of FGF signalling in the late chick tailbud. She further demonstrated this correlation using in vitro and in vivo models where attenuation of FGF signalling can mediate loss of Tbra expression upstream of Wnt signalling, while high levels of FGF maintain Tbra expression and induce ectopic CNH-like cell foci. These studies indicate that Cdx2 and Tbra are essential for NMP maintenance in the embryonic posterior growth zone, while the NMP niche is dependent on both Wnt and Fgf signalling. This indicates that these transcription factors are actively contributing towards axial growth at the time embryos generate

their trunk. Other suggested candidate molecules involved in this process are Fgf4, Fgf8, Fgf17, FgF18 and Wnt8a/c. Given the nature of this thesis, I will elaborate further upon their roles in axial elongation and patterning as well as their role in pluripotency and neural contribution in mammals.

WNT ("wingless-related integration site") signalling plays a critical role in developmental patterning (reviewed in Clevers, 2006) and can be separated into three modes of action upon the activation of a cell-surface WNT receptor. The canonical Wnt/β-catenin signalling, which requires signal transduction through β-catenin, the non-canonical planar cell polarity pathway, and the Wnt/Ca2+ pathway. The canonical WNT signalling pathway plays different roles in several biological processes (reviewed in Clevers 2006), such as regulating the proliferation of mesenchymal progenitor cells involved in vertebrate limb and tail development (Kawakami et al., 2006). In vitro, WNT signalling promotes the self-renewal of mouse ESCs and prevents differentiation towards EpiSCs. During the maintenance of EpiSCs, WNT was found to be dispensable yet essential to induce a posterior PS-like subpopulation at the expense of an anterior epiblast-like subpopulation (Tsakaridis et al., 2014). This is further supported by studies which show that the addition of Wnt3a into neural differentiation cultures is enough to prevent ESCs from adopting neural fate (Faunes et al., 2013). Wnt3a is a direct inducer of Tbra expression (Yamaguchi et al., 1999) and contributes to giving rise to paraxial mesoderm (Chalamalasetty et al., 2014). The loss of this ligand results in the loss of posterior mesodermal structures and the gain of ectopic neural tissue. By contrast, an excess of Wnt causes the opposite effect, with mesoderm being induced over neurectoderm (Takada et al., 1994, Yoshikawa et al.,1997). However, studies have shown how the effects of Wnt3a can vary depending on the target tissue. High expression levels of Wnt3a in the epiblast block the formation of the neural tube but does not prevent NMPs from producing different mesodermal lineages. In the paraxial mesoderm, appropriate Wnt/β-catenin is required for somitogenesis and to provide proper anterior-posterior polarity to somites. Wnt signalling also plays an important role in the induction and maintenance of NMPs and the subsequent differentiation of their derivatives (Wymeersch et al., 2016).

As mentioned previously, FGF plays an important role in neural induction but also contributes to the formation of mesoderm (reviewed in Stern., 2005). FGF promotes

the expression of genes found in the Caudal Lateral Epiblast (CLE), such as Nkx1.2 and Wnt8c. In addition, the loss of FGF4 and FGF8 in late-gastrula mouse embryos results in defects during axial elongation due to the production of posterior neural and mesodermal tissues becoming compromised (Naiche et al., 2011, Boulet and Capecchi, 2012). Downregulation of FGF receptor FGFR1 in the chick embryo results in a premature exit of NMPs from the progenitor pool (Mathis et al., 2001). Moreover, cells lacking the Wnt response gene Cdx2, crucial in axis elongation, can be rescued by transplantation to a wild-type environment (Bialecka et al., 2010). This suggests that NM bipotency is not intrinsically determined and relies on the combination of extrinsic cues of other signalling pathways such as FGF and Notch (reviewed in Wymeersch, Wilson & Tsakaridis et al., 2021).

FGF also plays important roles in cell proliferation, survival, and motility (Goetz and Mohammadi, 2013). In vitro, FGF is important to produce and maintain EpiSCs in a pluripotent state by inhibiting cells reversing back to a lif-serum-ESC state and preventing further differentiation towards a neural lineage (Greber et al., 2010; Sterneckert et al., 2010). At the same time, FGF plays an important role in neurogenesis, promoting neural precursor production, proliferation, differentiation, and migration in the brain (Yaguchi et al., 2009).

However, there are some contradictions in the current literature regarding the role of FGF in the neural differentiation of pluripotent cells. As mentioned previously, some studies have found that FGF can promote neural induction from lif-serum (Kunath et al., 2007; Stavridis et al., 2007); while others show that blocking FGF signalling in EpiSCs promotes neural differentiation (Greber et al., 2010; Jaeger et al., 2011). Furthermore, in vivo data has shown no existing evidence of FGF acting as a neural inducer in the post-implantation embryo (Di-Gregorio et al., 2007). These contradictions can be explained by viewing neural differentiation as a progression through different stages of pluripotency where naïve ESC cells become primed for the neural lineage, exiting primed pluripotency, and becoming ready to initiate neural differentiation. In other words, FGF promotes the conversion of cells from naïve to primed while also inhibiting the pathway to encourage the exit of the primed state and enter the neural lineage (Stavridis et al., 2010; Sterneckert et al., 2010). Therefore, having different roles during pluripotency, priming and neural commitment. These concepts will be explained further on in the introduction.

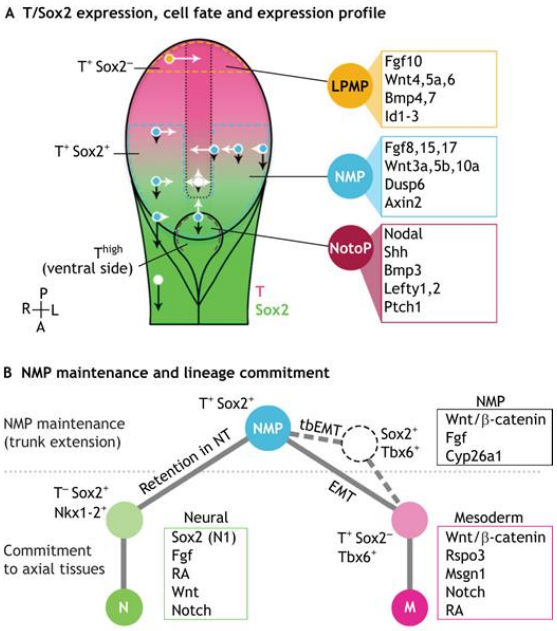

Figure 1.2. NMP gene regulatory network.

Schematic of the dorsal posterior embryo illustrating Sox2 (green) and T (magenta) expression in relation to neural (N) versus mesodermal (M) fate choices of NMPs (cyan dashed line). (B) Model for T+Sox2+ NMP maintenance and N or M differentiation in vivo. Reproduced from Wymeersch, Wilson and Tsakiridis., 2021.

1. 4. Patterning of the CNS.

Hox genes can be classified into three major categories based on their anterior expression boundary: anterior or head PG1-3, cervical PG4-8 and posterior PG9-13 (reviewed in Philippidou & Dasen et al., 2013). Since Hox genes are not expressed in the forebrain and midbrain, 'head' Hox genes are expressed in the hindbrain.

The hindbrain goes through a process of segmentation resulting in the formation of eight rhombomeres (r). Each segment has a characteristic Hox code that is important in specifying its identity.

During axial elongation the Wnt/FGF signalling pathway becomes activated and induces activation of transcription factors Tbra and Cdx2, activating early Hox genes PG1-4. Posteriorisation is further enhanced by RA signalling. RA acts by recruiting retinoic acid receptors (RARs) to genomic sites located in the 3' end of Hox clusters (Mahony et al., 2011) and by promoting rapid removal of the repressive chromatin mark histone3 lysine27 trimethylation (H3K27me3) and polycomb repressive complex (PRC) 1 and 2 (Mazzoni et al., 2013a). These events result in the induction of posterior hindbrain identity PG 4-8.

As the CNS reaches thoracic identity, the β-catenin pathway becomes upregulated as a result of the activation of the Wnt/FGF signalling pathways. This leads to NMPs becoming induced and PG5-9 becoming activated. Pluripotent factor Oct4 allows trunk growth by maintaining the NMP population and delaying the activation of PG10-13 until GDF11 starts becoming expressed. The FGF signalling pathway (Hackland et al., 2019) and expression of GDF11 (Aires et al., 2019) result in the downregulation of Pou5f1 and upregulation of Cyp26a1 (enzyme responsible for the degradation of RA). This results in PG13 becoming induced and in a complete exhaustion of NMP progenitors due to the downregulation of the canonical Wnt/β-catenin pathway symbolising the end of axial elongation.

1. 5. Termination of axial growth.

As previously described, Tbra and Cdx2 are important transcription factors involved in trunk axis extension. Work by Amin et al., 2016 shows that Cdx2 binds to sites in the anterior and middle part of the Hox clusters in EpiSCs and in embryos and upregulates gene expression in both systems. However, this changes upon trunk-to-tail transition. At E12.5, Cdx genes become downregulated and Tbra by E14.5. Work by Young et al., 2009 indicates that PG13 represses axial growth when expressed precociously, antagonizing the action of anterior and central Hox and Cdx genes. Young describes a model by which Cdx genes and trunk Hox genes promote posterior axis elongation by maintaining posterior growth signalling needed for the maintenance of progenitor activity. This process occurs until the expression of the most posterior Hox genes accumulates and competes with trunk Hox proteins causing the termination of axial growth. As the posterior trunk becomes formed, central Hox genes instruct a phase of tissue growth and of slowing down (trunk-tail transition) which results in an arrest of tissue being added at the end of body axis extension. This model would couple posterior axial elongation of the developing embryo with patterning of the emerging tissue by the Hox combination expressed in the growth zone at that time. According to this model, Hox13 proteins antagonize Cdx2 binding and repress more anterior Hox genes. This results in Wnt and Fgf signalling becoming downregulated, resulting in a complete depletion of NMPs and, therefore, termination of axial extension. Signalling molecules retinoic acid (RA) and Growth differentiation factor (GDF11) play an

important role providing a feedback loop which helps determine the end of axis elongation.

1. 5. 1. Retinoic acid.

Retinoic acid (RA) signalling plays various roles during development. During early embryonic development, retinoids are known to act as a crucial morphogen in the correct embryonic axis formation. RA is derived from retinol (vitamin A), where its synthesis and degradation are regulated by enzymatic reactions carried out by two main enzymes: 1. Retinaldehyde dehydrogenase (RALDH), specifically RALDH2, a crucial enzyme required for the synthesis of RA across different organisms. As mentioned previously, RA levels of signalling have a direct effect on Wnt and Fgf signalling. This effect is mediated by the induction of posterior hox genes and contributes to the cessation of body axis elongation. This feedback mechanism is shown in the work of Olivera-Martinez et al., 2012 where reduction of retinoid signalling at stages HH19-22 correlated with elevated levels of Fgf activity and ectopically maintained mesoderm gene expression. This would suggest endogenous retinoid signalling in loss of mesoderm identity. Furthermore, axis termination can be determined by local cell death in the tail bid; however, this was reduced upon blocking retinoid signalling. As somites, anterior to NMPs, express RALDH2, it is possible to suggest that as cells migrate out of the CLE they are likely to be exposed to increasing concentrations of RA, downregulating levels of Wnt and Fgf signalling.

Mentioned Cdx genes play an important role in axis elongation by maintaining expression of Cyp26a1. Mutant mice lacking cyp26a1 results in ectopic RA signalling in the posterior growth region. Abu-Abed et al., 2001 also describes transformations of the cervical vertebrae, abnormal patterning of the rostral hindbrain and defects in the tail bud. Cytochrome P450 hydroxylase A1 (cyp26a1), is an enzyme required in the degradation of previously synthesized RA. RA binds with the retinoic acid receptor (RAR) and retinoic acid receptor (RXR) to regulate target gene expression (reviewed in Kam et al., 2012). These two enzymes are required to maintain spatial and temporal patterns of RA signalling during embryo development, which results in the correct anteroposterior patterning of the central nervous system and trunk axis. This is evident through several studies which show the importance of these two enzymes. Knockout

of RALDH2 in mice results in impaired rhombomere segmentation, altered homeobox gene expression and pattern, and defective neural crest cell migration (Niederreither et al., 2000). During the post-implantation stage, embryos with a complete knockout of RALDH were unable to survive (Niederreither et al., 1999). Retinoids on mouse embryos can induce ectopic expression of Hoxa1 and Hoxb1, causing the posterization of rhombomeres from rhombomere 1-3 to rhombomere 4 (Conlon and Rossant., 1992). This further suggests that RA, alongside FGF and WNT signalling pathways, must form a complex regulatory network to ensure correct anteroposterior axis formation during gastrulation.

In addition, in zebrafish, the knockdown of RALDH2 causes downregulation of RA signalling, which results in the malformation of the central nervous system and disruption of left-right asymmetry (Grandel et al., 2002, Kawakami et al., 2005). In RALDH mice mutants, it was possible to observe asymmetric somite formation due to left-right desynchronization of the segmentation clock oscillations (Vermot et al., 2005). These defects were also observed in chick and zebrafish (Vermot and Pourquie et al.,2005, Kawakami et al., 2005). This suggests that RA can form a protection zone, protecting somites from the left-right asymmetric signals to maintain the bilateral symmetry of somites columns. On the other hand, besides anteroposterior patterning, RA also plays a crucial role in the formation of the dorsoventral axis by establishing a feedback loop (or simply interacting with Nodal). This is observed in a study by Uehara et al., 2009, where mouse embryos carrying a complete knockout of Cyp26 showed formations of secondary body axis due to unbalanced expression of Nodal as a result of RA not being synthesised.

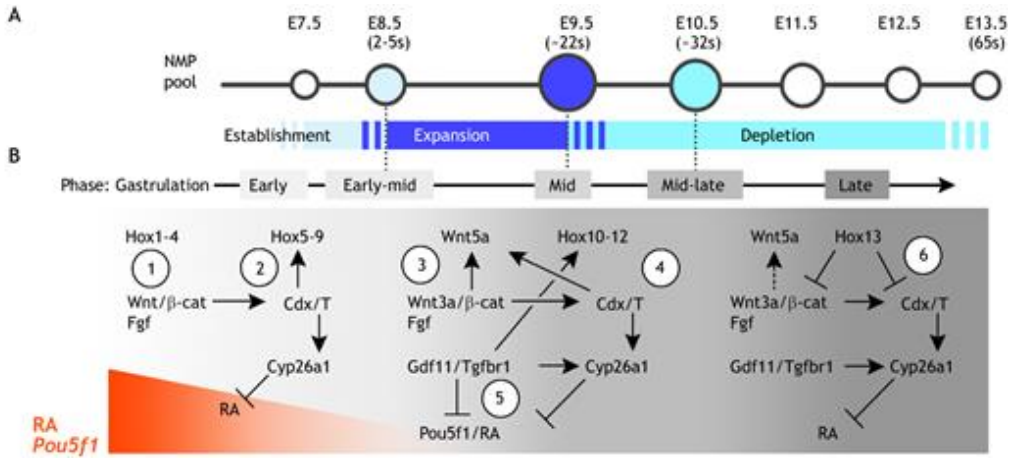

Figure 1.3. A dynamic regulatory mechanism in NMPs drives axial patterning.

Model of how the mouse vertebral pattern is ultimately shaped by the signalling dynamics sensed by NMPs. Reproduced from Wymeersch, Wilson and Tsakiridis., 2021.

1. 5. 2. GDF11.

Growth differentiation factor (GDF11), also referred to as bone morphogenic protein 11 (BMP11), belongs to the transforming growth factor-β (TGF-β) superfamily. GDF11 was first reported in 1999 as a novel differentiation factor for odontoblasts (Nakashima et al., 1999), and ever since, scientist have aimed to investigate its role in development, erythropoiesis, ageing, cardiovascular disease, diabetes mellitus, cancer, and other diseases. Given the scope of this thesis, I will be focusing on its role in development.

GDF11 is expressed at different levels across a wide range of embryonic tissues, including tailbud, limbs and nervous system, as well as adult tissues like the spinal cord, brain, olfactory system, and other endoderm derivatives such as pancreas, intestine, spleen, and kidney (reviewed in Zhang et al., 2017).

GDF11 signalling pathway initiates by binding to activin receptor II (ActRII), which subsequently recruits activin receptor I (ActRI), including ALK4, ALK5 and ALK7. Upon binding, GDF11 activates smad and non-smad signalling pathways by activating receptor-Smad (R-smad), which includes smad2/3 and Smad1/5/8. This causes the recruitment of Smad4, which together with the R-smad, migrate into the nucleus and transcribe the target genes.

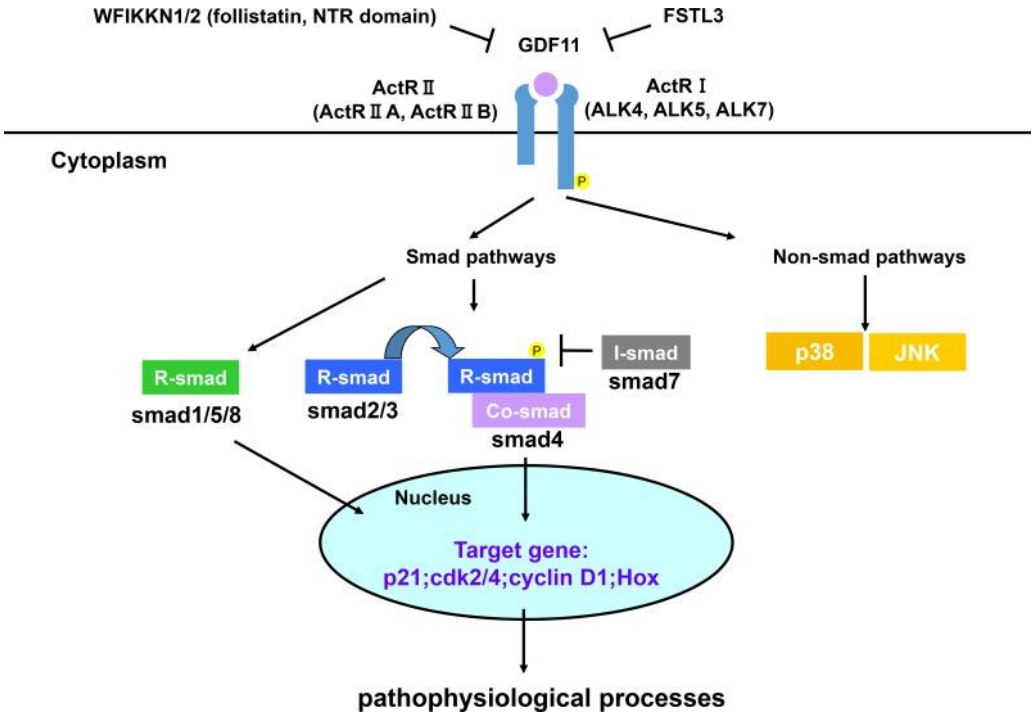

Figure 1.5. GDF11 signalling pathway.

Schematic representation of the multiple proteins and negative feedbacks loops involved in the GDF11 signalling pathway. Reproduced from Zhang et al., 2017.

As briefly mentioned, during early embryo development, GDF11 can be found to be expressed in the primitive streak and tail bud regions, playing a crucial role in anterior-posterior regionalization (McPherron et al., 1999). Studies using GDF11 mutant mice have found defects in their axial skeleton, with a more severe phenotype being observed in GDF11 complete knock-out mice showing posterior displacement of the hindlimbs. This can be due to a direct impact on hox gene expression, as GDF11 is required for Hox gene regulation through phosphorylation of Smad by type I receptor ALK5 upon binding to ActRIIA and ActRIIB (McPherron et al., 1999, Andersson et al., 2006).

GDF11 is also involved in olfactory neurogenesis and optic nerve development, but it has also been observed to be involved in spinal cord neurogenesis. Studies have shown how GDF11 secreted by newly born neurons in the developing spinal cord promotes cell cycle exit, decreases proliferation, changes differentiation potential, and facilitates the temporal progression of neurogenesis (Shi and Liu et al., 2011). In addition, a study observed that old mice treated with daily doses of recombinant GDF11 resulted in an increase of Sox2+ve neural stem cell population in the brain,

indicating that GDF11 is capable of restoring neurogenesis in aged mice (Katisimpardi et al., 2014).

1. 6. Exploring Hox gene plasticity during development.

1. 6. 1. How are Hox genes regulated during development?

To answer this question, researchers have transplanted tissue or a small number of cells and analysed gene expression in the transplanted cells. These experiments, described in detail below, have revealed different levels of plasticity in Hox gene expression across different tissues in the CNS (Noden., 1983, Couly et al., 1998). For context, I will be referring to as plasticity the ability to respond to different stimuli/environments and adjust/adapt to them. to Gain-and-loss of function analysis carried out across several vertebrates has helped reveal the importance of Hox gene transcription in rhombomeres and neural crest cells (NCC) in head development (Krumlauf et al., 1994). Moreover, alterations to the spatial organization of rhombomeric tissue can result in the reorganization of the neural crest (NC), resulting in craniofacial abnormalities. Therefore, can Hox genes change depending on the site of transplantation, and if capable, is the response equal across the different antero-posterior levels of the CNS?

It is important to highlight that the cranial neural crest can be divided into two domains: the anterior neural crest (diencephalon, mesencephalon, and r1 and r2 of the metencephalon), where hox expression is never observed, and the posterior neural crest, where cells present the same hox signature as the rhombomere from which they originate.

Rhombomere transplantation experiments in chick showed that prior to emigration from the neural tube, neural crest cells (NCCs) have a fixed axial identity which remains unaltered by the signals from the surrounding environment when placed in ectopic sites (Couly et al., 1998). However, when rhombomeres are rotated rather than exchanged, NCCs change their Hox gene expression showing some degree of plasticity (Saldivar et al., 1996, Hunt et al., 1998).

To study the plasticity of NCC cells, Trainor and Krumlauf., 2000 grafted rhombomeric cells at homotopic and heterotopic locations into mouse embryos. Cells from r3, r4 and r5 were taken from each region and placed back into the same anteroposterior

position (homotopic) in the hindbrain of host embryos. Grafted cells incorporated into the hindbrain, mixed with their immediate neighbours, and retained appropriate axial expression for Hoxb1, Hoxb2 or Hoxa2. Cells from r3, r4 and r5 were then grafted into r2 (heterotopic). Cells integrated into the host population while also retaining their original axial anteroposterior identity. In contrast, while homotopically grafted NCCs maintained their original hox gene expression, those grafted in heterotopic sites. completely lost it. Neural cells grafted in the embryo showed mismatched Hox expression in the heterotopically-grafted neural tube while the crest-derived from it matches the environment. This suggests that at head level, anteroposterior identity is not completely fixed, furthermore suggesting that the surrounding environment may play a critical role in cells' axial identity.

At the hindbrain level, there appears to be a higher degree of plasticity. Rhombomeres transposed anteriorly to the otic vesicle retain their original anteroposterior Hox gene expression (Kuratani & Eichele., 1993, Couly et al., 1998). However, when grafted posterior to the otic vesicle, cells' Hox gene expression appears to undergo reprogramming to match their anteroposterior location. (Grapin-Botton et al., 1995, Itasaki et al., 1996). This is also observed in grafts carried out by Prince & Lumsden., 1994, where grafts of r4 grafted in anterior r2 retain expression of Hoxb-1, while grafts of r2 grafted in posterior r4, downregulate Hoxa-2 and adapt to the surrounding tissue. These observations appear to suggest that the induction of different Hox genes is dependent upon the anterior-posterior position of the graft, indicating that a change in anteroposterior identity can only occur when cells are grafted more posteriorly. This is hypothesised to occur via progressively stronger signals emanating from more posterior sites.

1. 6. 2. The importance of mesoderm and community effects on axial identity.

The grafting work described so far argues for hox gene plasticity based on observations made from the analysis involving manipulations of blocks of tissue. This approach, however, carries the risk of transferring other factors, such as signalling molecules and cell-community effects, which might regulate Hox gene expression and mask the real effects upon cellular plasticity.

As mentioned previously, work carried out by Trainor and Krumlauf., 2000 showed that cranial NCCs, which migrate as dispersed cells after grafting, are unable to maintain Hox expression in an ectopic environment. However, when grafted in a homotopic environment, these cells maintain their regional identity. In the same work, Trainor and Krumlauf identified the cranial mesoderm from the same axial level as the main source of the signals cells required to maintain Hox expression. However, the mesoderm signals appear to have a more permissive role rather than an instructive role, as they are incapable of inducing Hox gene expression in NCCs. Treating embryos 7.5-8.5 d.p.c in utero with retinoic acid expands Hoxb1 expression anteriorly into r2 and transformed r2 to an r-4 like character. However, expression of Hoxb1 was not induced in NCC. To further test the effects of RA on Hox gene expression on NCCs, embryos were cultured in RA after being grafted with transgenic r4 tissue into a r2 site. However, expression of Hoxb1 was not found in the graft-derived NCC migrating to the first arch. Same RA treatment was applied to embryos following transplantation of r2 cells from a Hoxb1/lacZ embryo into r4 wild-type host. Results showed once again graf-derived NCC being unable to express Hoxb1. Embryos were also cultured in the presence of BMP493 (RA inhibitor), however reporter expression in NCCs and arches were unaffected. Together these results show that RA is not the mesoderm signal required to induce and maintain Hoxb1 expression in NCCs migrating from r4 into ba2.

This model suggests that the rhombomeres provide their derivative NCCs with an initial anteroposterior identity which prepares them to respond to a particular set of environmental signals in each branchial arch. Therefore, when NCCs are transplanted to an ectopic environment, they fail to activate or maintain Hox expression as there is an absence of the appropriate signals. This raises the interesting question whether all mesoderm secretes anteroposterior instructive signals. However, cranial mesoderm and trunk mesoderm are different, as cranial mesoderm is a loosely packed mesenchymal population that does not form epithelial-like condensations or express somitic markers. Somites release RA, which helps establish Hox expression in the hindbrain (Itasaki et al., 1996, Gould et al., 1998). (Trainor and Krumlauf., 2000). Furthermore, sets of three somites of different anterior-posterior levels were grafted adjacent to either r1-r3 or r-5 in the hindbrain of stage 10 host embryos. Somites 8-10 could induce ectopic Hoxb4 expression in r3-r5 when placed adjacent to the selected

rhombomeres. This indicates that somites have the potential to reprogram Hox expression in the anterior hindbrain. Therefore, paraxial mesoderm is a source of environmental signals capable of altering Hox expression depending on the A-P origin.

In addition, Trainor and Krumlauf., 2000 also observed that in homotopic grafts, NCC cells which dispersed from the primary graft site maintained their original Hox pattern. However, in heterotopic grafts, cells which separated from the original grafts and dispersed failed to maintain reporter expression, while those which remained in a cluster at the graft site maintained their original (heterologous) Hox expression. Therefore, dispersed cells can exhibit plasticity regarding their Hox gene expression and change their fate. This adds an additional layer of complexity and suggests that in ectopic locations (outside their normal location), single cells lack the supporting signals from their neighbours to reinforce the Hox expression and that community effects play an important role in maintaining Hox identity.
On the other hand, cells of a rhombomere identity that become separated from the primary graft and intermingle with the surrounding population have been shown to be plastic and unable to maintain their appropriate Hox expression patterns, reinforcing the idea that community effects are also important to specify regional identity in rhombomeric populations.

1. 6. 3. Does the stage of development have an impact on Hox plasticity?

The work described so far shows that Hox gene expression can be modified by a cell's environment along the anteroposterior axis; however, these observations are limited to a stage in development where the CNS has been established. Can Hox genes change ounce boundaries have been established? Lance-Jones & Landmesser., 1980, addressed whether motor neuron axial identity is specified prior to outgrowth by giving lumbosacral motor neurons a choice of targets within the limb region. Specific lumbosacral spinal cord segments were reversed prior to limb bud formation and lumbosacral motor neurite outgrowth at developmental stage (9.5). Axons from reversed segments were therefore offered a choice between targets that were appropriate for the original anteroposterior identity of the spinal cord, or for its new location originally appropriate and spatially appropriate targets. The study showed that motor neurons in reversed cord segments projected initially to targets in accord with

their new anterior-posterior position, “recognized” the incorrectness of the muscle and then altered their course to establish connections with the correct muscle. A further study later published (Matise and Lance-Jones., 1996), following the same experimental design but at a younger developmental stage (2.5), showed that motor neurons in reversed cord segments projected and formed connections with muscles in accord with their new anterior-posterior position. Experimental design illustrated in figure 1.6. This indicates that neurons become specified prior to outgrowth, but only once a specific stage in development has been reached.

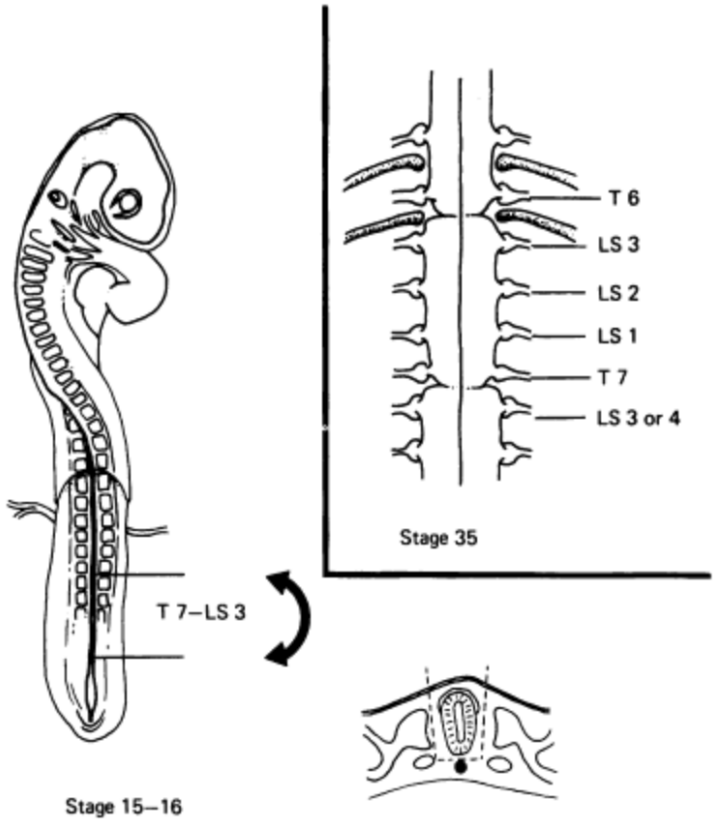

Figure 1.6. Grafting experiment elucidating Hox gene plasticity in the developing embryo.

Diagram of the position and morphology of the cord segments reversed at the time of operation (left) and at a representative time of examination (top right). Structures removed and reversed in the operation are shown in the cross-section at the bottom right (within dashed lines). Reproduced from Matise and Lance-Jones., 1996.

1. 6. 4. Is there a posterior dominance in Hox plasticity?

In some of the work previously described (Couly et al., 1998, Trainor and Krumlauf., 2000), anteriorization is never observed in posterior-to-anterior (P-A) transpositions. In contrast, anterior tissues switch to posterior identities when grafted in posterior locations, a phenomenon that may be connected to ‘posterior dominance’. The

proposed model to defend this idea, anterior segments would express low-inducing signals, while more posterior segments would be exposed to increasing levels of signals, causing them to adopt more posterior identities. Anterior tissues grafted in posterior regions would become exposed to higher signals and switch fate. Posterior tissue grafted to the anterior would move tissues from a high signal area to a lower one resulting in no changes regarding their axial identity. Therefore, plasticity is revealed only in A-P rhombomere transposition, suggesting a ratchet-like mechanism where changes in cell fate can occur only on one direction (posteriorly). This idea is later supported with the work by Gurdon et al.,1995 who shows how once exposed to high levels of signal, cells can't then express a Hox profile typical of low signalling – which he refers to as a 'ratchet'.

This can be the result of cells retaining or 'remembering' (potentially implying conserved chromatin changes) the signals they were being exposed to, resulting in a posterior dominance. Furthermore, suppose the graft is not in a sufficient range, e.g., a graft from r2 to r4. In that case, the signalling levels may not be distinct enough with regards to the relative levels of signalling and, therefore, not be able to induce changes in expression. However, this idea was disputed by work previously described by Itasaki et al., 1996 when donor segments identical in size were grafted into successively more posterior positions along the A–P axis. Grafted segments between r2 and r6 were capable of inducing Hoxb4; however, the response was not the same across all segments, with the more anterior segments requiring to be grafted into more posterior positions to induce similar changes in gene expression. This work indicates that the response of the cells is not as simple as mimicking the surrounding environment and that the preprogrammed identity of each segment does influence the nature of the response. Thus, the degree of plasticity is more closely related to the A-P position of the graft and the required level of signalling.

1. 7. Introduction to stem cells.

1. 7. 1. A brief history in stem cells.

Self-renewal, the capability of a cell to create multiple identical copies of itself indefinitely and pluripotency, the ability to differentiate to produce every cell type in the organism, are defining features of embryonic stem cells. These two features have attracted the interest of the scientific community for decades, as they can be used as powerful tools in the discovery of novel approaches in regenerative medicine. The work in pluripotency began with the study of teratomas, germ cell line tumours which spontaneously rise in mice strains, such as the 129, and contain cells of one or more of all three germs layers (ectoderm, mesoderm, and endoderm) (Steven and Little 1954). Kleinsmith and Pierce, 1964 demonstrated the potential of embryonal carcinoma (EC) cells, a subset of individual cells from teratomas, to give rise to a new tumour containing derivatives of all germ layers, as well as extraembryonic tissues, when grafted into host mice. This experiment was the first to show that a single cell can generate multiple embryonic lineages. The self-renewing cells of the tumour were later known as embryonal carcinoma cells (ECs) and further invigorated the interest in the field.

Further work showed that tumour-derived ESCs contribute to normal embryo development when injected into the blastocyst (Papaioannou et al., 1975) and generate chimeric mice (Papaioannou et al., 1978). In 1981, their work resulted in the isolation and in vitro propagation of pluripotent cells from the inner cell mass (ICM) of mouse blastocysts, referred to as ‘embryonic stem cells or ESCs (Evans and Kaufman., 1981; Martin., 1981). Later experiments confirmed that, unlike ECs, ESCs can remain karyotypically normal upon repeated passages making it possible to generate high levels of chimaerism and can transmit their genetic information through the germ line to their offspring (Bradley et al., 1984). This allowed the beginning of an exciting new era in developmental biology.

1. 7. 2. Stages of pluripotency.

The increasing knowledge in the field of stem cells has led to a bigger understanding of the different stages of pluripotency during early development and to the establishment of in vitro culture conditions. These include naïve pluripotency, formative pluripotency, and primed pluripotency. Naïve pluripotency can be described as a stage of development which closely resembles the pre-implantation epiblast identified at E4.5 (reviewed in Nichols and Smith., 2009). Cells at this stage are known to express general pluripotent markers such as Oct4 and Sox2 and other unique markers such as Nanog, Tbx3 and Esrrb, just to name a few. At this stage, cells hold the potential to become any cells derived from the three germs layers, except for extraembryonic tissue. As cells lose naïve pluripotency and become more receptive to different stimuli, they enter a stage known as formative pluripotency (reviewed in Kalkan and Smith., 2014, Smith, 2017). As cells commit to a particular fate they will enter a stage known as primed pluripotency. As the work described in this project will focus on the generation of neural cells from epiblast stem cells (EpiSCs), a primed stage of pluripotency, I will describe in greater detail this last stage.

1. 7. 3. Primed pluripotency.

Primed pluripotency is a property of the post-implantation epiblast (Nichols and Smith, 2009). As described with embryonic stem cells (ESCs), primed cells can self-renew and differentiate towards all germ cell derivatives; however, they are also biased towards a particular fate. In a developing embryo, primed cells remain pluripotent until the onset of somitogenesis (Beddington, 1981; Beddington, 1982; Osorno et al., 2012 Huang et al., 2012). EpiSCs are in vitro analogues of the primed epiblast (reviewed in Nichols and Smith, 2009; Tesar et al., 2007). Using teratoma assays, these cells have shown to be able to generate all three germ layers but fail to contribute to chimaera formation when injected into recipient blastocysts, not being able to contribute to the germline, unlike earlier-stage ESCs (Vallier et al., 2007., Huang et al., 2012). These cells can be derived from the embryonic epiblast between E5.5 and E8.0, but the transcriptome of EpiSC lines derived from different stages of development converge to resemble that of late gastrulation-stage epiblast (Kojima et al., 2014a). Expression of pluripotency markers Oct4 and Sox2, and early-post implantation markers Fgf5, Otx2 and Oct6 (reviewed in Kalkan and Smith, 2014) are characteristic markers which

help define EpiSCs. These cells contain two large and mutually exclusive subpopulations, which either express markers of either early PS (such as Tbra) or the neural lineage (such as Sox1), resulting in high levels of heterogeneity on a gene expression level. The PS-like subpopulation represented a more un-differentiated and dynamic population, while the neural-like subpopulation was less dynamic, with some cells having already committed to neural differentiation (Tsakaridis et al., 2014).

1. 7. 4. In vitro culture conditions.

Several culture protocols exist for the recapitulation of established pluripotent states in vitro. I will explain here those employed in this study.

1. 7. 4. 1. Embryonic stem cells (ESCs).

ESCs isolated from the ICM of E4.5 embryos were first grown basal media supplemented with serum on a layer of feeder cells or mouse embryonic fibroblasts (MEFs) (Evans and Kaufman, 1981; Martin, 1981). These cells provided cells with an environment which encouraged adhesion and prevented differentiation (Smith & Hooper 1987). The component was later identified as Leukaemia Inhibiting factor (LIF) (Smith et al. 1988, Williams et al. 1988). The second component required for ESC culture is foetal calf serum (FCS), which allows cells to maintain pluripotency. Both of these factors appear to be essential for ESC culture as cell cultures in the presence of LIF, but in the absence of FCS, cells are unable to remain undifferentiated and form neural ectoderm (Ying et al. 2003a,b). MEFs were found to be able to be replaced by the addition of recombinant LIF and coating the plates with a gelatine substrate (LIF/FCS). When placed in the environment of the host embryo, ESCs exhibit all attributes of epiblast identity and potency, being equivalent to the ‘naïve’ preimplantation epiblast (reviewed in Nichols and Smith, 2009). However, ESCs cultured in LIF/FCS conditions showed to exert differences in their transcriptome and their potential to self-renew and contribute to development (reviewed in Morgani, Nichols and Hadjantonakis, 2017).

1. 7. 4. 2. Primed stem cell culture in EpiSC conditions.

EpiSCs can be maintained in vitro in basal media supplemented with activin and FGF once isolated from the post-implantation epiblast at stages E5.5-E8.0 (Brons et al., 2007; Osorno et al., 2012; Tesar et al., 2007). The addition of Activin stimulates the activation of the Activin/Nodal signalling pathway. The Activin/Nodal signalling pathway negatively regulates transcription of pluripotency-inducing BMP target genes in ESCs; therefore, any changes in this balance may result in the capabilities of ESCs to maintain pluripotency and proliferation becoming affected. (Galvin et al., 2010). On the other hand, Fibroblast Growth Factors (FGFs) are molecules which act by stimulating the mitogen-activated protein kinase pathway, where the activation of FGF receptors, Grb2, Ras, Raf, Mek and Erk leads to transcription activation of target genes (reviewed in Villegas et al., 2010). In culture, the main role of FGFs is to promote cell proliferation (Thisse & Thisse 2005). In comparison to ESCs, EpiSCs must be passaged in small clumps, as they fail to survive if passaged as single cells. This effect is tied to the hyper-activation of Rho-associated protein kinase (ROCK)/myosin signalling, which leads to apoptosis in response to changes in cell-cell adhesion (Ohgushi et al., 2010).

EpiSCs can also be produced by exposing ESCs to EpiSC conditions over long periods, which results in extensive cell death and differentiation, but also propagation of EpiScs (Turco et al., 2012). Functional differences between ESCs and EpiSCs are further shown by demonstrating the inability of EpiSCs to incorporate in pre-implantation embryos but to be able to do so in post-implantation embryos (Huang et al., 2012). In contrast, ESC incorporates well into pre-implantation embryos but not into post-implantation embryos (Evans and Kaufman, 1981). At a genetic level, ESCs and EpiSCs express pluripotent markers Oct4, Sox2 and Nanog; however, they do not show pluripotency markers Esrrb and Nr5a2 typical of a naïve state (Guo et al., 2009; Tesar et al., 2007), but do express markers observed in the post-implantation embryo such as Fgf5 and Otx2, characteristic of a primed state.

Transcriptome analysis of multiple EpiSC lines from embryos staged throughout gastrulation revealed that these cells do not resemble the post-implantation stage, as was believed (reviewed in Kojima et al., 2014a). The study revealed that these cells have a unique identity which much closely resembles those of the early primitive streak

based on the expression of mesoderm markers Tbra, Eomes and Mixl1, and endoderm markers Foxa2 and Sox17 (Kojima et al., 2014b). Further comparison studies between EpiSC lines show variation between levels of gastrulation markers Tbra and overall differentiation potential (Bernemann et al., 2011), which causes EpiSCs cultures not to be homogenous and to be vulnerable to spontaneous differentiation (Han et al., 2010). Add as a potential point in the discussion.

1. 7. 4. 3. Neuromesodermal progenitors in vitro.

The generation of neuromesodermal progenitors (NMPs) in vitro offers an attractive approach to produce cell types of the posterior spinal cord and mesoderm, which can be used for disease modelling or therapeutic applications. Generation of NMPs in vitro was first reported by Tsakiridis et al., 2014, where EpiSCs treated with CHIR, FGF2 and activin resulted in the emergence of cell populations positive for hallmarks of NMP identity Tbra and Sox2. Upregulation of characteristic markers of axial progenitors cdx2, Fgf8 and Gox genes were also upregulated. Ever since several other protocols have been published in an effort to optimise the generation NMPs from human and mouse pluripotent stem cells (Amin et al., 2016; Cooper et al., 2020 preprint; Diaz-Cuadros et al., 2020, 2019b; Frith et al., 2018; Gouti et al., 2014; Hackland et al., 2019; Lippmann et al., 2015; Tsakiridis and Wilson, 2015; Turner et al., 2014; Verrier et al., 2018, Metzis et al., 2018). All protocols have in common the stimulation of Wnt and, in most cases, the FGF signalling pathways. The efficiency of these protocols to generate NMPs was assessed using three determinant factors: First, the expression of caudal markers in the derived cultures (Gouti et al., 2017). Second, the ability to generate neural and mesodermal cell types in vitro. Thirdly, the ability to contribute to the neural tube and paraxial mesoderm upon being grafted to chick or mouse embryos. Cultures of NMPs are not limited to 2D cultures. Recently, these cells have been shown to be able of self-organising into 3D aggregates following a pulse of CHIR (Veenvliet et al., 2020). These make an attractive model to study morphogenic events during axis elongation as these organoid-like structures show A-P and dorsoventral axis formation, polarised colinear Hox gene activation and somitogenesis (Beccari et al., 2018; van den Brink et al., 2020; Veenvliet et al., 2020). NMPs derived from different pluripotent stem cell populations have shown to resemble quite closely their in vivo counterparts; however, they appear to be quite different when comparing their transcriptome and differentiation potential. This is thought to be due to differences in

culture and starting PSC populations which are at different developmental stages ranging from late gastrula caudal epiblast up to tail-bud stages (Edri et al., 2019a,b; Frith et al., 2018; Gouti et al., 2017; Gouti et al., 2014; Verrier et al., 2018).

The study of NMPs is rapidly expanding as their potential use for disease modelling and therapeutic application are becoming increasingly evident. However, there are still limitations to the generation of these axial progenitors in vitro. These cells are considered a transient population both in vivo and in vitro, making it very challenging to retain a homogenous culture of $T^{+}Sox2^{+}$ cells over prolonged periods of time (>3 passages) in the presence of Wnt and Fgf agonist. Cultures eventually commit to a particular lineage, either becoming mesoderm by downregulating Sox2 and maintaining Tbra, or becoming neural by downregulating Tbra while maintaining Sox2 (Tsakiridis and Wilson, 2015; Wind et al., 2020 preprint). The inclination towards a neural fate is due to lower levels of Wnt and Fgf signalling, which in vivo has been shown to control Sox2 expression in the caudal epiblast through N-1 enhancer activation (Takemoto et al., 2006).

1. 7. 5. Neural differentiation.

Differentiating embryonic stem cells have become an experimental tool for the analysis of molecular events that accompany lineage specification. The ability of ES cells to differentiate towards neural lineages has been demonstrated by Martin *et al*., following the isolation of mouse ES cells (Martin, 1981., Evans & Kaufman, 1981). Initial approaches included the culture of Embryoid bodies (EBs) with retinoic acid (Bain *et al*., 1995) or the co-culture with PA6 stromal cells or conditioned media (Kawasaki *et al*., 2000, Perrier *et al*., 1994). However, these cells present low efficiency of differentiation, heterogeneity and need for purification via lineage selection techniques (Li *et al*., 1998). In addition, EBs contain a mixture of different cell types, making it very challenging to study individual cell types.

Differentiating ES cells in adherent monolayers offers a solution to these problems. Culturing ES cell monolayers in defined feeder-free conditions in the absence of exogenous FGF and BMP inhibitors allows cells to undergo efficient neural commitment (Ying *et al*., 2003., Chambers *et al*., 2009). These cells were cultured at low density (reviewed in Pollard *et al*., 2006; Ying *et al*., 2003), suggesting that they

differentiate by default rather than by induction, paralleling the default induction of neural identity in the epiblast. Further studies demonstrated an early requirement for Fgf signalling in the exit from naïve pluripotency (Kunath *et al*., 2007, Stavridis *et al*., 2007). ES cells differentiating in this medium, N2B27, appear to have a similar gene expression pattern to those present *in vivo*, indicating a developmentally relevant *in vitro* differentiation system (Aiba *et al*., 2006). Therefore, adherent monolayer N2B27 cultures represent an efficient *in vitro* paradigm for *in vivo* neural induction.

1. 7. 6. The role of Sonic hedgehog (Shh) in the generation of neural cells in vitro.

Sonic hedgehog (Shh) is a secretory protein released from the mesoderm in the spinal cord shortly after connecting to the ventral midline of the neural plate (reviewed in Lin et al., 2020). Shh is essential in the development of multiple tissues and organs, especially of the central nervous system (CNS). Shh is found to be expressed ventrally, resulting in the development of the ventral hindbrain, midbrain, and forebrain (reviewed in Jessell., 2000, Altaba et al., 2003). Activation of Shh through the Gli pathway induces differentiation of the different classes of neurons which populate the brain and controls the development of the ventral midbrain and cerebellum (Hynes et al., 1995., Kohtz et al., 1998, Agarwala et al., 2001). Shh signalling is also essential in determining tissue polarity and pattern formation, which results in the formation of the neural tube patterns, the antero-posterior axis, and the dorsal-ventral axis, as well as the formation of somites and limbs (Chiang et al., 1996, Kvon et al., 2016). Besides patterning, Shh also plays important roles as a morphogenic factor in cell-fate specification, proliferation, differentiation, and survival of neural precursor cells along the neuraxis (Roelink et al., 1995). The effects of Shh during development have been elucidated using Shh mutant mouse embryos as a study model. Embryos bearing this mutation presented defects in the establishment or maintenance of midline structures, including the notochord and floorplate. Later defects include the absence of distal limb structures and ventral cell types within the neural tube and the absence of the spinal column and most ribs (Chiang et al., 1996).

Shh is expressed in the floor plate and notochord in the vertebrate neural tube. At this location, studies have identified a gradient along the dorsal-ventral axis during embryonic development (reviewed in Ribes and Briscoe., 2009). This gradient results

in the formation of distinct neuronal subtypes, including motor neurons (MNs) and four groups of interneurons (V0-V3). This evidence is further supported by gain-and-loss-of-function experiments showing that Shh is necessary and sufficient to induce ventral neural cell types (Roelink et al., 1995, Marti et al., 1995). At the same time, a deficiency of Shh does not only affect the formation of spinal cord structures but also brain development (Chiang et al., 1996). Shh is capable of such tasks by regulating the expression of numerous proteins found in the spinal cord. These genes include Nkx2.2, Olig2, Nkx6.1, Nkx6.2, Dbx1, Dbx2, Irx3, Pax6, and Pax7 organised from ventral to dorsal and regulated by graded Shh signalling (reviewed in Ribes and Briscoe., 2009).

1. 7. 7. Motor neuron progenitor induction.

Specification of motor neuron (MN) identity depends on three critical steps: neural induction, caudalization, and ventralization of precursors (Wichterle *et al*., 2002). Chambers *et al*., 2009 showed that dual inhibition of SMAD signalling by a combination of recombinant noggin protein and SB431542 neuralizes hESCs with very high efficiency. Currently, a combination of RA and sonic hedgehog agonist purmorphamine (PUR) is used for the differentiation of neuralized hESCs into motor neurons (Patani *et al*., 2011). In this case, RA acts on cells committed to a neural identity to change their rostrocaudal position, and to accelerate their differentiation, while sonic hedgehog or hedgehog agonist further specifies a ventral positional identity which causes a significant proportion of ES cells to initiate a motor neuron-specific transcriptional pattern and acquire features of mature neurons observed through immunohistochemistry. A later study compared the ventralizing activity of different Shh agonists on motor neuron yields after neural induction. Human-specific Shh agonist (HAG) gave rise to 10% Hb9+ cells, shh agonist (SAG) gave rise to 16% Hb9+ cells and (PUR) gave rise to 22% Hb9+ cells. The combination of SAG + PUR gave rise to 27% Hb9+ cells showing the highest yield of MNs from hESCs over a long period of culture (31 days) (Amoroso *et al*., 2013). Conversion of motor neurons from mESCs has also been described by Gouti *et al*., 2014 using SAG + RA. MNs generated using a combination of RA and SHH resemble bona fide MNs with the ability to form functional neuromuscular junctions (NMJs) and the capacity to engraft into the developing spinal cord (Amoroso *et al*., 2013).

MNs arise from the ventral domain of the neural tube. However, further specification of MNs allows the coordinated movement of hundreds of distinct muscle groups. MNs can be classified based on their anatomical and functional properties. The positional identity of MNs along the rostrocaudal axis is determined by the coordinated action of multiple signalling molecules. High levels of RA promote rostral (e.g. cervical and brachial) identity, whereas FGFs and Gdf11 activity give rise to more caudal (e.g. thoracic and lumbar) MNs (Liu *et al*., 2001). Determining which factors allow to produce cells with homogenous axial identities and NPCs expressing the most posterior genes (HOX PG11-13) will be the focus of the result chapters presented in this thesis.

Aims of the thesis.

Generating cells of the correct axial identity hold potential for cell therapies and models to study a range of developmental disorders. Grafting studies have shown that grafting not only the correct tissue type but matching axial identity is an important factor which increases the efficiency and overall success of the grafting (Kadoya et al., 2016). In the same way, different birth defects and neurodegenerative disorders can affect cell types in an axial-dependent manner; therefore, a need to create of not only the correct cell type but also of the correct axial level is of high interest.

Historically, most protocols aiming to generate posterior NPCs induce predominantly cells of a mixed hindbrain/ cervical axial identity marked by expression of Hox PG (1-5) members but are inefficient in producing high numbers of the more posterior, lumbosacral Hox PG (10-13)-positive spinal cord cells. One of the reasons for this is that differentiation of PSCs towards neural derivatives have been influenced by Nieuwkoop's 'activation-transformation' model. As mentioned, the idea of this model is that anterior neuroectoderm is induced 'by default' without posteriorising signals relying on RA/Wnt signals to induce progressively more posterior neural cells (Chambers et al., 2009., Nieuwkoop & Nigtevecht, 1954). More recently, the generation of neural cells with a thoracic and lumbosacral identity determined by the expression of Hox PG9 is possible by neuralising NMP-like cells via the addition of RA and inhibiting TGF/Nodal/BMP signalling pathways (Gouti et al., 2014,). However, cells presented a heterogenous axial identity and did not express the most posterior Hox PG (10-13).

Modulation of FGF and WNT plays essential roles in forming axial progenitors and in coordinating posterior identity. Work from Lippmann et al., 2015 showed that supplementation with GDF11 to an NMP culture including FGF and WNT produces a shift towards the more PG groups corresponding to lumbosacral levels. Activation of lumbosacral Hox paralogs after adding GDF11 can be due to its role as a key regulator of trunk-to-tail transition during embryonic axial elongation and caudal expression. However, regardless of the generation of lumbar motor neurons (MNs), they do not show single-cell quantification data being unable to determine whether lumbosacral PG groups are expressed at a protein level. Therefore, there is still limited quantitative/ functional evidence regarding its efficiency. More research is required to understand

the optimal conditions to generate tissues of defined sections of the postcranial axis.

Despite extensive published work on the generation of NPCs of different axial identities, there is limited evidence of how efficiently these cells can integrate into an in vivo model. Wind et al., 2021 showed that human pluripotent stem cells (hPSCs) of thoracic identity can integrate into the ventral side of the neural tube and project axons towards muscle target cells when grafted at a 'homotopic' site in a stage 10-13 chick embryo. However, they did not show the efficiency of these cells to integrate and form axonal projections at different axial levels of the spinal cord ('heterotopic') or whether their axial identity altered to adapt to the host site.

My hypothesis, tested in this thesis, is that matching anteroposterior identity is essential for optimal grafted neural progenitor cell integration, and that achieving spinal cord matching requires NMP differentiation.

To test this hypothesis, the aims of this project can be summarised into the following:

1. Identify contributing factors and conditions to achieve the differentiation of neural progenitors with defined and consistent axial identity in culture.

2. Determine the importance of axial identity upon transplantation by evaluating NPC axial plasticity, survival, and integration.

Chapter 2: Materials and Methods.

2.1.General Reagents.

Table 2.1. List of general reagents used in the thesis.

Details of General Reagents		
Product	Manufacturer	Catalogue Number
10 mM dNTP Mix	Thermo Fisher Scientific (Life Technologies)	18427-013
50 mM 2-Mercaptoethanol (x1000)	Life Technologies	31350010
96 Well microplate with Cell-Repellent Surface, clear, U bottom, sterile, with lid, case of 6	Greiner Bio-One	650970
Absolutely RNA Miniprep Kit	Agilent	400800
Accutase® Solution	Sigma-Aldrich	A6964
Activin-A (Human/murine/rat raised in E. coli)	Peprotech	120-14E
Anti-Fade Fluorescence Mounting Medium - Aqueous, Fluoroshield	Abcam	Ab104135
B27 Supplement (50x) Serum Free	Thermo Fisher Scientific (Life Technologies)	17504044
Bovine Serum Albumin solution,7.5% in DPBS	Scientific Laboratory Supplies Ltd.	A8412-100ml
CHIR99021 (CHIR)	Tocris Bioscience	4423/10
Corning® Matrigel® Growth Factor Reduced (GFR) Basement Membrane Matrix, LDEV-free, 10 mL	Corning	354230
Costar® 10 ml Stripette®	Corning Incorporated	4101
Costar® 12 well clear TC-treated multiple well plates, individually wrapped, sterile	Corning	3513
Costar® 24 well clear TC-treated multiple well plates, individually wrapped, sterile	Corning	3524
Costar® 25 ml Stripette®	Corning Incorporated	4251

Costar® 48 well clear TC-treated multiple well plates, individually wrapped, sterile	Corning	3548
Costar® 5 ml Stripette®	Corning Incorporated	4051
Costar® 50 ml Stripette®	Corning Incorporated	4501
Costar® 6 well clear TC-treated multiple well plates, individually wrapped, sterile	Corning	3516
Costar® 6 well clear TC-treated multiple well plates, individually wrapped, sterile	Corning Incorporated	3516
Cover glasses, 12 mm diameter	Marienfeld-Superior	0111520
CryoTube™ Vial	Thermo Scientific	377224
DAPI 10mg/ml in H2O	Cambridge Bioscience	40043
Dimethyl Sulfoxide (DMSO)	VWR Chemicals	23500.26
DMEM/F-12, no glutamine	Invitrogen Life Technologies	21331-020
Donkey Serum	Sigma-Aldrich	D9663-10ml
Dulbecco's Phosphate Buffered Saline (PBS)	Sigma-Aldrich	D8537
Eppendorf PCR Tubes, 0.2 mL, PCR clean, 8-tube strips, 120 pcs. (960 tubes)	Eppendorf UK	0030124359
Eppendorf Safe-Lock microcentrifuge tubes, volume 0.5 mL, assorted colors	Scientific Laboratory Supplies Ltd.	T3670-500EA
Ethanol absolute 100%	VWR Chemicals	20821.330
Filter Tip Bevelled 10 µl	StarLab	S1121-3810
Filter Tip Bevelled 100 µl	StarLab	S1121-2810
Filter Tip Universal 1000 µl	Greiner Bio-One	740288
Foetal Calf Serum (FCS)	Life Technologies	10270106
Geltrex LDEV-Free Reduced Growth Factor Basement Membrane Matrix	Thermo Fisher Scientific (Life Technologies)	A1413201

Glasgow minimum essential medium	Sigma	G5154
GlutaMAX Supplement	Thermo Fisher Scientific (Life Technologies)	35050-061
Glycerol	CalBiochem	356350
iSpacer 0.1mm	SUNJin Lab	IS306
KnockOutTMSerum Replacement	Gibco	10828028
L-glutamine, 200mM	Invitrogen	25030-024
LDN 193189	Tocris Bioscience	1509
Leica™ Immersion Oil type F	Leica™ Microsystems	11513859
LightCycler 480 SY Green Master	Roche Applied Science	04887352001
Lightcycler® Multiwell Plate 384, White	Roche	4729749001
M2 Medium	Sigma	M7167-100mL
MEM non-essential amino acids (NEAA) (100x)	Invitrogen Life Technologies	11140-036
Microscope Slide Polysine 75x25x1mm	Gerhard Menzel GMBH	MIC3050
Microscope slides	VWR	ECN 631-1553
Microtube 1.5 ml	Sarstedt	72.692.005
Molecular Biology Grade Water	Hyclone	SH30538
N-2 Supplement (100x)	Thermo Fisher Scientific (Life Technologies)	17502048
Neurobasal ® Medium	Thermo Fisher Scientific (Life Technologies)	21103049
Paraformaldehyde (PFA)	Fisher Chemical	F/1501/PB08
Penicillin (10,000 U/mL) / streptomycin (10,000 µg/mL)	Invitrogen	15140-122
Phosphate Buffered Saline (PBS) Tablet	Sigma	P4417

ProLongTMGold Antifade Mountant	Thermo Fisher Scientific	P36930
Random Primers	Promega Corporation	C1181
RapiClear 1.49	SUNJin Lab	RC14900
Recombinant Human FGF Basic/ FGF2 (145aa)	R&D Systems, Inc	3718-FB-100
Recombinant Human/Murine/Rat GDF-11	Preprotech	120-11
Retinoic acid	Sigma-Aldrich	R2625
RNAse-free ddH2O	Roche	39369-21-8
RNaseOut™ Recombinant Ribonuclease Inhibitor	Scientific (Life Technologies)	10777-019
RNAseZap® RNAse decontamination solution	Ambion	AM9780
SB 431542	Tocris Bioscience	1614
Smoothened Agonist (SAG)	Calbiochem	364590-63-6
SuperScript III Reverse Transcriptase	Thermo Fisher Scientific (Life Technologies)	18080044
Triton™ X-100	Sigma	T8532
Trypsin 2.5%, 100x	Invitrogen	15090-046
Tube, Round-bottom; With cell strainer cap	Falcon	352235
UltraPure ™ Dnase/Rnase-Free Distilled Water	Gibco	10977
White Filter Cards	Thermo Fisher Scientific (Life Technologies)	11922355
µ-Plate 24 Well Black ibiTreat: #1.5 polymer coverslip, tissue culture treated, sterilized	Thistle Scientific Ltd	IB-82406
µ-Slide 8 Well ibiTreat: #1.5 polymer coverslip, tissue culture treated, sterilized	Thistle Scientific Ltd	IB-80826

Table 2.2. List of equipment used in this thesis.

Table 2.2	Instrument/Equipment Details
Equipment	Company
Centrifuge 5702	Eppendorf
Cytospin for Cytocentrifuge	Thermo Scientific
DNA Engine thermal cycler	BioRad
Glass Coplin Staining Jar, cat 107	Thermo Fisher
IncuShaker, 10 L H1010 BR13-00	Benchmark Scientific
LightCycler® 480 Instrument II	Roche
LSR Fortessa (4 Laser) Analyser	BD
LSR Fortessa (5 Laser) Analyser	BD
Mr. Frosty™ Freezing Container	ThermoFisher Scientific
Nanodrop ND1000 Spectrophotometer	Thermofisher Scientific
Sanyo CO2 incubator	Sanyo
SciSpin Mini Microfuge	Sciquip
Sigma 1-14 Microfuge	Sciquip
SUB Aqua 18 Plus Water bath	Grant
TCS SP8 Confocal Microscope (5 Detectors)	Leica
Vortex Mixer	SLS Lab Basics
Widefield Observer	Zeiss

2.2. Solutions Prepared

Standard molecular biology solutions were prepared according to (Sambrook and W Russell, 2001). Frequent solutions included:

- 4% (w/v) PFA: PFA dissolved in PBS (pH 7.4)
- PBS (not for cell culture): 5 PBS tablets/L water
- 15% sucrose (w/v) solution: sucrose dissolved in PBS (pH 7.4)
- PBS-T: PBS with 0.1% Triton X-100
- Blocking buffer: 5% Donkey serum and 0.01% sodium azide in PBS

2.3. Primary Antibodies

Table 2.3. Primary antibodies used for ICC.

Epitope	Host	Dilution	Manufacturer	Catalogue number
Brachyury	Goat	1:200-400	R&D	AF2085
SOX2 [EPR3131]	Rabbit	1:200	Abcam	Ab92494
Hoxb4	Rat	1:25	DSHB	I12
Hoxc9	Mouse	1:50	Abcam	Ab50839
Hoxc13	Rabbit	1:200	Abcam	Ab188043
TubIII	Rabbit	1:500	Abcam	Ab18207
Islet1	Mouse	1:200	DSHB	39.4D5
FoxA2	Rabbit	1:400	Cell signalling technology	8186
Pax3	Mouse	1:50	DSHB	Pax3

2.4. Secondary Antibodies.

Table 2.4. Secondary antibodies for ICC.

Host species	Species recognised	Alexa excitation wavelength (nm)	Manufacturer	Catalogue number
Donkey	Mouse	488	Invitrogen	A21202
		555	Invitrogen	A31570
		647	Invitrogen	A31571
	Rabbit	488	Invitrogen	A21202
		555	Invitrogen	A31572
		647	Invitrogen	A31573
	Rat	488	Invitrogen	A21202
		555	Invitrogen	A48270
		647	Invitrogen	A48272

2.5. qPCR primer sequences.

Table 2.5. qPCR primer sequences.

Gene	Forward sequence	Reverse Sequence
ChAT	GGTTCGGTGCGTAACAGC	GCGATTCTTAATCCAGAGTAGCA
En1	TGGGTCTACTGCACACGCTAT	TTTTCTTCTTTAGCTTCCTGGTG
FoxP1	CTGCACACCTCTCAATGCAG	GGAAGCGGTAGTGTACAGAGGT
Hoxa13	CCAAATGTACTGCCCCAAAG	TCTGAAGGATGGGAGACGAC
Hoxa4	TCCTCGTCCTCGTTACTGCT	TCCAATCCTGGCAAAGTTGT
Hoxa5	CAAGCTGCACATTAGTCACGA	GCGGTTGAAGTGGAATTCTT
Hoxa7	GTCCCCAACCTGCACTCTAC	CGCTCAGTCCACAAAAGTTG
Hoxa9	GGATGAGCTGAGCGTTGG	CTTGGACTGGAAGCTGCAC

Hoxb1	AAGAGAAACCCACCTAAGACAGC	GCTCAGGTATTTGTTGAAATGAAA
Hoxb2	GTCCCCAACCTGCACTCTAC	CGCTCAGTCCACAAAAGTTG
Hoxb8	CAGCTCTTTCCCTGGATGC	ATAGGGATTAAATAGGAACTCCTTCTC
Hoxc13	CAGCTGTAGAGGTGGGTTCG	AAAGGCCAGGGGTTTAGAGA
Hoxc6	GAATTCCTACTTCACTAACCCTTCC	TCATAGGCGGTGGAATTGAG
Hoxc9	GCAGCAAGCACAAAGAGGA	CGTCTGGTACTTGGTGTAGGG
Hoxd10	CTGAGGTTTCCGTGTCCAGT	TTGGAGTATCAGACTTGATTTCCTC
Isl1	GCAACCCAACGACAAAACTAA	CCATCATGTCTCTCCGGACT
Lhx2	CAGCTTGCGCAAAAGACC	TAAAAGGTTGCGCCTGAACT
Lhx3	CAAGTCCGACAAGGACAGC	TAGCAGGCCCCATGTCAG
Noto	TTG CAA AGC AGC ACA ACC T	TTT GGA ACC AGA TCC TCA CC
Olig2	AGACCGAGCCAACACCAG	AAGCTCTCGAATGATCCTTCTTT
Pax2	AGGGCATCTGCGATAATGAC	AAGGCTGCTGAACTTTGGTC
Pax3	GCCCACGTCTATTCCACAA	GAATAGTGCTTTGGTGTACAGTGC
Tbx6	CGCTGTGGGGACAGAGAT	TGACTGATACTCGGCAAGCA
Tuj1 (Tubb3)	GCGCATCAGCGTATACTACAA	TTCCAAGTCCACCAGAATGG

2.6. Cell lines.

2.6.1. E14JU09 EpiSCs.

The E14JU09 EpiSCs cells are derived from the ESC to EpiSC conversion of the existing E14JU09 ESC cell line. These ESCs are a clone line derived by the Transgenic Unit at the Centre of Regenerative Medicine from ESCs obtained from chimeric embryos generated with E14tg2a ES cells. They have a 129/Ola genetic background and are hypoxanthine phosphoribosyl transferase deficient, with a high propensity for germline colonisation.

2.6.2. r04-GFP EpiSCs.

The r04-GFP EpiSCs are derived from cells obtained from an E6.5 embryo of mixed genetic background. These cells were then genetically engineered to carry a random integration of a CAG-driven GFP, conferring ubiquitous GFP expression (Huang et al., 2012).

2.6.3. R04-GFP ESC.

The r04-GFP ESCs are derived from the E14Ju09 ESC cell line, which was genetically engineered to carry a pPyCAG-EGFP-IRES-PuroR-polyA plasmid delivered by lipofection (Tesar et al. 2007).

2.7. Cell culture and conditions.

2.7.1. Incubation

All cultures were incubated 37°C with 5% CO_2. A Fastread haemocytometer (Kisker Biotech) was used to count cell numbers when required.

2.7.2. N2B27 Medium

Components of chemically defined medium hereinafter termed N2B27 are outlined in the following table:

Table 2.6. Reagents used to make N2B27 media.

Table	**N2B27 Media Composition**
Component	**Volume**
DMEM/F12 (Gibco)	25ml
Neurobasal (Gibco)	25ml
L-Glutamine (Invitrogen)	500µl
2 -mercaptoethanol	100µl
Non-Essential Amino Acids (NEAAs)(Invitrogen)	500µl
N2 (Gibco)	250µl
B27 (Gibco)	500µl

2.7.3. EpiSC Culture.

The composition of EpiSCs culture media, herein termed N2B27/Activin/FGF is the same as the composition of N2B27 as described above, except that it is supplemented with fresh:

- 20ng/ml (final) –Recombinant human/rat/Mouse activin A (Peprotech)
- 10ng/ml (final) –Recombinant human Fgf Basic (R&D systems)

To passage EpiSCs, plates were coated with 7.5µg/ml bovine fibronectin (Sigma-Aldrich) and were left at RT°C for at least 5 minutes. EpiSCs were passaged when they reached 60-80% confluency. The medium was aspirated from the cells, the cells were washed with sterile PBS (Sigma), and 200µl of accutase (Sigma) was added. Cells were incubated at 37°C for about 2 minutes and then tapped carefully against the bench to detach and break cells into small clumps. Accutase was quenched through the addition of un-supplemented N2B27 media. The desired density was then transferred to a universal (Sterilin) containing more N2B27 media. Cells were then pelleted through centrifugation at 1300 rpm for 3 minutes, the excess media aspirated, and the cell re-suspended in Activin/FGF/N2B27 and plated onto the prepared fibronectin-covered plates after aspiration of the fibronectin solution. EpiSCs were routinely passaged in 6 well plates at a density of 1:8 to 1:15 every other day depending on the cell line.

2.7.4. ESC medium,

The composition of ESC culture media is the same as described in Table 2.6.

To passage ESCs, plates were coated with 5% gelatine and were left at RT°C for at least 10 minutes. ESCs were passaged when they reached approximately 80% confluency. The medium was aspirated from the cells; the cells were washed with sterile PBS (sigma), and 200µl of accutase (Sigma) was added. Cells were incubated at 37°C for about 2 minutes and then tapped carefully against the bench to detach and break cells into small clumps. Accutase was quenched through the addition of ESC media. The desired density was then transferred to a universal (Sterilin) containing more ESC media. Cells were then pelleted through centrifugation at 1300 rpm for 3

minutes, the excess media aspirated, and the cell re-suspended in ESC media and plated onto the prepared gelatine-covered plates after aspiration of the gelatine solution. ESCs were routinely passaged in 6 well plates at a density of 1:6 every other day depending on the cell line.

2.8. Cryopreservation.

2.8.1. Cell Freezing.

For cryopreservation, cells were subjected to accutase and pelleting following the standard passaging routines described above. Once the supernatant was aspirated off, the cells were in knockout serum replacement (KSR)(Gibco) +10% DMSO. 500µl of FCS/KSR +DMSO solution was used for each aliquot frozen (usual cells from a single 6-well plate well per aliquot). The resuspended cell solution was then aliquoted to a cryovial and immediately placed on dry ice. These were then transferred to -80°C for short-term storage or to liquid nitrogen tanks for long-term storage.

2.8.2. Cell Defrosting

To defrost cells, prewarmed media appropriate to cell type was placed into a universal. The frozen aliquot of cells was thawed in a water bath at 37°C and immediately added to the aliquoted media. Cells were then pelleted and the supernatant aspirated. The cells were re-suspended in the appropriate culture medium and plated onto pre-coated plates.

2.9. Cell differentiation protocols.

2.9.1. In vitro derivation of Neuromesodermal Progenitors (NMPs) from Mouse EpiSCs.

Differentiation of EpiSCs into neuromesodermal progenitors (NMPs) *in vitro was* carried out as described in (Gouti et al., 2014). Following treatment with accutase and spinning as per normal passaging, EpiSCs were re-suspended, counted and plated at approximately 6000 cells/cm^2 on fibronectin (Sigma)-coated wells in N2B27 medium supplemented with CHIR99021 Wnt 3µM (Axon) and bFGF 20ng/ml (R&D systems). Cells were cultured in these conditions for 48 hours.

2.9.2. In vitro derivation of Neuromesodermal Progenitors (NMPs) from Mouse ESCs.

To differentiate ESCs into neuromesodermal progenitors (NMPs) in vitro, ESC colonies were lifted using accutase and then spun at 1500 rpm for 3 minutes. ESCs were then re-suspended, counted and plated at approximately 6000 cells/cm^2 on gelatine-coated wells in N2B27 medium supplemented with bFGF (1µL/ml) (R&D systems) for 48h. Media was then aspirated, and N2B27 media supplemented with CHIR99021 Wnt (3µM) (Axon) and bFGF (20ng/ml) was added for a further 24h.

2.9.3. Differentiation of Neural precursor cell (NPC) of different axial identity.

To induce ventral anterior identity, NPCs (N_A) 100 nM RA (Sigma) was added to EpiSC cultures from D0–D2. To induce ventral hindbrain identity, NPCs (N_H) 100 nM RA (Sigma) and 500 nM SAG (Calbiochem) was added from D0–D2. Spinal cord identity (N_P) was induced by the addition of 0.3µL/ml CHIR99021 (Chir) (Tocris Bioscience, final concentration 3µM) and 2µL/ml bFgf (R&D, final concentration 20ng/ml) from D0 to D2 followed by 100nM RA and 500nM SAG from D2–D4. To induce terminal differentiation, cells were trypsinised and plated on plates coated with Matrigel (BD Biosciences) at a density of 1×10^5 cells cm^2 in N2B27 medium supplemented with bFGF (10 ng/ml). The next day bFGF was removed and cells were left to differentiate for an additional three days.

Note: Matrigel must be thawed on ice for approx. 12h at 4°C to prevent heterogenous gelation. Plates are then prepared by diluting ~10mg/ml Matrigel to 200µg/ml with PBS. Tips and strippetes must be stored at -20°C for approx. 1h before use to prevent matrigel from clumping.

Table 2.7. Illustration of NPCs differentiation protocol describing reagents, concentration, and length of time.

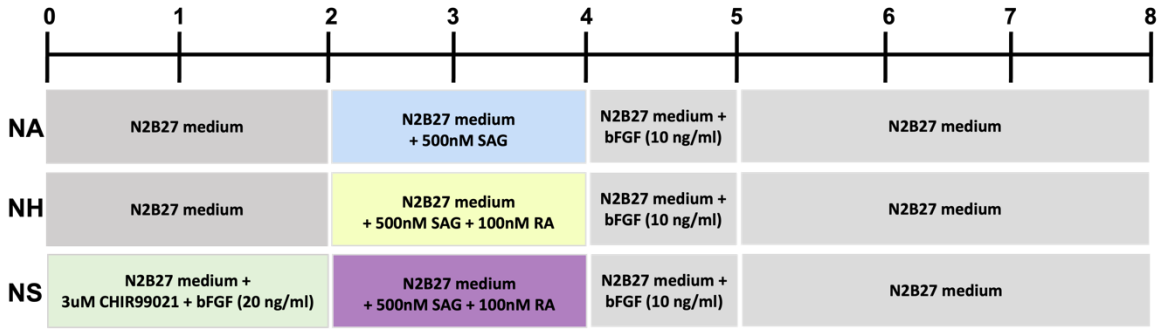

2.9.4. GDF11 cultures cells.

To induce differentiation of endoderm-derived cells, EpiSCs were plated on matrigel-coated wells in N2B27 medium supplemented with CHIR99021 (0.3µL/ml), bFGF (2µL/ml) and GDF11 (50ng/ml) from D0-D2. Media was then removed, and cells were exposed to fresh N2B27 for additional 24-48 hours. To induce intermediate cells, EpiSCs were plated on matrigel-coated wells in N2B27 medium supplemented with CHIR99021 (0.3µL/ml) and bFGF (2µL/ml) from D0-D1 followed by the addition of GDF11 (50ng/ml) from D1-D2. Media was then removed, and cells were exposed to fresh N2B27 for additional 24-48 hours. To induce tail cells, EpiSCs were plated on matrigel-coated wells in N2B27 medium supplemented with CHIR99021 (0.3µL/ml) and bFGF (2µL/ml) from D0-D2. Media was then removed, and cells were exposed to fresh N2B27 supplemented with GDF11 (50ng/ml) for additional 24-48 hours.

2.10. Molecular biology.

2.10.1. RNA isolation.

RNA was extracted from cultured cells using the Absolutely RNA Miniprep Kit (Agilent Technologies), following the manufacturer's instructions. Each well was washed with PBS (Sigma-Aldrich), and cells were collected using 350µl of RNA lysis buffer (containing 2.5µl B-Mercaptoethanol). This amount was scaled depending on plate confluence and the volume of the culture. When performing the spin steps, tube racks, globes, pipettes, and benches were wiped with RNAse-Zap (Ambion) to prevent RNAse contamination. The concentration of the isolated RNA was measured using a NanoDrop^{TM} Lite spectrophotometer (Thermo Fisher).

2.10.2. cDNA synthesis from RNA.

First-strand cDNA synthesis was performed using Superscript III (Invitrogen) following the manufacturer's instructions. 500ng of RNA, 50ng of random primers (Invitrogen), and 1µl of 10mM dNTP mix (Invitrogen) were combined in a nuclease-free PCR tube (Sarstedt), and nuclease-free water (Fisher-Scientific) was supplemented to a total reaction volume of 13µl. Samples were heated to 65°C for 5mins in a thermocycler (Biometra), and then cooled at 4°C for 5 min in ice. The following components were then added: 4µl First-strand buffer (5x), 1µL DTT (0.1M) (both Invitrogen), 1µL RNaseOUT^{TM} recombinant ribonuclease inhibitor (40U/µL, Invitrogen) and 1µL (200U) of Superscript III adding up to a total volume of 20 µL. The reactions were incubated at 50^{o}C for 1 hour, then 70^{o}C for 15min for heat inactivation of the enzymes. The RNA template was digested using 1µl (5U) RNase H (NEB) according to the manufacturer's instructions. Finally, the reaction was then diluted in 180µl of RNAse-free water and stored at -20^{o}C.

Each sample is calculated accordingly based on the measured content of RNA and diluted separately in the same volume of water.

2.10.3. Quantitative polymerase chain reaction (qPCR).

All qPCRs were carried out in a 384-well plate (Roche) with a total reaction volume of 10µL using Roche Sybr Green master mix on a Roche LightCycler® 480 Real- Time PCR system.

Table 2.8. qPCR reaction components.

Component	**Volume per reaction**
LightCycler®480ProbesMaster(Roche)	5ul
Forward primer (10µM)	1ul
Reverse primer (10µM)	1ul
Template cDNA	3ul

Table 2.9. qPCR reaction conditions.

Step	Temperature (ºC)	Duration (min:s)	Ramp rate (ºC/s)	Number of cycles
1 Pre-incubation	95	5:00	4.8	1
2 Denaturing	95	0:05	4.8	45
3 Annealing	60	0:10	2.5	
4 Extension	72	0:01	4.8	
5 Cooling	40	2:00	2.5	1

For each gene tested, a 10:1 dilution series of cDNA was prepared to contain the gene of interest. This was used in the Roche LightCycler® software (Roche) to determine the primer efficiency for each primer used. In each experiment, housekeeping gene TBP was analysed, and levels were used to normalize readings for other genes within each sample. For each gene tested, three technical replicates were set up on the qPCR plate to account for small-volume pipetting errors. To normalise the expression values, the value of the gene of interest as the average of its three technical replicates is divided by the average expression value of the housekeeping gene. All samples are relative to EpiSC samples.

Note: Cycling conditions according to manufactures instructions (45 cycles).

2.11. Animal Embryology.

2.11.1. Animal Husbandry/ Maintenance of mice.

Wildtype (WT) MF1 (outbred) Mouse strains were housed and bred in the Animal Unit of the Centre for Regenerative Medicine (CRM) according to the provisions of the Animals (Scientific Procedures) Act (1986).

All mice were kept under the same conditions, 10 hours light, 14-hour dark cycle. Embryos of specific developmental stages were obtained by setting up timed matings overnight and inspecting the presence of vaginal plugs the following morning. Embryonic day (E)0.5 was designated to the day at noon when plugs were observed.

2.11.2 Embryo and adult tissue collection and dissection.

Pregnant females were culled by cervical dislocation by Animal Unit staff. The uterus was extracted from the abdominal cavity, and the decidua was then placed in M2 Medium (Sigma) at room temperature. Adult tissue was removed at the same time and placed in M2 medium (Sigma) at room temperature (RT°C). Using forceps, the decidua and Reichert's membrane were removed from the embryo, and when necessary, adult tissue was further dissected in M2 medium under a zoom stereo microscope (Olympus, Nikon).

Special care was taken for embryos for *ex vivo* culture for which the yolk sac and amnion were carefully parted to evert the embryo, keeping the placenta attached to the embryo via the umbilical cord.

2.11.3. Grafting cells from in vitro culture into embryos.

Grafting was performed under a dissecting stereomicroscope using a hand-pulled micropipette. Cells were cultured in 6-well plates and then scraped from the plate using a 20-200 µl pipette tip. The resulting cell sheets were placed close to the embryos and drawn into the micropipette by gentle suction using a mouth pipette. Next, the cells were gently blown out, and a small cell clump containing ~20-100 cells was sucked into the micropipette again and placed close to the opening of the micropipette. The embryo was held loosely in place with forceps while the micropipette was inserted in the region of interest to create an opening. Cells were then gently expelled as the micropipette was drawn out of the embryo, leaving cells lodged in the neural tube (Huang et al., 2012).

2.11.4. Rolling culture of embryos.

Each embryo was cultured in separate bottles containing 3ml of media per embryo, previously warmed at 37°C and gassed with 5%CO2:95%O2. Gassing was repeated every 8-10 hours.

2.11.5. Organotypic embryo spinal cord slice culture.

Using forceps, the head and extraembryonic membranes were removed from embryos with their Reichert's membrane already dissected. These embryos were manually sectioned transversely into three sections using small bow scissors following the anterior-posterior axis. Sections were then transferred onto a cell culture insert on a Petri dish (PICMORG50, Millicell) and gently moved with forceps to position them flat on the insert. Cells were collected by scraping from the bottom of the dish to collect coherent groups of cells in a droplet of M2 which served as the reservoir for cells ready for grafting. Grafting was performed under a dissecting stereomicroscope using a hand-pulled micropipette. Inserts then were placed in 6-well plates and cultured in a 6-well plate. Excess media was removed to allow sections to attach to the membrane, followed by addition of 1ml of neural culture media. Slices with cells were incubated at 37°C+5% CO2 for four days, with fresh NSC medium added daily. Grafted cell growth was observed every day, and brightfield images were taken every 24h using a fluorescence stereo microscope to track the changes in tissue morphology throughout the extended culture. The ventral neural tube was labelled with DiI to identify the tissue's ventral site after four days of culture.

2.12. Immunofluorescence.

2.12.1. Preparation of tissue explants for Immunofluorescent staining.

After the 4th day of culture, explants were fixed with 4% (w/v) PFA in PBS at 4°C overnight. Sections were permeabilised with 0.5% (v/v) Triton-X100 in PBS for at least 15 minutes. Non-specific antigens were blocked with a blocking buffer of 5% Donkey serum (v/v) in PBS overnight. Primary antibodies were diluted in blocking solution according to manufacturers' suggested or optimised concentrations and added to the sections overnight at 4°C. Explants were washed with PBS three times for 5 minutes. Secondary antibodies were diluted 1:1000 in a blocking solution alongside a nuclear stain, in this case, hoescht (1:1000) and added to the sections overnight at 4°C. The explants were then washed with PBS three times for 5 minutes. After staining, the explants are transferred to a glass slide and mounted. Before mounting, explants were

cleared using the clearing solution Rapiclear. The clearing solution was preheated at 42°C and then added to the explants for 1-2 hours or until tissue appeared clear.

2.12.2. Wholemount immunohistochemistry for embryos E10.5 - E.12.5.

Dissected embryos were washed in PBS for 5 minute to remove M2 media and then fixed with 4% (w/v) PFA in PBS overnight at 4°C with gentle shaking. Samples are then washed three times with PBS for 15-20min each time (depending on embryo size) at RT. Each sample was then transferred into a small tube containing 2% PBST (2% Triton-X100 and 0.2% sodium azide) solution and placed on an orbital shaker for three days at 4°C to allow permeabilization. Each day the tube containing the embryo sample was checked to ensure that the embryo was not sticking to the edges of the tube. Samples are then washed in PBS for 15-20min/time (depending on embryo size) at RT and then transferred blocking buffer (10% normal goat serum, 2% Triton-X 100, and 0.2% sodium azide in PBS) and placed on an orbital shaker for two days at 4°C. Blocking solution can be kept at 4°C for 24h. Each embryo was then incubated with 2.5mls of primary antibody and placed again on the orbital shaker at 4°C for 5 days. Length of the incubation depends on the size of the sample and overall efficiency of the primary antibody. After incubation samples are washed twice with washing buffer (3% NaCl and 0.2% Triton-X 100 in PBS) for 2 hours each time, and then incubated with the secondary antibody at 4°C on an orbital shaker for 2-3 days. After incubation samples are washed with washing buffer for 2 hours each time once again. Samples are then incubated in 2% PBST containing DAPI at a working solution, 1:1000, at 4°C on an orbital shaker overnight. Samples are then washed three times with PBS for 15-20min each time (depending on embryo size) at RT. Samples can be stored in PBS at 4°C.

Note: DAPI can be added to the secondary antibody solution.

2.12.3. Clearing protocol.

To ensure highest quality of imaging, samples were incubated in 2-3mls of Rapiclear 1.49 solution. Visual clarity is then checked periodically until the sample is transparent. For mouse embryos E10.5 – E12.5, samples are incubated for 24-48 hours. For spinal cord sections, samples were incubated for 1-2 hours until fully clarified. For shorter

periods of clearing warm up the RapiClear 1.49 solution before using. Samples can be stored in RapiClear 1.49 at 4°C for several weeks without the image quality resulting affected. Samples are the mounted between two coverslips separated by an iSpacer. Remove the stricker and press to seal the coverslip. Any extra solution was removed using kimwipes.

Note: RapiClear 1.49 can be reused up to three times.

2.12.3. Embryo sample fixation.

Dissected embryos for embedding and sectioning were fixed with 4% (w/v) PFA in PBS at 4°C overnight.

2.12.4. Preparation of cryostat sections.

Following washes, fixed samples for embedding were transferred into a bijou vial with 15% (w/v) sucrose solution for between 2 hours and overnight at 4°C, depending on sample size. The sucrose solution was then replaced with melted 15% (w/v) sucrose and 7% gelatine (Sigma-Aldrich) solution. Samples were kept at 37°C and allowed to sink to the bottom of the vial. The samples were transferred and orientated in a metal mould underneath a dissecting microscope using forceps tools. Once in position, the sucrose/gelatine solution was placed carefully on ice to set. Samples were frozen by holding the metal base of the mould close to the surface of liquid nitrogen. Blocks were stored at -80°C and allowed to equilibrate for at least a few hours in the chamber of the cryostat (Leica CM1900, Leica Microsystems). Samples were mounted onto a cryostat and allowed to adjust to the machine's temperature set at -20°C temperature. The sample was then sectioned at 10-12 µm thickness on frost glass slides and stored at -80°C until required.

2.12.5. Immunofluorescent staining on mouse cryosections

Slides containing cryostat sections were thawed at RT°C for 5 minutes. To remove the gelatine, slides were then placed in a slide holder, which was then immersed into an empty pipette box containing preheated PBS and left in a water bath at 50°C for 20 minutes. Sections were carefully circled with a PAP pen (Vector) to keep reagents localized on tissue specimens.

Sections were permeabilised with 0.5% (v/v) Triton-X100 in PBS for at least 15 minutes. Non-specific antigens were blocked with a blocking buffer consisting of 5% Donkey serum (v/v) in PBS for at least 1 hour. Primary antibodies were diluted in blocking solution according to the manufacturer's suggestions or at optimised concentrations and added to the sections overnight at 4°C. Sections were washed with PBS three times for 5 minutes. Secondary antibodies were diluted 1:1000 in a blocking solution alongside a nuclear stain, in this case, hoescht (1:1000). and added to the sections for 2 hours at RT°C. The sections were then washed with PBS three times for 5 minutes. Upon completion of staining, the slides were mounted using either Prolong® Gold Antifade Reagent (Molecular Probes) or Vectasheild non-hardening medium (Vecta Labs) with a coverslip. Mounted sections were stored at 4°C until imaging. Mounted sections were imaged using a confocal microscope 4xD.

2.12.6. Immunocytochemistry on cells.

2.12.6.1. Fixing cells.

Once cultures were ready for imaging, the supernatant was removed, cells were washed once in PBS (Sigma), and overlaid with 4% paraformaldehyde solution for 10-15 min at 37ºC for 10-15 min. The fixative was then removed, and cells were washed three times for 5min each time in PBS.

2.12.6.2. Antibody staining for immunocytochemistry.

Fixed cells were incubated in a blocking solution containing PBS, 5% donkey serum and 0.1% Triton X-100 for one hour at room temperature; this will prevent antibody binding to any non-specific sites. The blocking solution was then removed, and cells were washed with PBS three times for 5 min each time. Primary antibodies were diluted in a blocking solution at a concentration recommended by the manufacturer. Cells were overlaid with diluted primary antibody solution and left overnight. The primary antibody solution was then removed and stored at 4ºC to be re-used. Cells were washed three times again with PBS and overlaid with a secondary antibody diluted 1:1000, unless stated otherwise, for two hours at room temperature. The secondary antibody dilution was removed and stored at 4ºC to be re-used. Cells were washed with PBS three times and overlaid with DAPI diluted 1:2000 in PBS for 10

minutes. After the DAPI solution was removed and cells were overlaid with PBS for imaging. The following primary antibodies were used: mouse anti-Hoxc9 (1:100) (DSHB) rat anti-Hoxb4 (1:100) (DSHB) rabbit anti-Tuj1 (1:500) (R&D) rabbit anti-Sox2 (1:200) (R&D) goat anti-Brachyury (1:500) (R&D) mouse anti-Islet1 (1:200) (DSHB). Secondary antibodies were anti-mouse, anti-rabbit, anti-goat and anti-rat, Alexa's (488, 555, 647) from Molecular Probes. In some instances, cells only had two washes between stages to prevent cell loss.

2.13. Imaging analysis.

2.13.1. Segmentation and cell quantification.

Images obtained on the fluorescent microscope Zeiss observer were exported as individual channels using the Zen software. Using the software ImageJ, background correction was applied to the fluorescent channel used to image cells stained with DAPI allowing the establishment of a min/max threshold (0-10,000). This allows for correcting for poor quality or incorrectly configured illumination. To do so, ImageJ plug-in rolling ball and background subtraction was applied. The first is correct for uneven illumination while preserving low-intensity fine specimen detail. The second removes low-intensity image information and background. Combination of these two features allows for improved segmentation and quantification. Nuclear segmentation is then applied on the same channel using the analysis software Ilastik. By selecting the pixel and object classification, Ilastik performs pixel classification and the thresholds the probability maps to be used to identify specific objects (Berg et al., 2019). Quality control measures were applied to reject incorrectly segmented nuclei using the training feature: which involved manually identifying cells from what the software establishes as background. Once nuclear segmentation appeared to be satisfactory, fluorescence intensity was measured using the software analysis package Cell Profiler (Carpenter et al., 2006). Nuclear intensities in the “nucleus” population were calculated using a Measure Object Intensity building block to quantify each channel selected. The mean intensity was calculated and exported as cvs. File, which was then imported into the analysis software package Flowjo for further quantification and visualisation purposes. Result values were plotted as scatter plots; negative controls were used to set the thresholds used to determine positive or negative cells for the markers of interest. Percentages of positive cells were then plotted as stacked plots.

2.13.2. Axon length measurement.

Length of TubIII positive cells were measured using the Simple Neurite Tracer feature in ImageJ/Fiji, a plug-in used for precise annotations of paths from elongated structures (such as neurons and blood vessels) in large image stacks (Longair et al., 2011). Two points were manually selected for each axon to determine the beginning and end points of the axon. The algorithm finds and measures the path length between and exports the values in table form. Values are then plotted using the analysis software package GraphPad.

2.13.3. Imaging.

Stained samples were imaged using different fluorescent microscopes depending on the sample selected for analysis and type of image required. Visualization parameters (magnification, exposure, gain, bit-depth, etc) were adjusted depending on the experiment and the genes of interest. Negative controls were carried out alongside each experiment and used to set reference values when possible. Across biological replicates, the same imaging and visualisation parameters were used. Each channel was individually optimized to achieve the highest quality signal.

2.13.4. Imaging on the Opera Phenix Plus High content spinning disk confocal.

The Opera Phenix plus, referred to as “Opera”, is a spinning disk confocal system capable of quickly imaging large volumes of samples. The height of acquisition and exposure time were adjusted for each channel to achieve the best focal plane and quality fluorescent signal. The parameters of each channel were adjusted depending on the experiment and genes of interest. The same processing was carried out across samples of a set experiment when possible.

2.13.5. Confocal microscopy.

Confocal microscopy was carried using the Leica TCS SP8 Confocal 4 Detector and Digital LightSheet (DLS). Imaging parameters were adjusted according to each experiment. Parameters that remained constant were the following:

Table. 2.10. Parameters used for confocal microscopy imaging.

Objective lens	10x or 20x (Dry)

Bit depth	16
Format	1024x1024 – 2048x2048
Scanning	Bidirectional
Z-step	1 µm

Gain and laser on the confocal were adjusted for each channel and checked against a negative control. The HiLo LUT on the Leica LAS-X software was used to ensure that images were not being saturated. On the confocal, two sequences were used during imaging, resulting in the simultaneous detection of two channels

Table. 2.11. Sequence of channels used for confocal imaging.

Seq 1	Seq 2
488 & 633	390 & 555

These parameters run through the entirety of the set z stack and allow to minimise any cross excitation between channels during simultaneous acquisition.

2. 13. 6. Quantification of grafted cells in spinal cord tissue slices.

To quantify the number of GFP+ve cells in a spinal cord tissue slice, a macro was created to analyse the grafted samples. The macro will first ask to open the image file selected for analysis. A halo (in pixels) is then defined, which will be used to measure the distance between the neural tube and objects. The macro then first segments the tissue and then will ask to outline the neural tube. From these, it creates a distance map with a maximum halo, as defined. The macro will then segment the grafts as ROIs and measure the brightness of the ROIs on the halo, as well as the area of the grafted cells, allowing to distinguish a large cluster or a single cell. It then calculates the distance between the neural tube and the grafted cells, in pixels and µm. Results are then saved, per image, as a csv table. An image of the distance map where the defined neural tube is superimposed in blue and grafted cells in green is also obtained.

2.13.7. Standards for Image analysis

Images were saved as .tiff files and processed using imageJ. Image processing included adjustment of brightness, contrast, bit-depth, the addition of scale bars and the creation of composite images.

2.14. Statistical analysis.

Data processing and statistical analysis were performed in Microsoft Excel, R and GraphPad. One-way ANOVA was used to compare levels of significance between experimental groups. Multiple comparisons corrections were performed using Bonferroni post hoc tests. Differences were significant at $P \leq 0.05$ and denoted with a single asterisk (*).

Chapter 3. Generation of neural progenitors of different axial identity.

3.1. qPCR on embryo shows expected collinearity and provides a baseline to compare data generated in vitro.

In order to test whether cells of a defined axial position can integrate better at that axial position, it was important to define differentiation conditions that produce cells that replicate expression states found in vivo. Although many Hox gene expression patterns have been characterised via wholemount in situ hybridisation, it was important to quantitate Hox gene expression in vivo at different axial positions at the time of grafting. E10.5 mouse embryos (n=3) were subdissected by Valerie Wilson along the anteroposterior axis and qPCR for a panel of Hox genes was carried out on individual embryo samples. The regions analysed were: forebrain + midbrain + rhombomeres 1-2, rhombomeres 3-8, somites 1-4, somites 5-7, somites 8-12, somites 13-24, somites 25-28 and somites 29 onwards. As expected, the most anterior part of the embryo did not express any of the selected Hox genes. In contrast, the more posterior regions of the embryo expressed progressively more 5' Hox PG members, with the hindbrain samples expressing PG1-2 members Hoxb1 and Hoxb2, and the tail sample expressing the PG12-13 members Hoxc12 and Hoxa13 (Figure 1B).

All Hox genes analysed by qPCR were also screened using the MGI resource (informatics.jax.org) to collect published images showing in situ hybridisation at E10.5 (Morrison et al., 1997, Liu et al., 1999, Zuniga & Zeller., 1999, Oosterveen et al., 2003., Gray, 2004., Yokoyama et al., 2009). The qPCR data was also plotted as a heatmap to allow easier visualisation of the different levels of expression. Anterior limits of expression previously assessed by wholemount in situ hybridisation match the qPCR data. Furthermore, additional aspects of the Hox expression pattern were evident in the qPCR data, for example elevated Hoxb1 expression in the tailbud and the somite29-tail qPCR sample, and high Hoxb8 expression in the somite 5-7 sample, more anterior than Hoxa7 in the somite 8-12 sample. This correlates with published microarrays and single-cell transcriptomics, where HoxB clusters are expressed earlier than HoxA and HoxC clusters in NMPs.

Furthermore, to further characterise the axial identity of generated NPCs I carried out wholemount immunostaining for markers Hoxb4, Hoxc9 and Hoxc13 in mice embryos E10.5 (Figure 3.3). This showed that selected markers are mutually exclusive, indicating different axial boundaries. In summary, this initial quantitative and qualitative assessment allows comparison of Hox expression levels during differentiation *in vitro* to those *in vivo*.

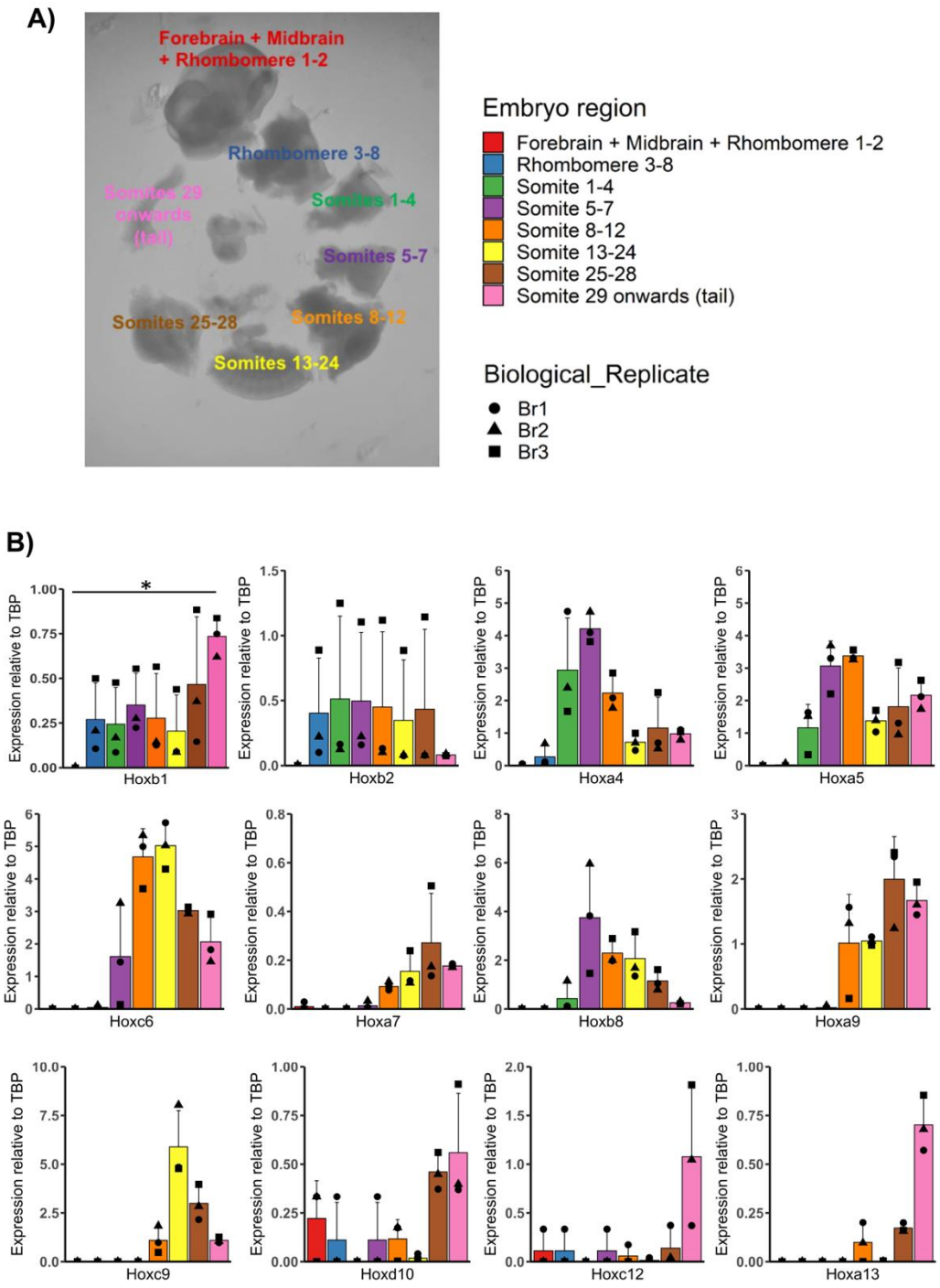

Figure 3. 1. In vivo quantitative standard series of Hox gene expression values.

(A) Dissected regions from a mouse embryo stage E10.5 (B) qPCR analysis for regions subdissected (*p≤0.05) (One-way ANOVA). Error bars represent the standard deviation for 3 biological replicates.

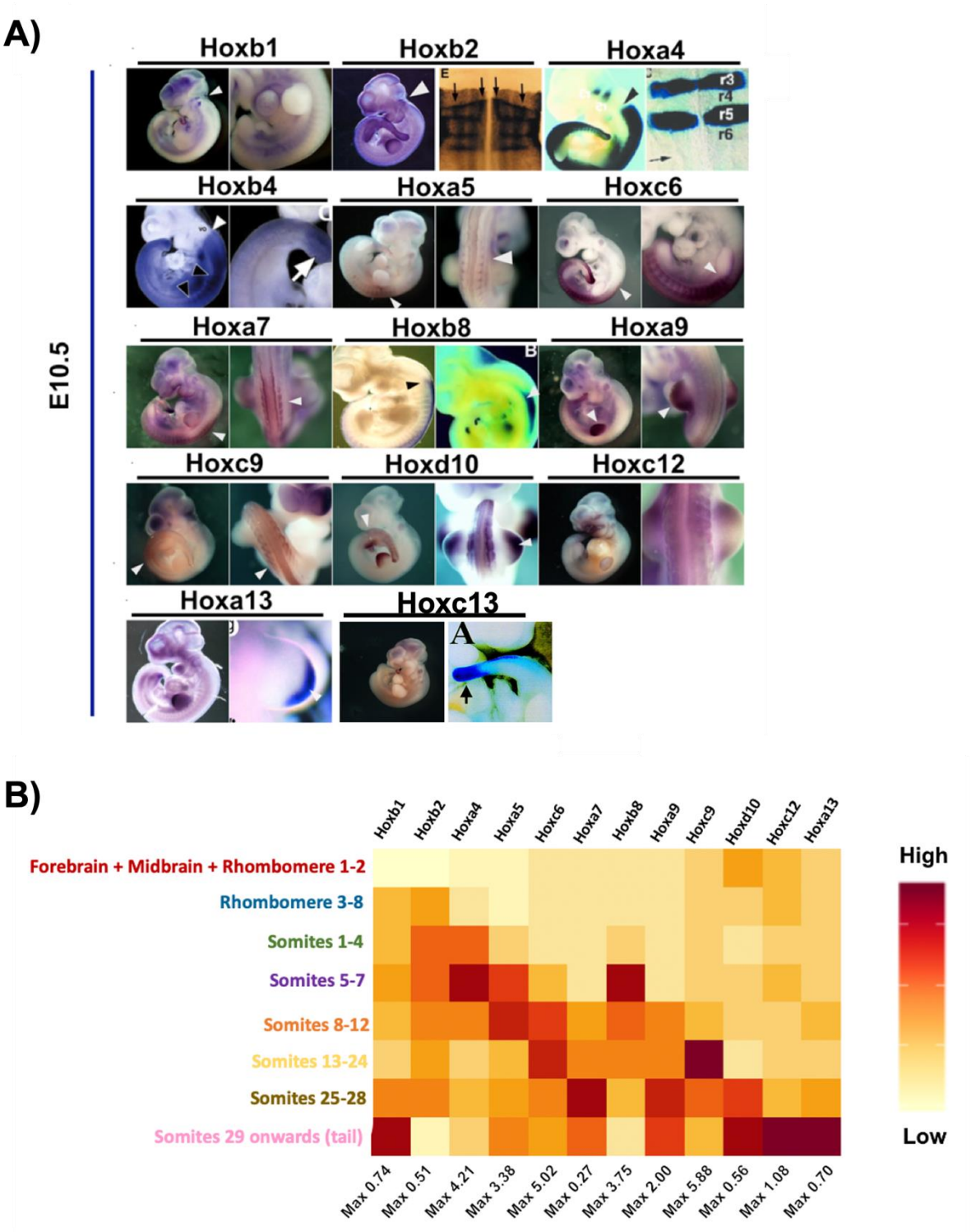

Figure 3. 2. Detection of Hox genes in E10.5 mouse embryos.

(A) In situ hybridization of Hox genes in an E10.5 mouse embryo (Morrison et al., 1997, Liu et al., 1999, Zuniga & Zeller., 1999, Oosterveen et al., 2003., Gray., 2004., Yokoyama et al., 2009) (B) Heatmap showing expression levels of Hox genes across regions of different axial identity. The heatmap is the result of the mean of three biological replicated divided by the standard deviation. Each column has an individual maximum range established from the highest expression value obtained from qPCR across subdissected regions.

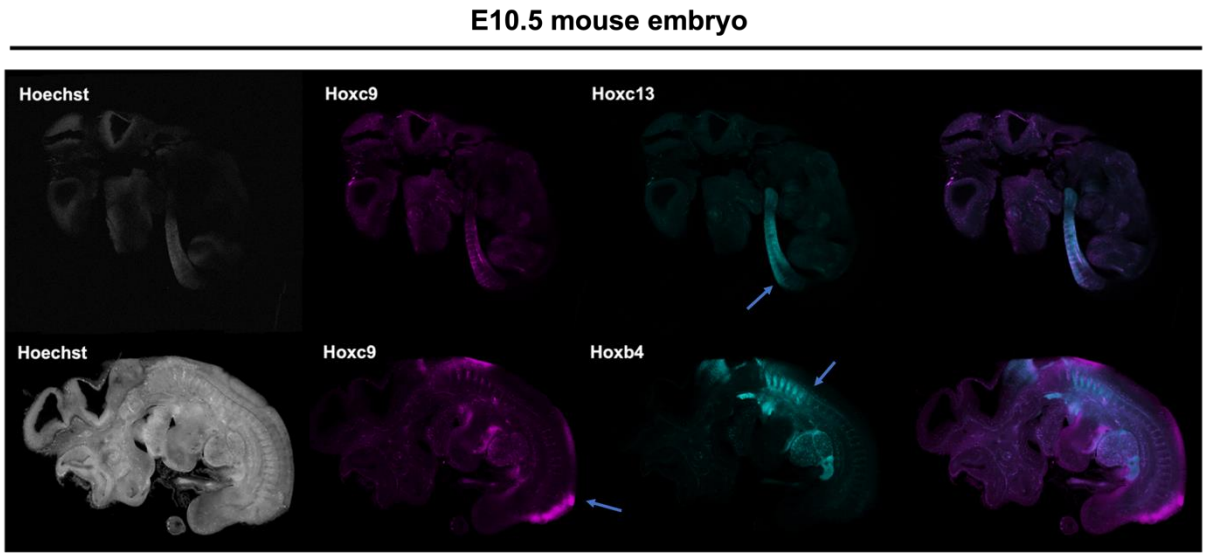

Figure 3. 3. Detection of different axial boundaries in E10.5 mouse embryos.

Wholemount immunostaining for Hoxb4, Hoxc9 and Hoxc13 axial markers of E10.5 embryos treated with clearing solution Rapiclear. The limits of expression for each hox gene are indicated by an arrow.

3.2. Making NA, NH and NS from EpiSCs.

In this section, I describe steps to define a protocol to generate NPCs of different axial identities in a consistent and reproducible manner using the E14Ju09 EpiSC cell line. To determine whether mouse EpiSCs can generate NPCs of different axial identities, I reproduced the protocol described in Gouti et al., 2014, who describes making anterior, hindbrain and spinal cord NPC identities from ESC. However, testing integration in mouse embryos was only performed with EpiSC-derived cells. Since I intended to graft cells in embryos, I decided to test whether EpiSCs could generate these NPC identities. To generate anterior NPCs (NA), EpiSCs were differentiated in standard neural-induction conditions (N2B27). Given the diverse population of cell derivatives that can rise from an NPC differentiation, they were also exposed to Shh agonist (SAG) which restricts NPC differentiation to motor neuron identity. To generate hindbrain NPCs (NH) same conditions are applied, except for the addition of retinoic acid (RA), an intercellular signalling molecule known to guide the development of the posterior portion of the embryo. Finally, to generate NPCs of spinal cord identity (NS), EpiSCs are cultured in NMP inducing conditions (Fgf/Chir) for an initial 48 hours prior to addition of media supplemented with SAG and RA for an additional 48 hours to initiate neural induction. To observe neurite outgrowth cells were then dispersed and replated onto matrigel-coated plates with serum-containing media supplemented with bFGF, which improves cell survival following replating. After 24h, the bFGF is removed, and cells remain in culture for an additional 3 days in basal media (Figure 3.4 A). To assess the axial identities of each condition, I carried out qPCR across the panel of Hox genes that had been calibrated against the embryo in section 3.1. Results were consistent with those published by Gouti et al., 2014 NPCs. Cells which had undergone NMP induction expressed higher levels of all selected Hox genes with exception of anterior Hox gene Hoxb1, expressed significantly higher in NA cells in comparison to NH and NS cells. NH cells showed upregulation of genes associated with hindbrain identity, such as Hoxb2 and Hoxa4; however, markers of spinal regions such as Hoxc6, Hoxa7, Hoxb8, Hoxa9 and Hoxc9 were barely detected. In summary, these results indicate that it is possible to generate NPCs of specific anterior (NA), Hindbrain (NH) and Spinal cord identity (NS) from mouse EpiSCs (Figure 3.4 B).

To determine the axial identity of the derived cultures at single cell protein level, I carried out ICC by staining cells with antibodies against Hoxb4 and Hoxc9. The neural

phenotype was also assessed using antibodies against Tub III. ICC shows cells positive for Tub III for all conditions, with higher numbers of cells positive for NH and NS cultures (Figure 3.4 C). The E14Ju09 EpiSC line showed to be heterogeneous, with no cells from NH cultures being positive for Hoxb4 or Hoxc9. NA cells also show an unexpected presence of cells positive for Hoxc9 and no cells positive for Hoxb4. On the other hand, NS cells show the presence of Hoxb4 and Hoxc9+ve cells matching the qPCR data and describing the same observation observed by Gouti et al., 2014. Expression of Hoxc9 in NA cells suggests that EpiSCs produce heterogeneous cultures that may be primed to express a posterior axial identity.

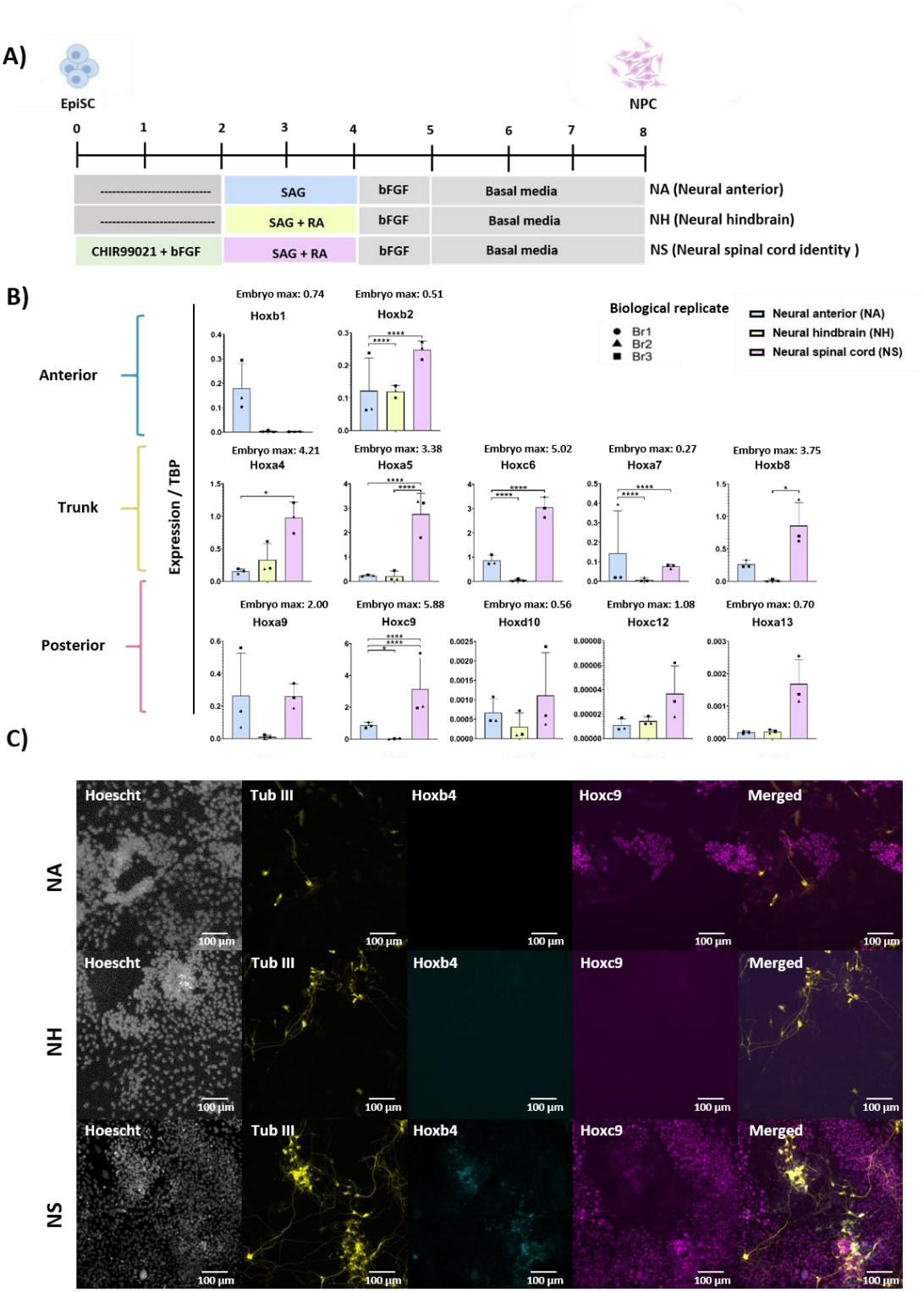

Figure 3. 4. Characterization of NPCs of different axial identities from the E14Ju09 EpiSC cell line.

(A) Schematic representation of differentiation conditions used for the generation of NPCs with specific Anterior (NA), Hindbrain (NH) and spinal cord (NP) identities from the E14Ju09 EpiSC cell line (B) qPCR analysis for NPCs with specific Anterior (NA), Hindbrain (NH) and spinal cord (NP) identities. Results are represented as values relative to housekeeping gene TBP (*p≤0.05, ***p≤0.001, ****p≤0.0001) (One-way ANOVA). Error bars represent the standard deviation for 3 biological replicates with 3 loading replicates each. Maximum expression levels detected in vivo for each Hox gene are shown above each qPCR plot, respectively. C) ICC staining for Tub III, Hoxb4 and Hoxc9 in NPCs of Anterior (NA), Hindbrain (NH) and spinal cord (NP) identities

3.3. NMP substrate does not affect NPC differentiation.

The protocol described in Gouti et al., 2014 generated NPCs of specific anterior (NA), hindbrain (NH) and Spinal cord identity (NS). However, the resulting cultures showed heterogenous axial identities, and the most posterior sacral motor neurons (PG11-13) were not produced. Therefore, further optimisation of these protocols may overcome these challenges. Unpublished preliminary data from the lab suggested that cells cultured in NMP media could be maintained for several days in a 3D suspension using Matrigel, resulting in posterior Hox genes (PG10-13) being induced. Matrigel is a basement membrane rich in extracellular matrix proteins, including laminin, collagen IV known for its capacity to recreate more in vivo-like environments for 2D and 3D cell culture applications. Matrigel may be able to provide an environment which resembles the NMP niche; therefore, by allowing cells to grow in conditions like those found in vivo, we might be able to induce the expression of sacral PG groups. To test the effects of cell-substrate on Hox gene expression in NPCs, I cultured NMPs in either fibronectin or matrigel and continued with the previously described protocol (refer to section 3.2 to generate spinal cord derivatives and figure 3.5 A). Gene expression for selected markers was assessed using qPCR, and efficient generation of NPCs was determined by ICC. Overall, the expression levels for most selected Hox genes were comparable in fibronectin and matrigel. This suggests that it is not the Matrigel components per se that allow posterior Hox expression (Figure 3.5 B).

As previously mentioned, RA is an intercellular signalling molecule known to guide the development of the posterior portion of the embryo and to induce neural differentiation (Zhao et al., 2009). However, the effects of adding RA to cultures already showing posterior axial identity remain unclear. Although the presumption in Gouti 2014 is that RA cannot posteriorise neural cultures beyond hindbrain level, it has not been formally shown that RA is acting independently of NMP induction, ie that RA has no posteriorising effect on NMPs, as opposed to anterior neural progenitors. To further test the effects of RA on derived NPC cultures, NMPs cultured in either fibronectin or matrigel were exposed to media containing SAG alone or supplemented with RA prior to being replated. No major differences for gene expression were found, although Hoxc6 and Hoxb8 were increased in matrigel cultures supplemented with RA versus those treated with SAG alone. On the other hand, Hoxa9 was increased in fibronectin cultures lacking RA in comparison to those with it (Figure 3.5 B). However, neither

matrigel nor RA generated NPCs with expression of PG10-13 Hox genes at levels seen in the embryo.

To determine the axial identity of the derived cultures at protein level and the efficiency of NPC differentiation, I carried out ICC by staining cells for Hoxb4, Hoxc9 and Tub III. All conditions show the presence of cells positive for Tub III, showing no visual differences between cultures grown in matrigel and in fibronectin. Cultures derived in each condition show cells positive for Hoxc9, confirming the presence of a thoracic identity (Figure 3.5 C). However, Hoxb4 levels seemed higher in cultures supplemented with SAG alone versus those supplemented with RA. The reason for this difference is unclear.

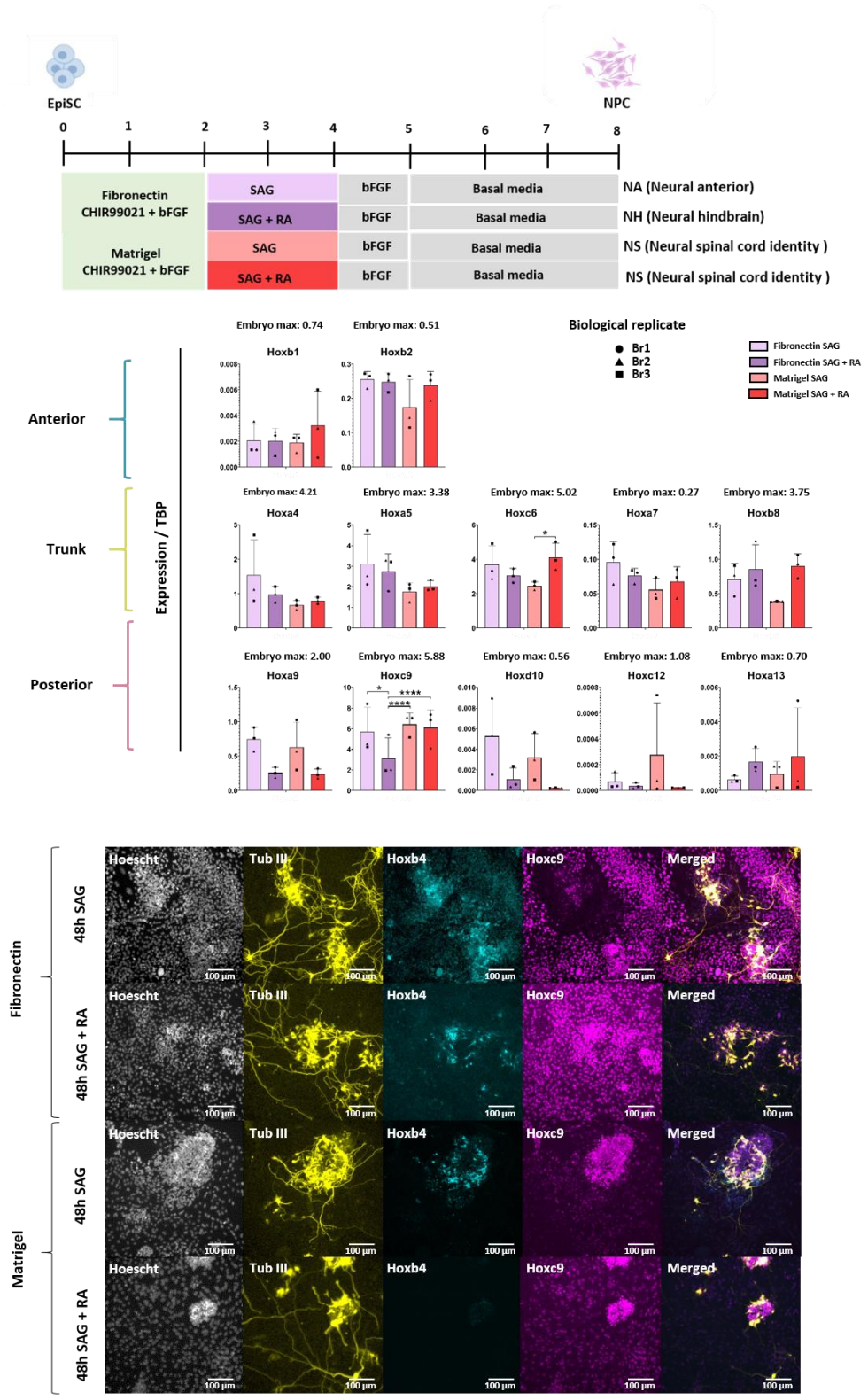

Figure 3. 5. Effects of cell substrate on NPC posteriorisation.

A) Schematic representation of NPC differentiation on different culture substrates from the E14Ju09 EpiSC cell line (B) qPCR analysis for NPCs of spinal cord (NP) identities cultured on Fibronectin and matrigel. Results are represented as values relative to housekeeping gene TBP (*p≤0.05, ****p≤0.0001) (One-way ANOVA). Error bars represent the standard deviation for 3 biological replicates with 3 loading replicates each. Maximum expression levels detected in vivo for each Hox gene are shown above each qPCR plot, respectively. C) ICC staining for Tub III, Hoxb4 and Hoxc9 in NPCs of spinal cord (NP) identities cultured on Fibronectin and matrigel.

3.4. Length of NMP culture does not posteriorize NPCs.

I have shown that extending the culture of NMPs in fibronectin and the culture of NMPs in matrigel are not factors which lead to the induction of the most posterior PG groups. However, I have yet to test whether extending the culture of NMPs prior to neural differentiation has any effects on the Hox gene expression or the efficiency of produced NPCs. To test this, I extended the culture of EpiSCs in NMP media from 48 hours to 72 and 96 hours, a period that mirrors the in vivo NMP induction around E7.0 until the appearance of posterior Hox gene expression around E10.5. In addition, to reach a conclusion about the role of RA after NMP induction in the generation of NPCs, cultured cells were treated with SAG alone or supplemented with RA to determine any effects on gene expression, number, or morphology. Gene expression was assessed using qPCR, showing similar levels of expression across cultures, once again achieving apparently physiological levels of Hox genes up to PG9, but not PG10-13. In addition, no noticeable differences are observed in cultures with or without RA.

These findings are further supported by ICC for Hoxb4, Hoxc9 and Tub III. Cultures show the presence of Hoxc9 positive cells, with a higher number of Hoxb4 positive cells being observed in cultures without RA. Overall, it suggests extending the culture of NMPs in vitro on matrigel up to 96 hours with/without RA prior to neurulation does not induce the expression of the most posterior Hox genes. All described protocols can generate NPCs determined by the presence of Tub III cells. However, the ratio of generated NPCs appears to be lower than those observed by Gouti et al., 2014. The highest number of NPCs generated was observed in cells which remained longest in culture and thus became most confluent, which suggested that cell density might be important in the generation of optimal proportions of NPCs.

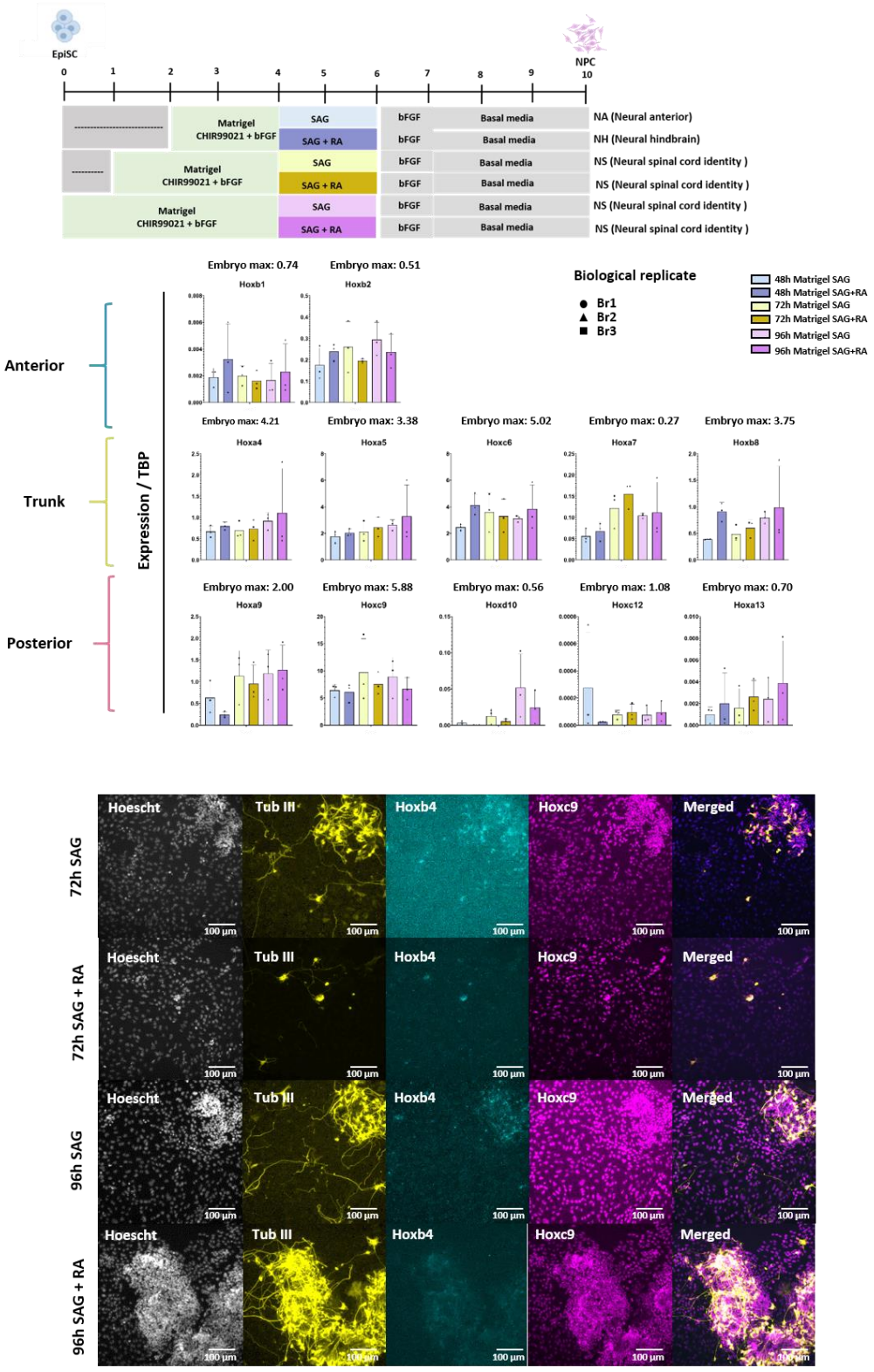

Figure 3. 6. Effects of prolonging NMP differentiation on NPC posteriorisation.

A) Schematic representation of posterior NPC differentiation with a prolonged NMP culture of 72h and 96h from the E14Ju09 EpiSC cell line (B) qPCR analysis for posterior NPCs with an NMP intermediate step at 48h, 72h and 96h. Results are represented as values relative to housekeeping gene TBP (One-way ANOVA). Error bars represent the standard deviation for 3 biological replicates with 3 loading replicates each. Maximum expression levels detected in vivo for each Hox gene are shown above each qPCR plot, respectively. C) ICC staining for Tub III, Hoxb4 and Hoxc9 of posterior NPC differentiation with a prolonged NMP culture of 72h and 96h.

3.5. Cell density has a direct impact on the number and neurite length of cultured NPCs.

To determine whether cell density affects NPC generation, I plated cells after neural induction in each condition at two different densities: low (10,000 cells/cm^2) and high (20,000 cells/cm^2). I carried out ICC and stained cells for Tub III and islet1 to determine the number of NPCs and motor neuron progenitors. At the higher cell density, more colonies formed, which coincided with dense areas positive for Tub III and islet1. This was observed across all cultures independently of the condition used. This suggests that cell density plays an important role in favouring NPC differentiation.

As mentioned, RA drives the posteriorisation of cells from a head (anterior) identity towards a hindbrain (posterior) identity; however, we are also uncertain whether this "push" results in NPCs becoming more mature, potentially explaining the lack of Hoxb4+ve cells in cultures supplemented with RA. To test this, I used a computer analysis tool known as simple neurite tracer and manually measured the length of axons in low and high-density cultures in the presence and absence of RA. This will also allow me to assess whether there are any morphological differences (length of axons) between cultures plated at low and high densities. The data shows that the length of axons between conditions with and without RA is very similar. On the other hand, longer axons formed in high- versus low-density cultures. This suggests that paracrine effects operate to enhance NPC differentiation.

I next compared the effects of cell density in cultures plated on fibronectin and matrigel. Similar to the results above, there were more NPCs in high-cell-density cultures. However, there are visual differences between NPCs grown in fibronectin and those grown in matrigel. With NPCs grown in fibronectin show loose and unorganized structures, while those grown in matrigel show nest-like structures with a higher degree of complexity resembling a neural network as those observed in vivo. This suggests that matrigel is a better substrate on which to culture NPCs for grafting.

Finally, to determine the effects of RA over prolonged periods of time on NPC efficiency and potential changes in morphology, I carried out ICC for Tub III and islet1 and recorded axonal length in the derived cultures. As previously shown, cell colonies are most prominent in cultures plated at high cell densities. However, colonies are also observed in low-density cultures extended for 96 hours. The colonies continue to be sites where a high number of cells expressing Tub III are found. At high cell densities,

NPCs in extended culture continue to show nest-like structures with a higher degree of complexity resembling those of neural networks. Across all conditions described so far length of axons remains to show no major differences, and the presence of Islet1 is barely observed. This suggests that cell density and substrate are the two major factors which contribute to generating higher numbers of NPCs which resemble those found in vivo.

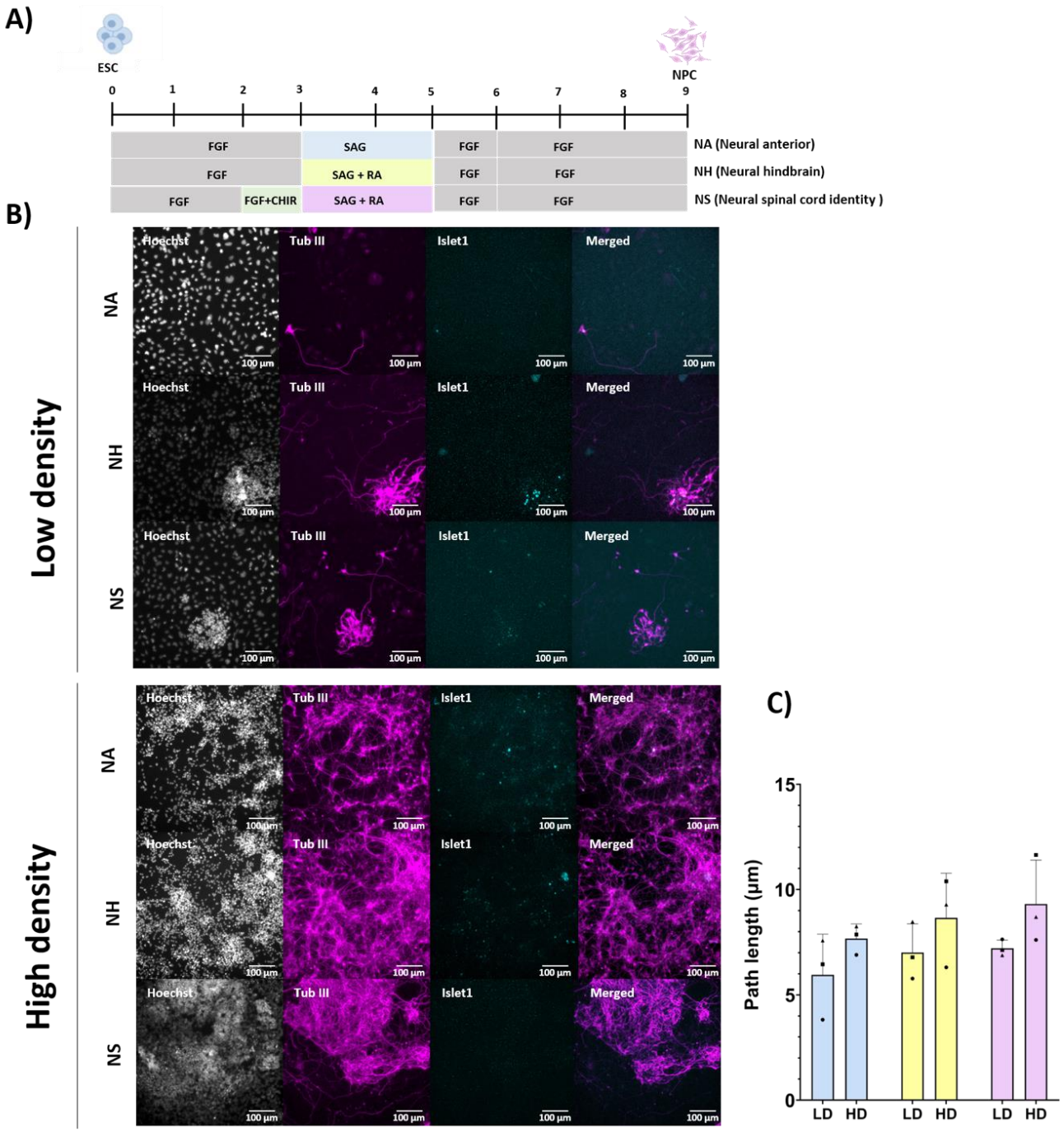

Figure 3. 7. Determining the importance of cell plating density on the generation of NPCs.

(A) ICC stained for Tub III and Islet1 for NPCs of anterior (NA), hindbrain (NH) and spinal cord (NS) identity cultured at low and high cel plating densities (B) Quantification of Tub III $^{+}$, Islet1^{+} and Tub III $^{+}$Islet1^{+} cells at low and high plating densities. DAPI was used as a nuclear counterstain. Error bars represent the standard deviation for 3 biological replicates.

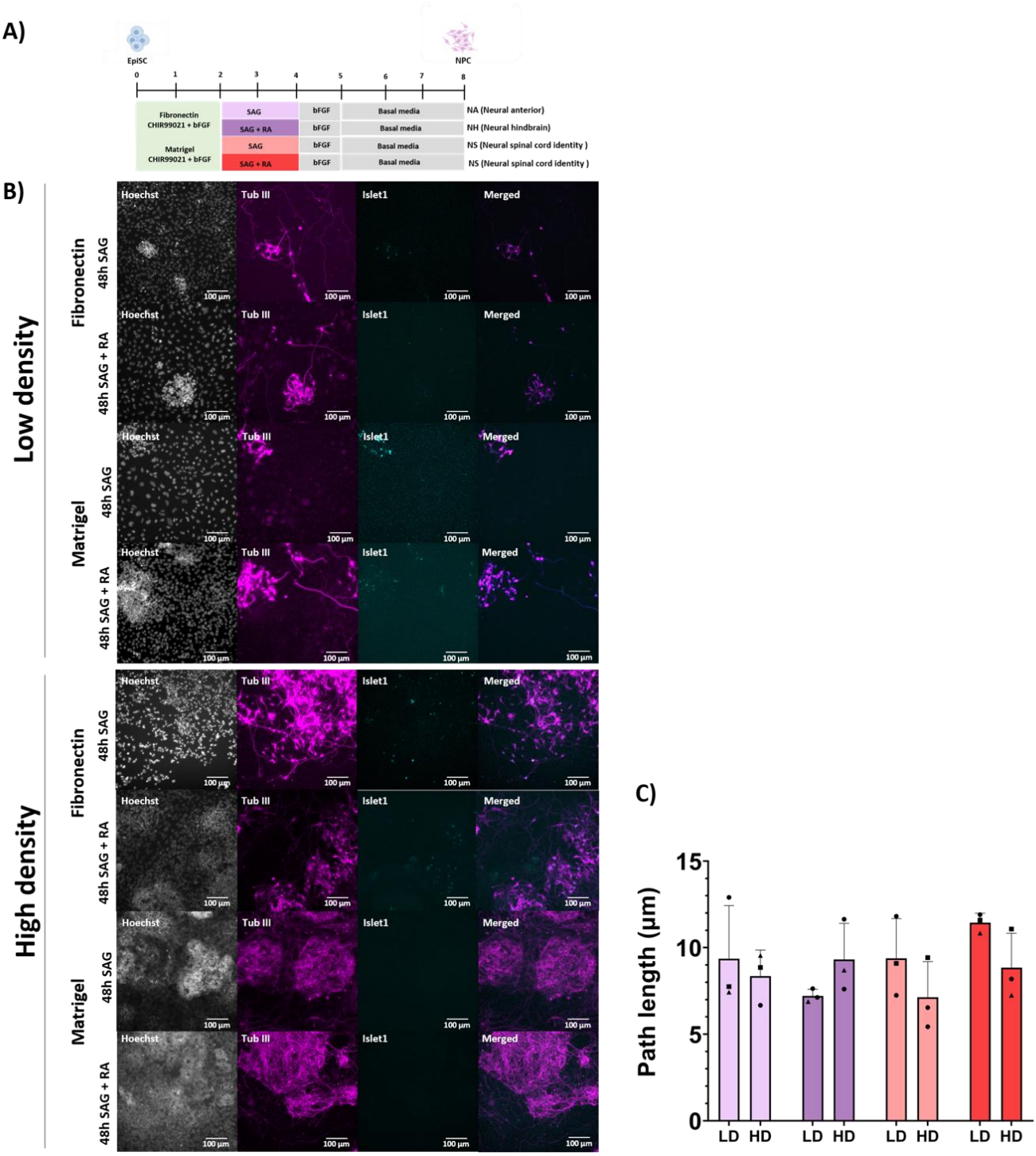

Figure 3. 8. Exploring the importance of cell-matrix in the generation of NPCs at low and high plating densities.

(A) ICC stained for Tub III and Islet1 for NPCs of spinal cord (NP) identities cultured on Fibronectin and matrigel at low and high cell plating densities (B) Quantification of Tub III^{+}, Islet1^{+} and Tub III^{+}Islet1^{+} of mentioned cultures. DAPI was used as a nuclear counterstain. Error bars represent the standard deviation for 3 biological replicates.

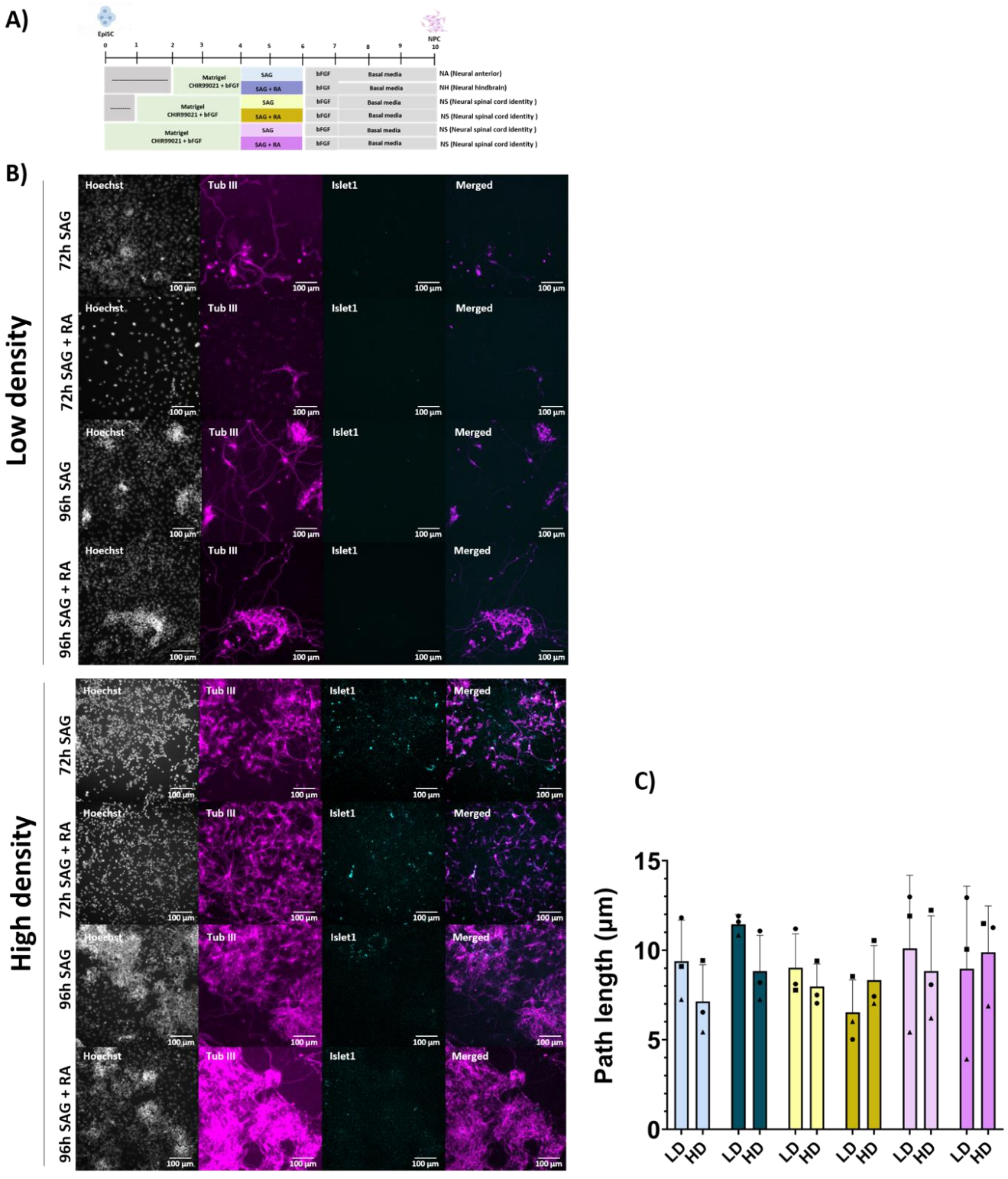

Figure 3. 9. Exploring the effects of prolonging NMP differentiation in the generation of NPCs plated at low and high plating densities.

(A) ICC stained for Tub III and Islet1 in posterior NPC cultures with a prolonged NMP culture of 72h and 96h at low and high cell plating densities (B) Quantification of Tub III $^{+}$, Islet1^{+} and Tub III $^{+}$Islet1^{+} cells at low and high plating densities DAPI was used as a nuclear counterstain. Error bars represent the standard deviation for 3 biological replicates.

3.6. Making NPCs of different axial identities using R4-cell line.

I have shown using the wildtype EpiSC cell line E14Ju09 that it is possible to generate NPCs of specific anterior (NA), Hindbrain (NH) and Spinal cord identity (NS) following the protocol described in Gouti et al., 2014. However, one of the major aims of the project is to graft NPCs of different axial identities into different homotopic and heterotopic sites. Therefore, to be able to track these cells, I tested an EpiSC line containing a GFP reporter. The R4 cell line was more homogeneous in culture than E14Ju09. It generated a higher proportion of NMPs with no cells negative for both Sox2 and Tbra. Neural differentiation of R4 EpiSCs was carried out in the conditions optimised above using E14Ju09 (Figure 3.10). Hox gene expression was measured using qPCR and ICC performed following the same parameters as previously described. qPCR showed that neural anterior (NA) cultures express PG1-2 Hox but not PGs posterior to these. Neural hindbrain (NH) express markers up to PG7; with low (non-physiological) expression of PG8-13. Neural spinal cord (NS) cultures showed expression up to PG9 but not PG10-13.

In addition, the role of RA after NMP induction was explored once again to determine that the effects observed are consistent across cell lines. I cultured spinal cord cells (NS) in the absence and presence of RA. No significant difference between these conditions was detected (*p≤0.05), although it remains possible that RA has a small positive effect on Hox expression (Fig. 3.10. B).

ICC further validated the specific axial and neural identity of cultured NPCs. Cultures were stained for Tub III, Hoxb4 and Hoxc9. It is possible to observe a strong presence of Tub III, across all different conditions. Neural anterior (NA) cultures showed no cells positive for Hoxb4 and Hoxc9 markers. Neural hindbrain (NH) cells showed a high number of Hoxb4+ cells and no cells positive for Hoxc9, indicating the presence of cells of a cervical identity. The neural spinal cord (NS) cultures showed few Hoxb4+ cells and many Hoxc9+ cells. Therefore, we consider thoracic identity only occurs in NPCs after NMP induction. In addition, when compared to the E14 Ju09 cell line, NA-derived cultures do not show cells positive for Hoxc9, demonstrating characteristic cell line-specific gene expression in addition to differences in heterogeneity.

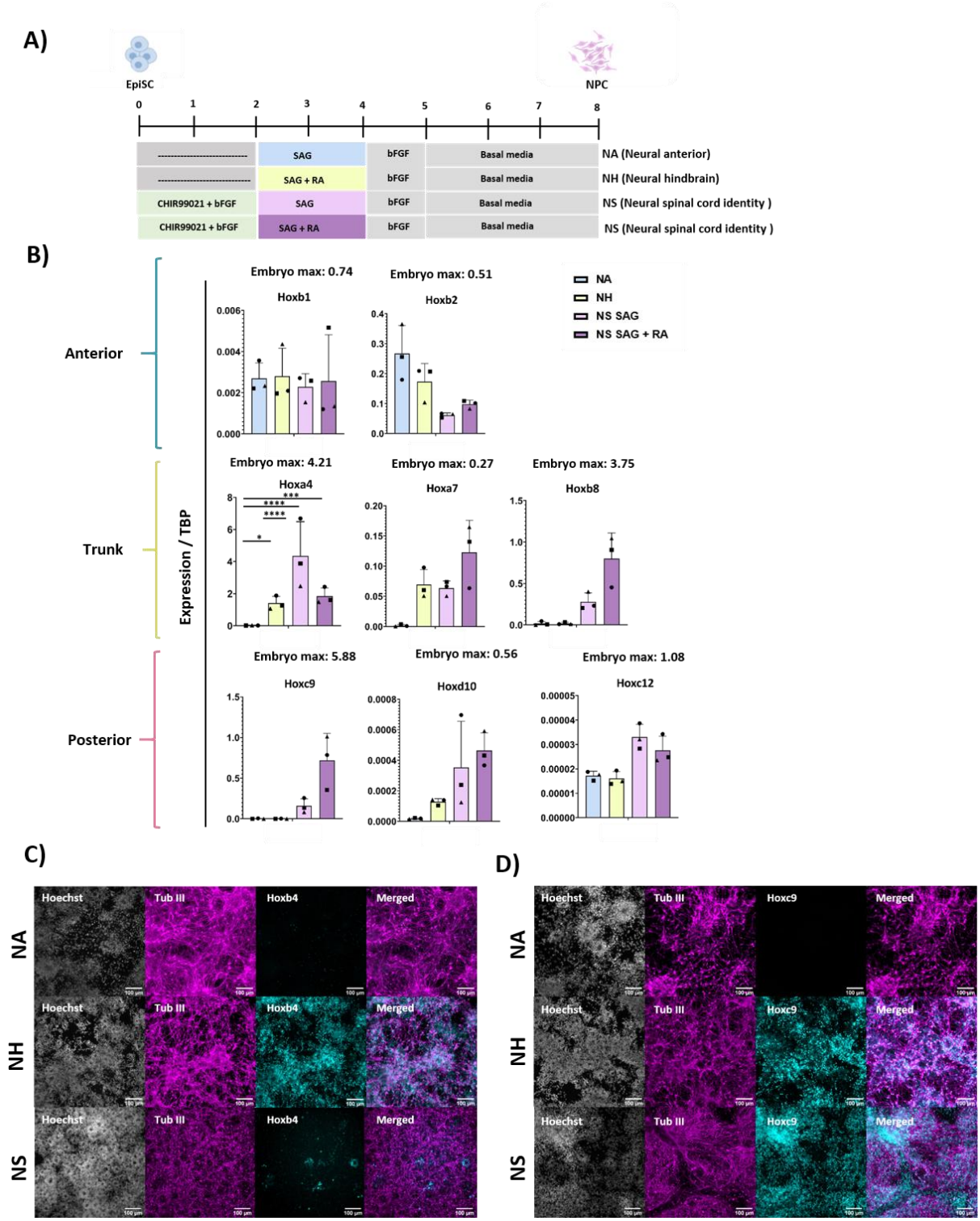

Figure 3. 10. Characterization of NPCs of different axial identity using the R4-EpiSC cell line.

(A) Schematic representation of differentiation conditions used for the generation of NPCs with specific Anterior (NA), Hindbrain (NH) and spinal cord (NP) identities from the R4-EpiSC cell line. (B) qPCR analysis for NPCs with specific Anterior (NA), Hindbrain (NH) and spinal cord (NP) identities. Results are represented as values relative to housekeeping gene TBP (*p≤0.05, ***p≤0.001, ****p≤0.0001) (One-way ANOVA). Error bars represent the standard deviation for 3 biological replicates with 3 loading replicates each. Maximum expression levels detected in vivo for each Hox gene are shown above each qPCR plot, respectively. C) ICC staining for Tub III and Hoxb4 D) ICC staining for Tub III and Hoxc9 in NPCs of Anterior (NA), Hindbrain (NH) and spinal cord (NP) identities.

3.7. NPCs generated from ESCs are comparable to those obtained with EpiSCs.

To compare ESC-derived NPCs with those derived from EpiSCs, I repeated the conditions I have described in section 3.3-3.6 using the E14Ju09 ESC cell line. The differentiation protocol to generate NPCs were the same as those described for EpiSCs, with the exception that cells were plated in N2B27 media supplemented with bFGF for an initial 48 hours prior to NMP induction for 24 hours. The Hox gene expression and neural phenotype of the resulting cultures were assessed using qPCR and ICC. Results were comparable to those shown generated using EpiSCs, Neural anterior (NA) cultures showed expression of PG1-2 Hox only. Neural hindbrain (NH) shows expression of anterior and trunk markers up to hoxa5 with low expression of posterior paralog groups. This appears to be different from cultures derived from EpiSCs, where NH cultures express the PG7 gene Hoxa7. In addition, expression levels of Hoxb4 in NPC cultures derived from EpiSCs were higher than ESCs. Neural spinal cord (NS) cultures expressed Hox genes of PG1-9 but not PG10-13. The addition of RA to cultures following NMP induction showed no major differences in selected marker expression, with the exception that RA increased the expression of Hoxc6.

ICC further validated the specific axial and neural identity of cultured NPCs. Cultures were stained for Tub III, Hoxb4 and Hoxc9. Tub III immunostaining was present in all conditions. Neural anterior (NA) cultures showed few cells positive for Hoxb4 and Hoxc9 markers. Neural hindbrain (NH) cultures contained many Hoxb4+ cells and some cells positive for Hoxc9. The neural spinal cord (NS) cultures showed few Hoxb4+ cells and many Hoxc9+ cells (Fig. 5A & B).

In summary, compared to the R4 cell line, NPCs derived from EpiSCs can generate differentiated neurons which are comparable to those generated from ESCs (Gouti et al., 2014); those generated from E14Ju09 are more heterogeneous, obscuring some of the inductive effects seen in ESCs and R4 EpiSCs.

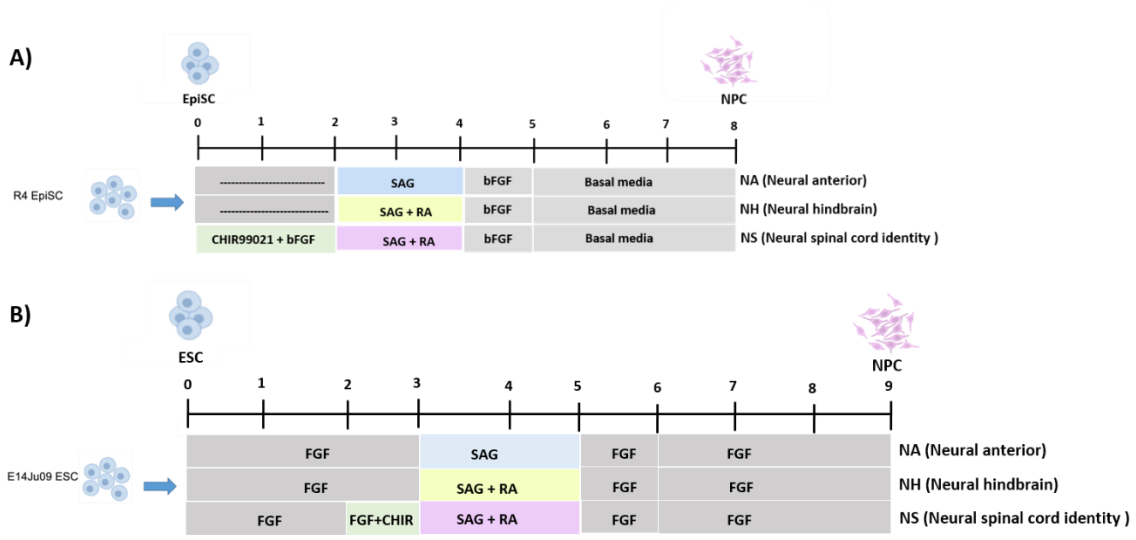

Figure 3. 11. Culture differences in the generation of NPCs using ESCs and EpiSCs.

Schematic representation of differentiation conditions used for the generation of NPCs with specific Anterior (NA), Hindbrain (NH) and spinal cord (NP) identities from A) EpiSCs and B) ESCs.

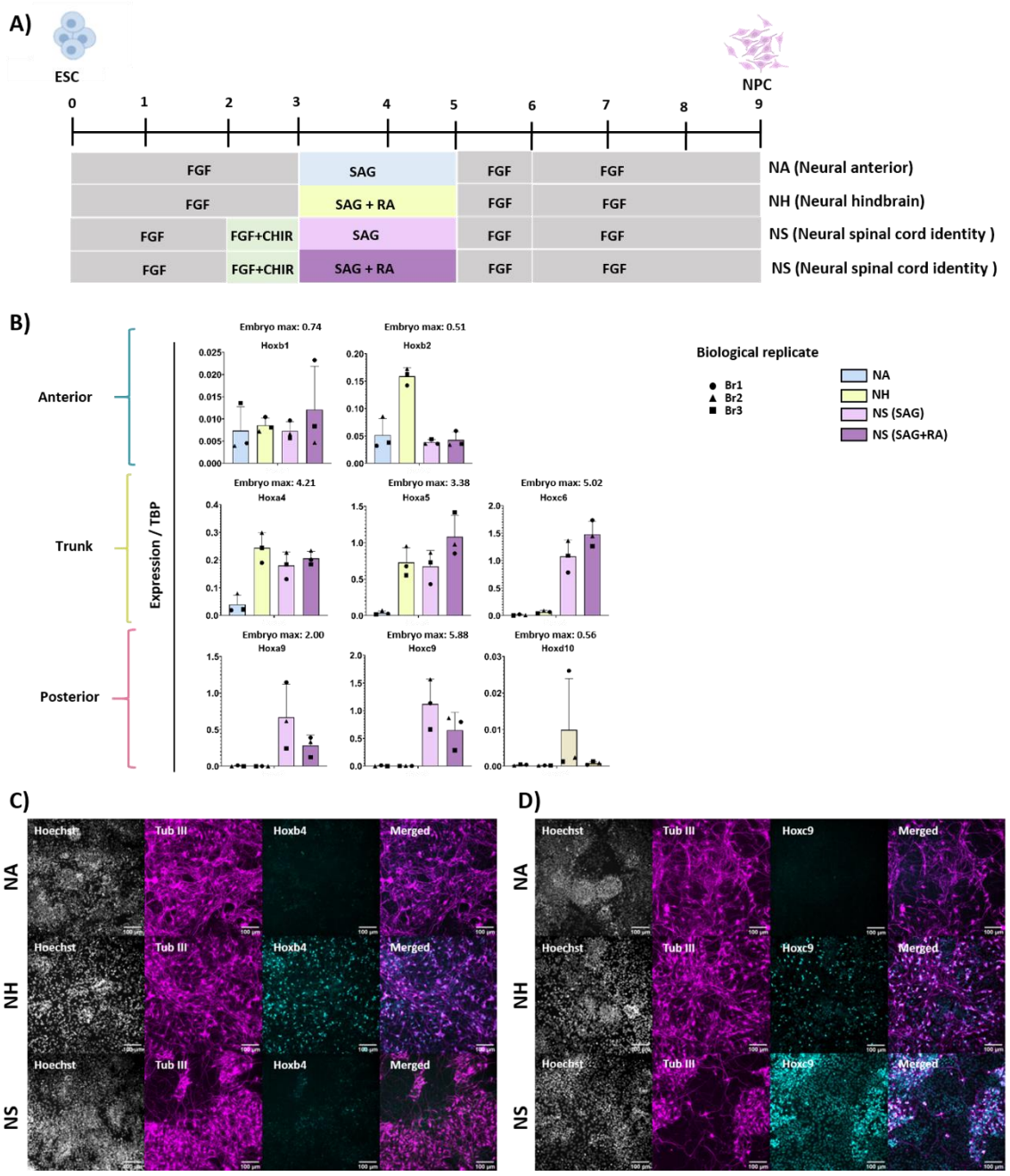

Figure 3. 12. Characterization of NPCs of different axial identity from the E14Ju09 ESC cell line.

(A) Schematic representation of differentiation conditions used for the generation of NPCs with specific Anterior (NA), Hindbrain (NH) and spinal cord (NP) identities from the E14Ju09 ESC cell line. (B) qPCR analysis for NPCs with specific Anterior (NA), Hindbrain (NH) and spinal cord (NP) identities. Results are represented as values relative to housekeeping gene TBP (One-way ANOVA). Error bars represent the standard deviation for 3 biological replicates with 3 loading replicates each. Maximum expression levels detected in vivo for each Hox gene are shown above each qPCR plot, respectively. C) ICC staining for Tub III and Hoxb4 D) ICC staining for Tub III and Hoxc9 in NPCs of Anterior (NA), Hindbrain (NH) and spinal cord (NP) identities

3.8. Validating the axial identity of pre-neural progenitor cells prior to grafting.

I have shown that generating NPCs of different axial identities is possible using ESCs and EpiSCs in two different cell lines. However, NPCs in cultures without growth factors will continue their developmental clock. Therefore, it is important to match not only their regional but also their temporal identities. This is a difficult task as matching cells cultured *in vitro* to an *in vivo* model is challenging as many factors that cannot be replicated in a culture environment come into play. The following considerations suggest that embryos at E10.5 are suitable for grafting. An embryo at this stage has around 30-35 somites and shows the expression of all PGs. Before this stage of development, expression of PG13 Hox genes is not detectable. The embryo at E10.5 has a spinal cord that includes caudal regions, but neurite outgrowth from the spinal cord has not begun. Finally, embryos at this stage can be cultured for 24 hours to assess integration and neural differentiation. The lack of axon outgrowth in E10.5 embryos suggests that grafting cells that have undergone neural induction in culture (addition of SAG and RA) without neural differentiation culture would provide an optimal match between the grafted cells and host embryos. I therefore assessed the axial identity of NPCs prior to neural differentiation.

NPCs of different axial identities were generated following the protocol previously described. However, the differentiation protocol only extended until day four after cells had been exposed to neuralising signals SAG or SAG and RA for 48 hours (Figure 3.13). Gene expression was measured using qPCR for selected Hox markers for each tested condition. Results showed the same Hox expression patterns as cells cultured for 8 days.

ICC further validated the specific axial and neural identity of cultured NPCs. Cultures were stained for Tub III, Hoxb4 and Hoxc9. The results shown are very similar to those in figure 3.12. It is possible to observe a presence of Tub III across all different conditions. Neural anterior (NA) cultures showed no cells positive for Hoxb4 and Hoxc9 markers. Neural hindbrain (NH) cells showed a high number of Hoxb4+ cells and no cells positive for Hoxc9, indicating the presence of cells of a cervical identity. The neural spinal cord (NS) cultures showed few Hoxb4+ cells and many Hoxc9+ cells. Therefore, we consider thoracic identity only occurs in NPCs after NMP induction (Fig. 3.13. C, D).

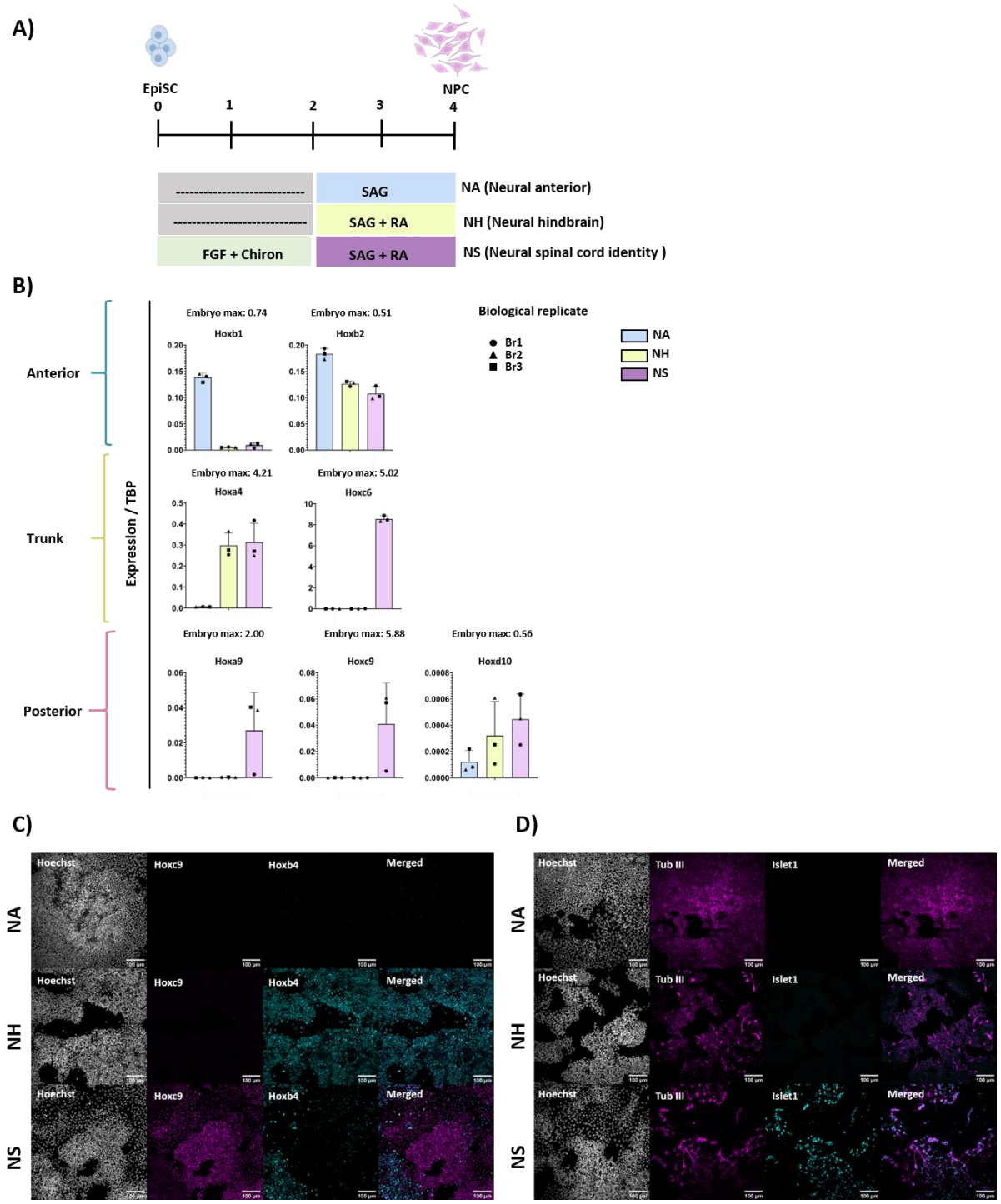

Figure 3. 13. Characterization of NPCs of different axial identity after neural induction for 48 hours.

(A) Schematic representation of differentiation conditions used to generate NPCs with specific Anterior (NA), Hindbrain (NH) and spinal cord (NP) from the R4-EpiSC cell line used to be transplanted at homotopic and heterotopic sites. (B) qPCR analysis for NPCs with specific Anterior (NA), Hindbrain (NH) and spinal cord (NP) identities at D4 of differentiation. Results are represented as values relative to housekeeping gene TBP (One-way ANOVA). Error bars represent the standard deviation for 3 biological replicates with 3 loading replicates each. Maximum expression levels detected in vivo for each Hox gene are shown above each qPCR plot, respectively. C) ICC staining for Tub III and Hoxb4 D) ICC staining for Tub III and Hoxc9 in NPCs of Anterior (NA), Hindbrain (NH) and spinal cord (NP) identities at D4.

3. 9. General discussion.

In this chapter, I have demonstrated that EpiSCs can be used to generate neural progenitor cells of anterior, hindbrain and cervico-thoracic spinal cord identities. Kojima et al. 2014 concluded from bulk RNA-seq analyses that EpiSCs have a posterior epiblast/primitive streak identity; I show that regardless of the characteristics mentioned, generation of anterior neural NPCs was just as efficient as posterior ones, suggesting either extensive EpiSC plasticity or that a subpopulation of EpiSCs has robust potential for anterior neural identity.

The primary objective of generating homogenous and reproducible protocols of different axial is to be used in transplantation studies to assess the importance of axial identity and determine whether they show differences in functional integration, including survival, neurite outgrowth and pathfinding. As a proof of concept, NPCs of anterior and posterior CNS identity will be grafted at different levels of the anteroposterior axis. Therefore, it is important to match expression levels observed in vivo to those in vitro to reduce the variability of factors and ensure the highest probabilities of success. Therefore, I wanted to be able to determine whether our cultures were expressing Hox genes to physiological levels seen in vivo. Therefore, we dissected an embryo into different segments along the antero-posterior axis and we performed qPCR to generate an in vivo quantitative standard of Hox gene expression (Figure 3.1). Interestingly Hoxb8 expression was found to be expressed more anteriorly than Hoxa7. This correlates with microarray analysis Wymeersch et al., 2019 in the tail bud which showed that HoxB cluster genes were activated earlier than their corresponding PG members in other clusters. Taken together with my observations, this suggests a cluster-specific correspondence between spatial and temporal collinearity.

The protocol used to generate cells of different axial in identity Gouti et al., 2014 uses either SAG alone to generate anterior identity, or in addition with RA to generate cells of a hindbrain identity. RA is an intercellular signalling molecule essential in patterning of the hindbrain and in organogenesis (Belle et al., 1990). However, the effects of adding RA to cultures already showing posterior axial identity remain unclear. The data generated from the E14Ju09 EpiSC cell line in figure 3.5 shows that cultures

treated in addition to RA after NMP differentiation show no major differences in gene expression. However, the same treatment on cultures derived from the R4 cell line (Figure 3.10) shows that treatment of RA increases Hox gene expression in late cervical markers Hoxa7 and Hoxb8, and posterior marker Hoxc9. These differences could be due to two alternative hypotheses. A) There are higher levels of heterogeneity in the e14Ju09 EpiSC cell line making it hard to see an RA effect on a subpopulation, or B) a genetic or epigenetic change in the whole population, as a result of the different ways in which the lines were derived, meaning that one line (R4) is RA responsive and the other one is not (E14Ju09). It would be interesting to compare both cells line by single-cell or bulk sequencing to observe any upregulated or downregulated genes that could explain these differences.

To generate NPCs of specific anterior (NA), hindbrain (NH) and Spinal cord identity (NS) Gouti et al., 2014 used mouse embryonic stem cells (mESCs) as a starting population to generate spinal cord derivatives by adding an NMP-intermediated step in a neural induction protocol. However, the authors did not show whether this could be replicated using mouse epiblast stem cells (EpiSCs). In contrast to ESCs, EpiSCs incorporate well and give rise to tissue of all three germ layers when introduced into post-implantation embryos (Huang *et al*., 2011). This grafting work, along with gene expression analysis and teratocarcinoma assay (Tesar *et al*., 2007), has highlighted the pluripotency and functional equivalence of EpiSCs to the post-implantation epiblast.

In contrast, no directly equivalent test has been reported from ESC-derived NMPs. In addition, work from the lab of Alfonso Martinez Arias suggests that NMPs derived from ESCs are phenotypically different from those derived from EpiSCs, which closely resemble those found in vivo (Edri et al., 2019b). In addition, this study shows that NMP differentiation from ESCs leads to heterogeneous progenitor populations with few NMP-like cells, whereas starting with EpiSCs yields a high proportion of cells with the embryo NMP signature. NMP-like cells derived from EpiSCs in vitro exhibit a gene expression signature which resembles their embryonic counterparts (Edri et al., 2019a). As such, EpiSC derivatives may be a more appropriate system than ESCs to examine the later differentiation events in the axis.

To test these claims, I compared NPCs from EpiSCs (Figure 3.10) with ESCs (Figure 3.12), as shown in (Figure 3.11). qPCR and ICC analysis show no major differences

in the derived cultures. This shows that both EpiSCs and ESCs can generate NPCs of different axial identities. Overall, I have established conditions to make anterior, hindbrain and cervico-thoracic spinal cord NPCs, but not cells expressing Hox10 onwards. In the next chapter, I will describe experiments to achieve differentiation of cells with a lumbo-sacral identity.

Chapter 4. Culture manipulations to activate posterior hox genes.

I showed in the previous chapter that prolonged culture of E14u09 EpiSCs did not result in activation of the most posterior Hox genes, but that I subsequently found greater homogeneity of differentiation with R4 EpiSCs. In this chapter, I continue to use R4 EpiSCs to test further conditions aimed at activating PG10-13 Hox genes.

4.1. Extending culture of NMPs in NMP media vs Basal media.

In chapter 3, I explored the effects of manipulating NMP conditions at the beginning of differentiation and whether these would result on posteriorisation of cells. However, it is uncertain at what point cells lose NMP signature and whether we can retain NMP identity in prolonged cultures by maintaining them in NMP media. By retaining NMP identity for longer periods of time we might be able to push axial identity towards the most posterior PGs. Furthermore, the effects of prolonging NMP culture in basal media remain uncertain. Although the presumption is that NMPs in the absence of Wnt and Fgf signalling would lose expression of Tbra and transition towards a neural fate, it has not been formally shown what the effects would be on NMP signature and on their axial identity. To test the effects of NMP media vs basal media in prolonged cultures, I plated R4 EpiSCs for 48h in NMP media. Media was then removed, and cells were supplemented with either fresh NMP media or N2B27 media for a further 24-48 hours. I carried out qPCR and ICC to examine Hox gene expression, NMP status and neural differentiation. Cells cultured in NMP media gained expression of Sox2 over time but also showed a higher level of expression when compared to cells growing in N2B27. The expression of Tbra remained similar across different conditions. Sox2+Tbra+ cells were not observed later than 24h of extended culture, and only in cells cultured in N2B27. Sox2+ve also appear to be arranged differently across conditions, with Sox2 positive in N2B27 being dispersed across the dish as a monolayer, while Sox2 single positive cells cultured in NMP media cluster together in the shape of rosettes. Intriguingly, not all rosette shaped clusters were Sox2 positive. The axial identity across conditions appears to be similar, with markers Hoxa5, Hoxb8 and Hoxc9 being expressed at higher levels in cells cultured in basal media. Expression of Hoxb4

decreased significantly across conditions by extending the length of the culture. In contrast, expression of Hoxb2 was the only marker increase by extending the length of culture.

ICC shows many Hoxc9 and fewer Hoxb4 positive cells across all conditions. Interestingly, Hoxc9 and Hoxb4 positive areas were segregated. As observed in the wholemount immunostaining of Hoxb4/Hoxc9 shown in Figure 3. 3, this indicates homogenous population of cells either cervical (Hoxb4+ve) or posterior (Hoxc9+ve). NPCs, marked by TubIII and islet1, were sparse or absent in NMP media. On the other hand, a large number of TubIII positive cells and a more modest number of Islet1 positive cells were observed in basal media, although none showed Tub-III+ve axon outgrowth. This appears to indicate that basal media is capable to retain NMP signature for an additional 24 hours but this does not result in the most posterior Hox genes becoming induced.

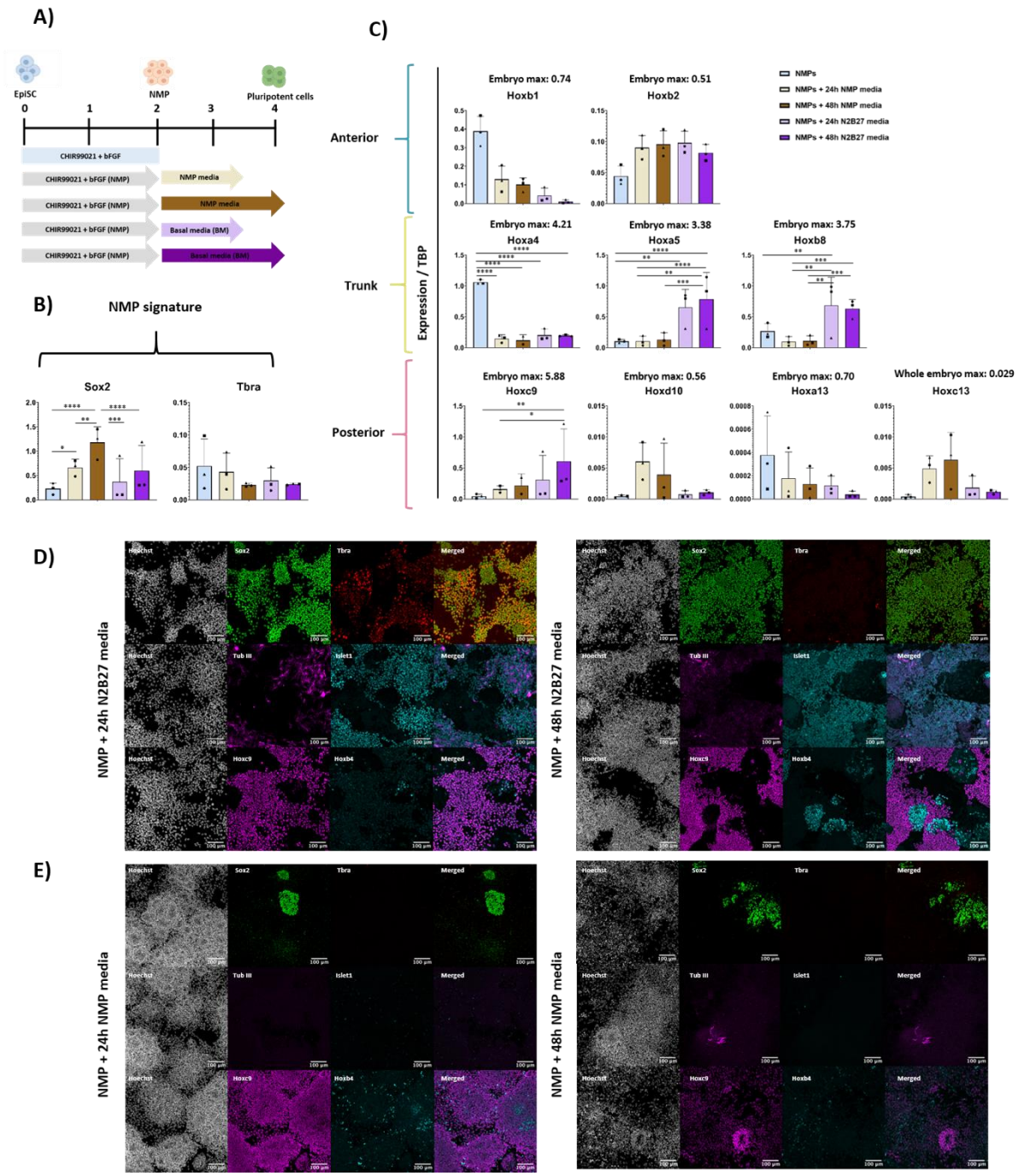

Figure 4. 1. Characterisation of prolonged NMP cultures in NMP or basal media.

(A) Schematic representation of prolonged NMP cultures in either NMP or basal media. qPCR analysis of (B) NMP signature genes and (C) hox genes of different axial levels. Results are represented as values relative to housekeeping gene TBP (*p≤0.05, **p≤0.01 ***p≤0.001, ****p≤0.0001) (One-way ANOVA). Error bars represent the standard deviation for 3 biological replicates with 3 loading replicates each. ICC staining combinations of Sox2 and Tbra, ßIII tubulin and islet1, and Hoxc9 and Hoxb4 in prolonged cultures of NMP in (D) basal media for 24h and 48h (E) NMP media for 24h and 48h.

4.2. Posteriorising axial identity by addition of GDF11.

Results so far suggest that factors such as time in culture, nature of the substrate, media composition and concentration of WNT agonist are insufficient to induce expression of the most posterior Hox genes PG10-13. Lippman et al., 2015 identified GDF11 as a candidate to induce posterior Hox gene expression in NMP cultures derived from hESCs, achieving expression of PG 10-11. However, they did not show single-cell quantification, and so it is unclear what cell types express these genes. GDF11 is expressed in the primitive streak at E8.0 and in tail bud regions at E9.5, where new mesodermal cells arise, and it has been suggested to play an important role in the specification of positional identity along the anterior-posterior axis either by local changes in levels of signalling or by acting as a morphogen. Homozygous mutations of GDF11 result in mice with patterning defects, extended trunks and shortened tails (McPherron et al., 1999). This highlights the important role of GDF11 in axial patterning. Furthermore, the effect of GDF11 on differentiating mESCs and EpiSCs remains unexplored. I first defined the timing of GDF11 action during NMP differentiation. GDF11 was either added at the start of NMP differentiation or 24 hours later. The expression of Hox genes and NMP markers Sox2 and Tbra were measured through qPCR to assess the effects of GDF11 on NMP differentiation. Culture in either condition showed a decrease in neural markers Sox2 while maintaining mesoderm marker T-bra.

Cultures exposed to GDF11 for 48 hours also lost the expression of multiple Hox genes in comparison to cultures grown in the absence of GDF11, with exception of posterior Hox gene Hoxa13. On the other hand, the addition of GDF11 for 24 hours to cultures growing in NMP media showed higher levels of expression for all selected markers, being statistically significant for genes Hoxb1, Hoxa4, Hoxc6 and Hoxc9. Expression of the most posterior PG Hox genes Hoxd10, Hoxa13 and Hoxc13 was also observed, out of which Hoxd10 and Hoxc13 are expressed at a physiological level.

To determine the extent to which I could increase expression of the posterior PGs shown, I next explored the effects of GDF11 concentration on axial and NMP identity markers. GDF11 was added 24 hours after NMP induction for a further 24 hours at concentrations ranging from 12.5 ng/ml-100 ng/ml. No differences were observed

across the different cultures, suggesting that the lowest concentrations of GDF11 used were saturating for the posteriorizing effect.

To determine whether cultures retained their NMP phenotype after the addition of GDF11, I carried out ICC for Sox2 and Tbra. Results further support what was observed by qPCR; loss of Sox2 expression is reflected in a low frequency of Sox2 positive cells while maintaining a similar level of Tbra expression, which is shown by a high frequency of Tbra+ve cells. Sox+Tbra+ colonies were observed; however, these were sparse and few. Cultures exposed to GDF11 for 48 hours showed no Sox+ve or Tbra+ve cells (Data not shown). This suggests that the addition of GDF11 blocks or prevents further NMP differentiation, indicated by the loss of NMP signature, and directs cells towards an alternative fate which I will proceed to explore.

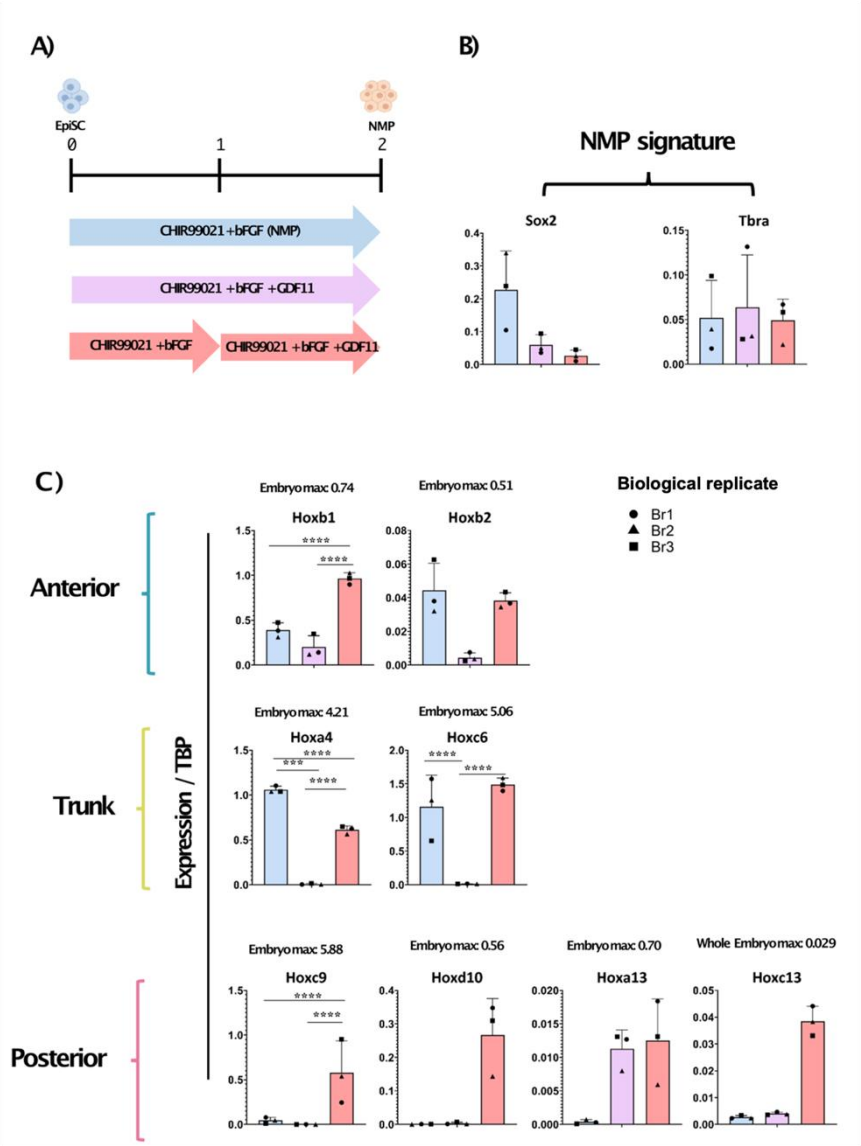

Figure 4. 2. Gene expression analysis of cultures treated with GDF11.

(A) Schematic representation of GDF11 added at different time points (B) qPCR analysis of cultures treated with GDF11 for NMP markers Sox2 and T-bra. (C) qPCR analysis of previous conditions for anterior, trunk and posterior identity markers. Results are represented as values relative to the housekeeping gene TBP (***p≤0.001, ****p≤0.0001) (One-way ANOVA). Error bars represent the standard deviation for 3 biological replicates with 3 loading replicates each. Maximum expression levels detected in vivo for each Hox gene are shown above each qPCR plot, respectively.

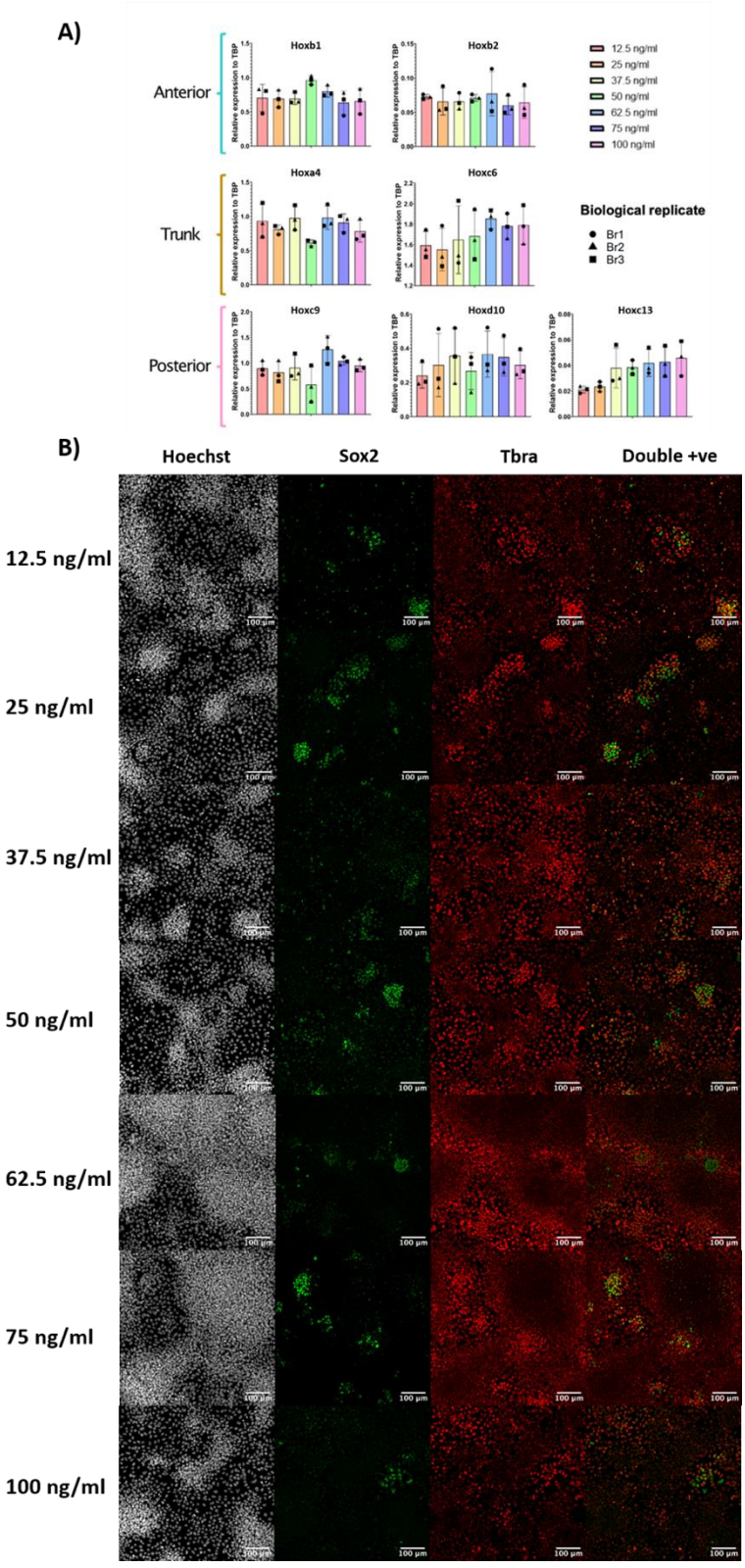

Figure 4. 3. Analysis of Hox gene expression and assessment of NMP populations in cultures treated with GDF11.

GDF11 titration on cultures treated with GDF11 for 24h (A) qPCR analysis of different axial markers for cultures treated at different GDF11 concentrations. Results are represented as values relative to housekeeping gene TBP (One-way ANOVA). Error bars represent the standard deviation for 3 biological replicates with 3 loading replicates each. (B) ICC staining of Sox2 and Tbra for EpiSC cells treated in the presence of GDF11 at different concentrations.

4.3. Further exploring the roles of GDF11

4.3.1. The addition of GDF11 to EpiSCs alongside Chiron and FGF leads to endoderm differentiation.

As shown, the addition of GDF11 can induce the expression of the most posterior paralog groups in mouse EpiSCs. This appears to be dependent on the time at which GDF11 is added during the NMP differentiation protocol. To explore how GDF11 addition at different times affects the eventual differentiation outcome, I extended the length of the culture of the previously shown protocols from 48 hours to 72 and 96 hours. The first condition, which I will refer to as condition A, consists of cells cultured in NMP media alongside GDF11 for 48 hours D0-D2. The media was then replaced with N2B27 for 24-48 hours. The second set of conditions, which I will refer to as condition B, consists of cells cultured in NMP media for an initial 48 hours. The media was then replaced with N2B27 containing GDF11 at 50 ng/ml for an additional 24-48 hours. In addition to analysing Hox expression and neural differentiation by qPCR and ICC, I also carried out ICC for Sox2 and Tbra to explore the effects of GDF11 on NMP signature markers to gain a better understanding of the new fate of derived cultures.
In condition A, the coexpression of Sox2 and Tbra decreased over time. ICC shows few to no double positive cells at 72 and 96 hours, indicating a loss of NMP identity. Hox expression was limited to Hoxd10 and Hoxa13. To determine whether lumbosacral PG groups are expressed at a protein level, I carried out ICC for Hoxc13 as well as Hoxb4 and Hoxc9. In support of qPCR data showing absence of most Hox gene expression, Hoxb4 and Hoxc9 were undetectable (Figure 4.6 D). Finally, I assessed their potential to become NPCs by staining for selective neural marker TubIII and islet1. The resulting cultures showed little or no expression of TubIII indicating that the cells were not neural. However, many islet1 positive cells, were observed, suggesting cells differentiating towards an endoderm identity, however further characterisation discussed in section 4.4 is required.

4.3.2. The addition of GDF11 after Chiron and FGF pulse induces cells with expression of the most posterior paralog groups.

In condition B, the expression of NMP/mesoderm marker Tbra decreased over time, showing almost no expression at 72 hours. On the other hand, the expression of NMP/neural marker Sox2 increases after 48 hours. Through ICC, it is possible to confirm a loss of NMP colonies as Tbra positive cells were absent. However, Sox2 positive cells were present. This data, alongside qPCR results, suggest that cells removed from NMP media adopt a neural fate. qPCR for axial identity markers shows that GDF11 added after NMP induction favours the expression of the trunk and posterior markers, evident by the expression of posterior hox genes Hoxd10 and Hoxc13, but not Hoxa13. I carried out ICC for Hoxb4 and hoxc9. I also performed ICC hoxc13 to determine whether lumbosacral PG groups are expressed at a protein level in condition B (Figure 4.6). Few Hoxb4 positive cells and many Hoxc9 positive cells were detected. When looking at expression of the different Hox genes, axial identity appears to be mutually exclusive, matching wholemount staining shown in Figure 3.3. ICC in condition B also confirms Hoxc13 positive cells showing that this protocol can produce cells expressing the most posterior PG at a protein level. Finally, the neural potential of these cells to become NPCs was further assessed by staining for selective neural marker TubIII and islet1. Cultures show the presence of cells positive for TubIII at 72 hours, showing early presence of axons at 96 hours, cells indicating a “recovery” in neural identity and becoming a candidate of interest in our grafting studies. These results suggest that it seems possible to have more control over axial identity by choosing when to add GDF11 to an NMP differentiation protocol. If GDF11 is added alongside Chiron and FGF, there is a loss of characteristic NMP markers making a type of cells still to be determined. While if added after an NMP induction, it is possible to induce posterior axial identity while maintaining a neural phenotype.

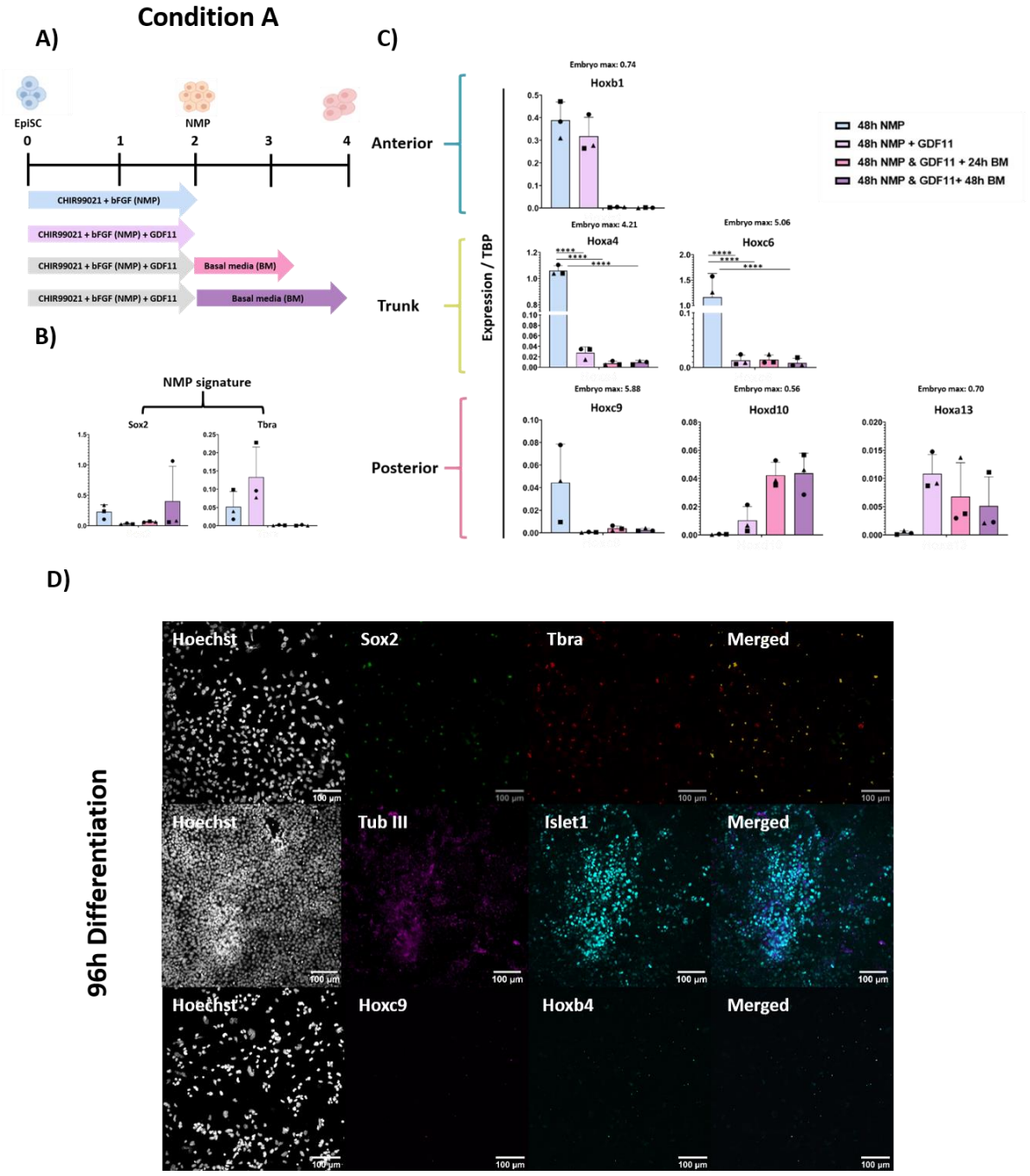

Figure 4. 4. Figure. Investigating the effects of GDF11 added to NMP differentiated media in cultured cells.

(A) Schematic representation of cultures supplemented with GDF11 alongside Chiron and bFGF for 48h with an additional extended culture of 24h and 48h in basal media (Condition A). qPCR analysis of cultures treated with GDF11 for (B) NMP markers Sox2 and T-bra and (C) anterior, trunk and posterior identity markers. Results are represented as values relative to the housekeeping gene TBP (***p≤0.001, ****p≤0.0001) (One-way ANOVA). (D) ICC staining combinations of Sox2 and Tbra, ßIII tubulin and islet1, and Hoxc9 and Hoxb4 in cultures supplemented with GDF11 alongside Chiron and bFGF for 48h with an additional extended culture of 24h and 48h in basal media.

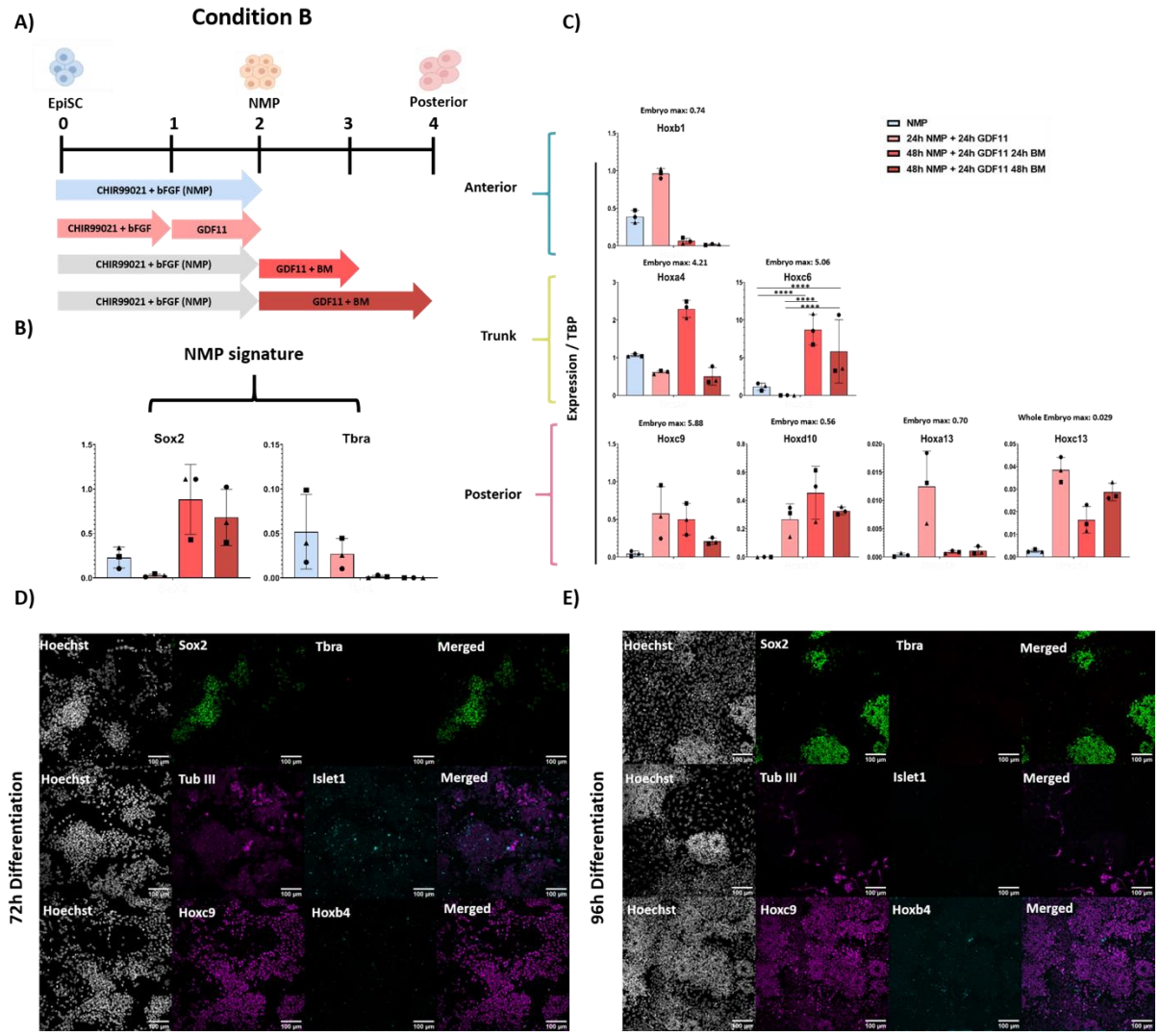

Figure 4. 5. Exploring the effects of supplementing NMP cultures with GDF11.

(A) Condition B Schematic representation of differentiation protocol of 'tail' cells (Condition B) qPCR analysis of cultures treated with GDF11 for (B) NMP markers Sox2 and T-bra and (C) anterior, trunk and posterior identity markers. Results are represented as values relative to the housekeeping gene TBP (****p≤0.0001) (One-way ANOVA). (D) ICC staining combinations of Sox2 and Tbra, TubIII and islet1, and Hoxc9 and Hoxb4 in 'tail' NPCs.

4.4. Further characterisation of GDF11 conditions.

In section 4.3, I show that addition of GDF11 can direct cells towards a different fate depending on when it is added to an NMP differentiation protocol. In condition A, the presence of GDF11 alongside Wnt and Fgf prevents generation of NMPs by suppressing Sox2 and Tbra expression. In condition B, cultures proceed to lose Tbra over time but recover expression of Sox2. While it is possible that condition B is directed towards a neural fate, the identity of cells in condition A remains unknown. To further understand the cell fate promoted by early treatment with GDF11, I carried out qPCR for markers of alternative non-neural fates. Endoderm marker Foxa2 and node marker Noto were highly expressed in condition A, in comparison to condition B, which expressed neural markers Sox2 and Foxp1. At 72 hours condition B also shows upregulation of somite marker Pax3 alongside mesoderm marker Tbx6. At 96 hours, expression of Pax3 remains to be upregulated but Tbx6 expression decreases, indicating a loss of mesoderm identity mesoderm. This further indicates condition B transitioning towards a neural fate. Previous ICC carried out for condition A derived cultures also showed expression of Islet1, which is both a motor neuron and a marker of the pancreas, an endodermal organ. Given the lack of expression of neural markers at RNA and protein level, this suggests that condition A promotes an endoderm fate. This can also explain the upregulation of the posterior Hox gene Hoxa13, which is associated with gut development (De Santa Barbara and Roberts., 2002). This also suggests that condition A is not capable of inducing posterior hox gene expression (with the exception of Hoxa13) in comparison to condition B. To further confirm the endoderm fate and gain of posterior axial identity to a protein level in these cultures, I carried out ICC for Pax3 and Foxa2 and axial identity markers Hoxc9 and Hoxc13. In condition A, a high proportion of cells were Foxa2 positive, and none were Pax3 positive cells. Conversely, in condition B, Pax3 positive cells were frequent, and Foxa2 positive cells were not detected. In condition A, Hoxc13 marked only a very few low-intensity cells, compared to condition B where strongly stained Hoxc13 positive cells were frequently observed. Taken together, these data suggest that condition A directs cells towards an endoderm fate while condition B induces neural cells with posterior axial identity, further indicating that an NMP intermediate is necessary to achieve posterior axial identity.

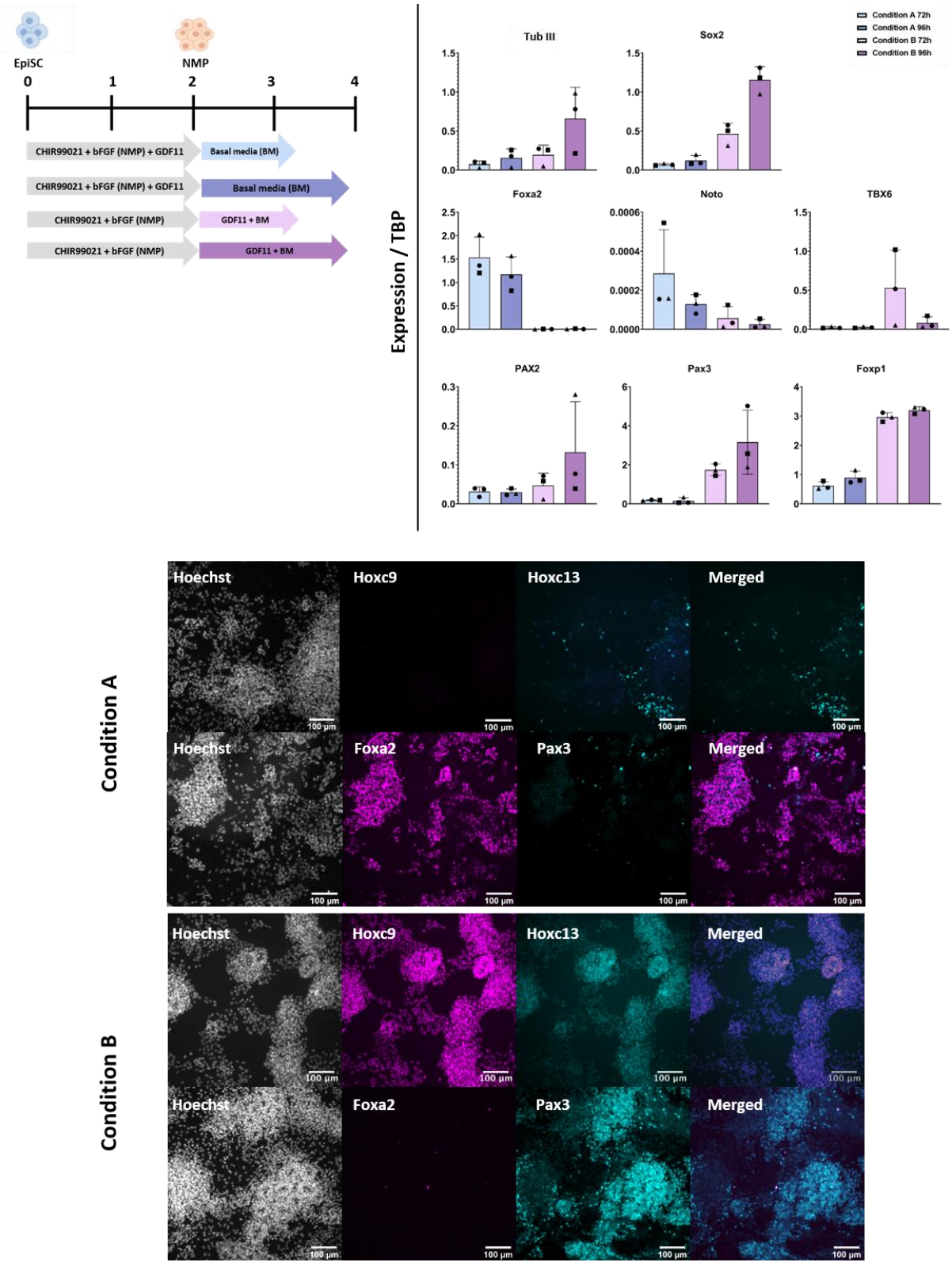

Figure 4. 6. Aiming to determine cell type identity in GDF11 treated cultures.

(A) Summary schematic for conditions previously described referred to as condition A and condition (B) qPCR analysis of markers of cell fate. Results are represented as values relative to the housekeeping gene TBP (One-way ANOVA). (C) ICC staining combinations of Hoxc9 and Hoxc13, and Foxa2 and Pax3 for conditions A and B at 96h.

4.5. Adding a pulse of GDF11 during NMP induction.

In section 4.2, I showed that a “pulse” of GDF11 for 24 hours to cultures growing in NMP media generates cells expressing PG Hoxd10 and Hoxc13 to levels found In vivo. Having shown the drastic effects of GDF11 pre- and post-NMP induction described in section 4.3, it appears that an NMP transition state is necessary to achieve expression of the most posterior PGs. However, the duration of GDF11 signalling necessary is unclear and the effects of prolonging NMP culture after a “pulse” of GDF11 remain uncertain. To test whether a short period of GDF11 treatment was sufficient to posteriorize cells that had been induced to become NMPs, cells were cultured in NMP media for 24 hours; media was then replaced with fresh NMP media supplemented with GDF11 for an additional 24 hours. Media was then replaced with basal media, where cells continued growing for 24 and 48 hours. I then carried out qPCR for markers of axial identity and NMP signature, showing similar levels of Sox2 and Tbra in comparison to cultures derived from a standard NMP differentiation protocol. Expression for Hox markers resemble those observed previously for condition B (Figure 4. 5), ie upregulation of all selected Hox markers, including the most posterior PGs Hoxd10, Hoxa13 and Hoxc13. Levels of expression for these markers appear to be higher than those previously shown for condition B. However, these cultures show a degree of variability amongst the different biological replicates, perhaps partly due to an observed increase in cell death upon the addition of GDF11. ICC was also carried out to further determine the identity of these cells when GDF11 is added. Cells were positive for Sox2, with varying intensity of immunoreactivity. Tbra expression was absent, indicating that no NMPs were present at the end of this protocol. NPC identity was then determined by staining with TubIII and Islet1. TubIII positive cells were present, some of which also appeared positive for islet1 suggesting that motor neuron progenitors were present. An alternative explanation could be a mixed population of endoderm and neural progenitors. Biological replicates collected for analysis showed a Hox expression profiler either to that observed in condition A or condition. This further suggests high heterogenous cultures of endoderm and neural progenitors. Finally, axial identity is determined by staining for Hoxc9 and Hoxb4. ICC shows Hoxc9- but not Hoxb4-positive cells, supporting qPCR results. Further characterisation is required to fully determine the fate of these cells. This data further supports that an NMP intermediate is necessary to achieve posterior axial identity.

Higher levels of expression for the most posterior PGs were observed in cultures supplemented with GDF11 for 24 hours growing in NMP media. However, these cultures were heterogenous and with higher levels of variability and cell death than those described for condition B.

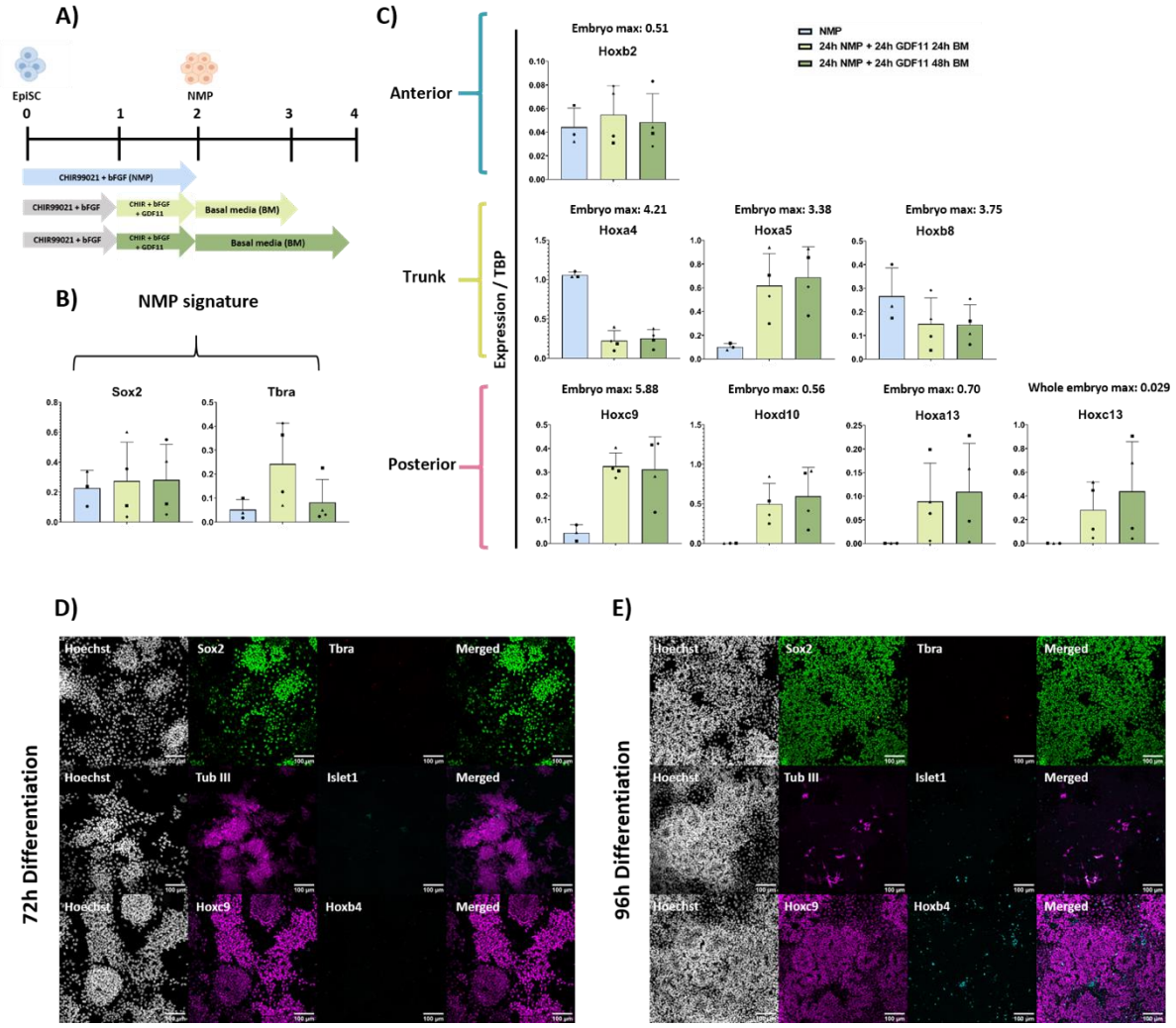

Figure 4. 7. Characterisation of generated cultures after a "pulse" of GDF11 for 24 hours.

(A) Schematic representation of differentiation of 'intermediate' cells. qPCR analysis of 'intermediate' cells for (B) NMP markers Sox2 and T-bra and (C) anterior, trunk and posterior identity markers. Results are represented as values relative to the housekeeping gene TBP (One-way ANOVA). ICC staining combinations of Sox2 and Tbra, ßIII tubulin and islet1, and Hoxc9 and Hoxb4 in 'intermediate' cells at (D) 72h and (E) 96h.

4.6. Discussion for chapter 4.

In chapter 4, I tested for the first time the effects of GDF11 on NMP cultures derived from EpiSCs. I show that the addition and timing of GDF11 during NMP differentiation is critical for the optimal expression of caudal/sacral Hox genes (Figure 4.2). This results in two different types of cultures showing distinct Hox gene profiles: Adding GDF11 added at day 0 results in upregulation of posterior marker Hoxa13 but not other Hox genes; adding it after at least 24 hours of NMP differentiation leads to upregulation of multiple Hox genes, including posterior PG10-13. This indicates that addition of GDF11 can induce PG13 Hox genes in cultured cells. However, the NMP signature also changes (Figure 4.2). At 48 hours the number of Sox2+ Tbra+ ve cells observed in figure 4.3 decreased considerably in comparison to what is observed in cultures in the absence of GDF11 (appendix 1 and 2). In chapter 1, I explained that GDF11 is involved in the downregulation of transcription factor Pou5f1 and upregulation of enzyme cyp26a1 (Aires et al., 2019). This contributes to late PG becoming induced and in the eventual disappearance of NMPs due to a downregulation of the canonical Wnt/β-catenin pathway resulting in the end of axial elongation. Therefore, this suggests that addition of GFD11 blocks or interrupts differentiation of EpiSCs into NMPs. Having observed a downregulation ofSox2 and Tbra at an expression and protein level I began to question the resulting fate of these cells.

One of the primary objectives of this thesis is to generate NPCs expressing the most posterior PGs. Prolonging cultures of NMP in basal media showed upregulation of neural marker Sox2 while also retaining expression of Hox genes up to PG9 (Figure 4.1). Other studies also show that ESC default towards a neural fate when cultured in the absence of extrinsic signals (Smukler et al., 2006). Therefore, I cultured NMPs for 48 hours and then treated them with GDF11 and basal media. NMP cultures treated with GDF11 and basal media retained expression of Sox2 and induced expression of Hox PG10-13 genes (Figure 4.5). I further confirmed their neural identity by measuring expression of important markers of CNS development Pax2, Pax3, Foxp1 and TubIII (Stoykova and Gruss., 1994, Li et al., 2015) (Figure 4.6). Axial identity was also confirmed at a protein level by staining for Hoxc13 (Figure 4.6). This indicates that it is possible to generate neural cells of posterior axial identity. This will allow us to study

their capacity to integrate and survive upon transplantation of cells expressing late axial markers in homotopic and heterotopic sites.

In an attempt to further induce expression of PG13 I prolonged the length of the cultures described in (Figure 4.2). Cells cultured in NMP conditions alongside GDF11 generated cells expressing Hoxa13 as the only axial marker (Figure 4.4). Hoxa13 has been shown to be expressed in the tail gut endoderm and is associated with gut/genitourinary/tail development (De Santa Barbara and Roberts., 2008). Hoxa13 also appears to be associated with gastric cancer (Qin et al., 2019). These studies associate expression of Hoxa13 with endoderm derived tissues, indicating that generated cells are endoderm progenitors. I found that these cells expressed Foxa2 and Islet1 consistent with an endoderm identity (Figure 4.4, 4.6). GDF11 is known to counteract the activity of Wnt and FGF by repressing the activity of Cdx2 proteins; therefore, adding GDF11 alongside Chiron and Fgf may give rise to a counteractive feedback loop which forces cells to exit towards an endoderm fate.

On the other hand, I show that extending the culture of cells after a 24-hour window of GDF11 treatment during NMP differentiation generates cultures expressing multiple Hox genes including the most posterior PG10-13 (Figure 4.7). However, gene expression observed is variable with individual cultures matching either an endoderm progenitor or a posterior axial profile. This suggests that the differential response to GDF11 is initiated in the first 24 hours of NMP differentiation. In this scenario, cultures that are slightly more advanced would respond by activating a posterior axis gene expression profile; those that are less differentiated would respond with an endoderm profile.
Both conditions showed high levels of cells death after addition of GDF11, for reasons that are unclear. RNA-sequencing analysis of these differential responses would lead to a better understanding of the affected pathways.

Chapter 5. Grafting cells of defined axial identity to the neural tube.

5.1. Investigating the importance of axial identity in grafted E10.5 mouse embryos.

As discussed in the Introduction, studies have shown that transplantation of NPCs could become an alternative approach to improve recovery after SCI (Mayer-Proschel et al., 1997, Peljto et al., 2010). Furthermore, work from Kadoya et al., 2016 has demonstrated that the engraftment of progenitors in the spinal cord may be optimal when they are matched to the correct anteroposterior level. In this chapter, I test whether grafting NPCs with matched axial identity leads to better integration and differentiation than unmatched cells. This approach will allow a deeper understanding of how cells behave in an in vivo environment.

I used the culture conditions previously defined in Chapters 4 and 5 to generate NPCs of anterior (NA), hindbrain (NH), anterior trunk spinal cord (NS) and posterior spinal cord identity (NS-P). These were grafted at homotopic and heterotopic sites in E10.5 mouse embryos that were subsequently cultured for 24 hours (Figure 5.1). An embryo at this stage has around 30-35 somites and shows expression of all PGs. Before this stage of development, posterior structures are not fully developed, and expression of the most posterior PG13 is not found. Furthermore, embryos at E10.5 have a developing CNS, with neural cells, including motor neurons, at early stages of differentiation. Neural progenitors at this stage have limited axon outgrowth, which starts to develop over the next 24 hours. To track grafted cells, I used R4 EpiSCs, which carry a ubiquitously expressed GFP reporter construct (Huang et al., 2012). Integration, survival, neurite outgrowth and axial identity of the grafts were assessed after sectioning and immunostaining. I will refer to these grafts as “whole-embryo culture grafts”.

The results from these experiments are shown in Figures 5.3 and 5.4 and tabulated in Tables 5.1, .2, .3 and .4. Each cell type NA/NH/NS/NS-P expressing Hoxb1,a4, c9 and c13 was grafted into three different regions along the antero-posterior axis: r6 (Region I), somite 5-7 (Region II) and somite 24-25 (Region III) (Figure 5.1).

In practice, in some embryos it was difficult to identify the precise graft site targeted in wholemount fluorescence microscopy after culture due to the small size of the graft. In addition, grafted cells that entered the neural lumen moved to unexpected locations before settling. Thus as a first step, I retrospectively determined the integration site after sectioning by comparing with standard embryo models on emouseatlas.org, where a virtual section of a similarly-staged embryo can be visually aligned with the physical embryo sections I generated (Figure 5.1). The success of integration was then determined by looking at the position of the graft and the extent of intermingling with the host. Staining with TubIII and islet1 determined neural identity of the graft and environment in the host, while staining with Hoxb4 and Hoxc9 determined the axial identity of the graft once integrated in the host, and of the adjacent tissue to the graft.

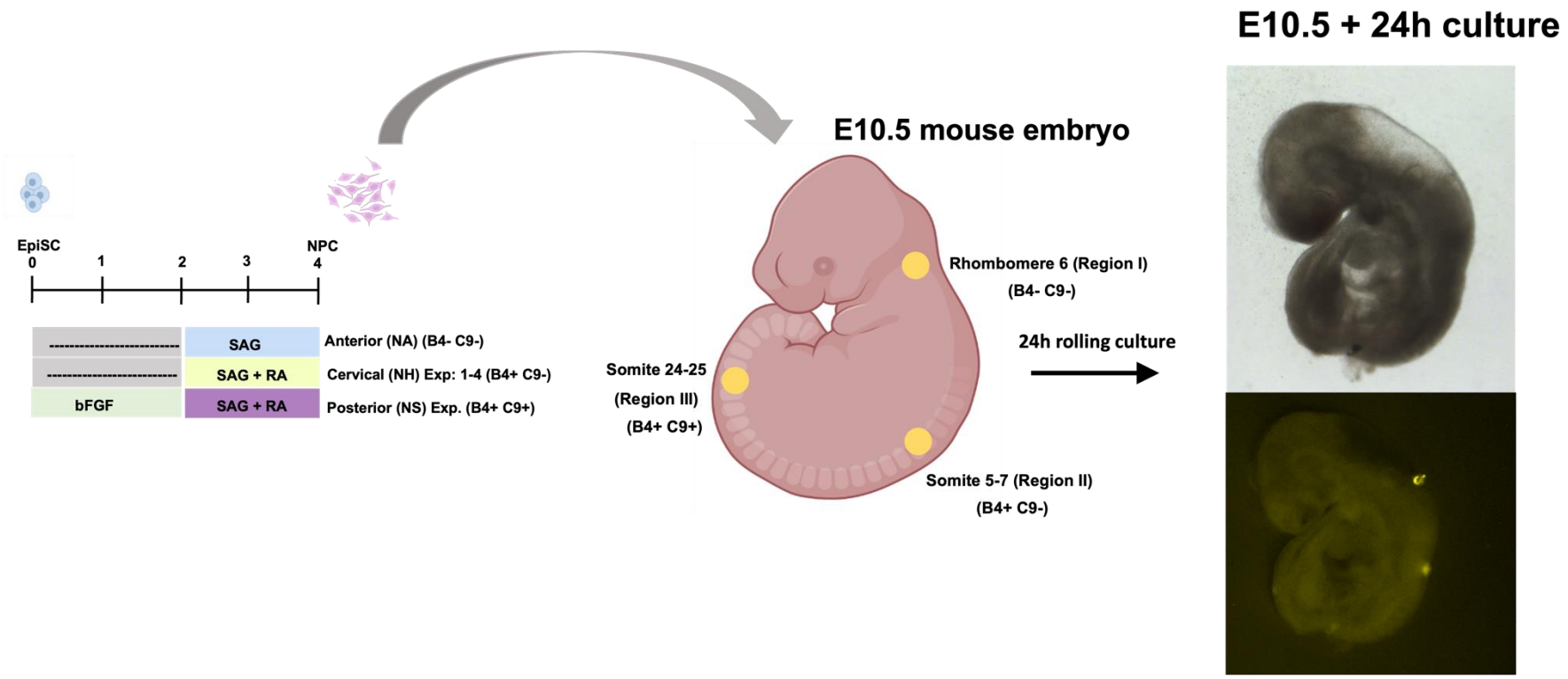

Figure 5.1. Diagram of cell engraftment protocol.

Schematic representation of grafting protocol employed to engraft cells of specific axial identity (NA, NH and NS) into specific homotopic and heterotopic locations (Region I, II and III). Expected Hox gene expression for the grafted cells and the host site is further indicated for each cell type and region. B4 (Hoxb4) C9 (Hoxc0) + (positive) – (negative). Number of grafts per embryo n=3 Graft.

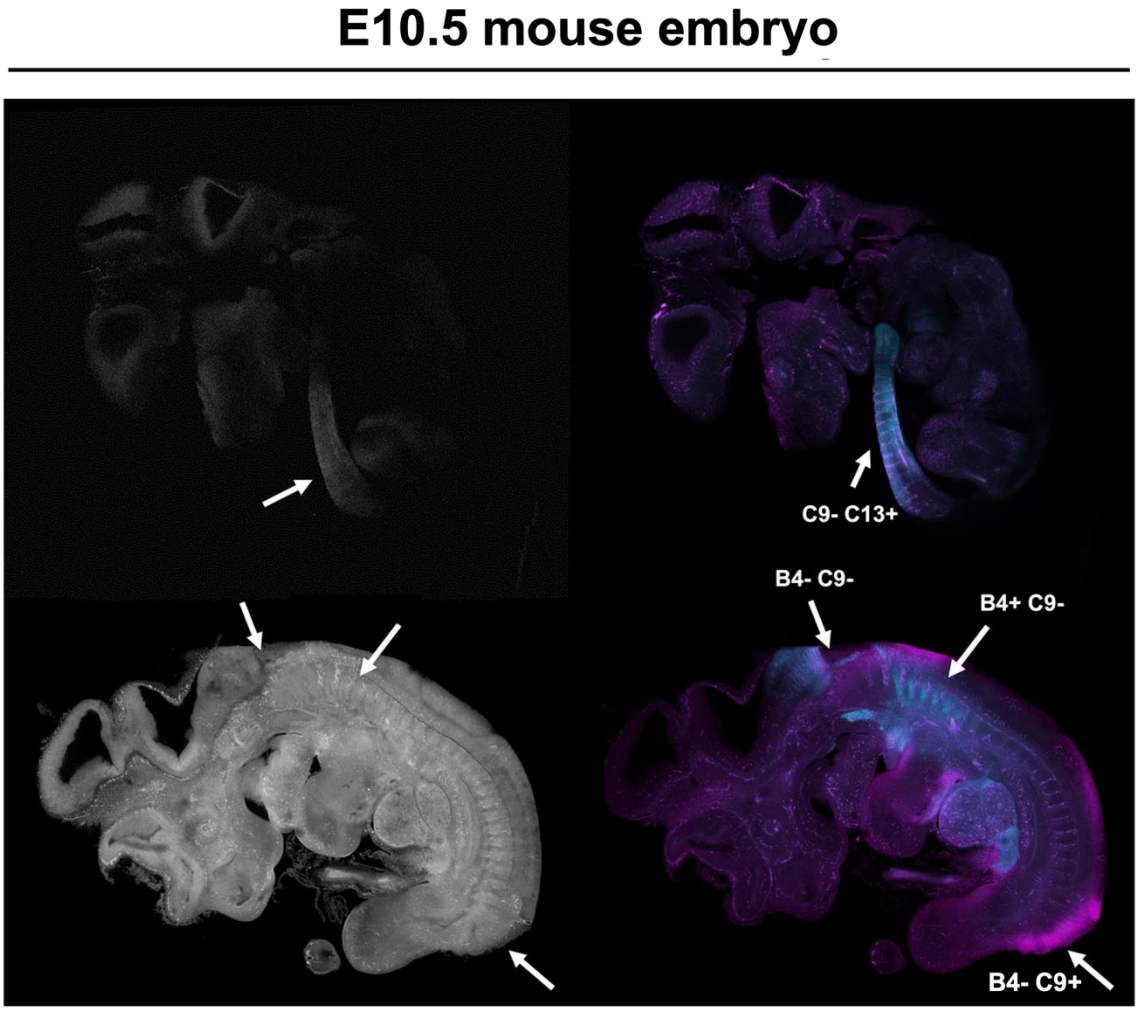

Figure 5.2. Allocation of different axial markers in wholemount embryos.

Wholemount staining of E10.5-11.5 embryos stained for Hoxb4 (B4), Hoxc9 (C9) and Hoxc13 (C13). Arrows indicate expression of selected markers at different regions of interest. + (positive gene expression) – (negative gene expression).

5.1.1. Grafted cells can retain neural identity and match the hosts neural site.

Table 5.1. represents a summary of grafted cells of different axial identity localised at three different sites. The neural tube (NT), the neural lumen, or adjacent tissue referring to an extraneural site. Results show that found grafts positive for TubIII would match the host environment when also positive for TubIII. This remained constant regardless of axial identity (Figure 5.3). Cervical cells in extraneural sites also retained neural identity in an environment which does not express TubIII. Furthermore, posterior grafted cells showed a higher number of posterior grafted cells negative for TubIII (n=9 out of 22) in comparison to anterior (n=6 out of 9) and cervical (n=11 out of 13). However, these grafts were found in regions of the host also negative for TubIII. These observations indicate that posterior cells can express neural identity when the surrounding tissue is expressing TubIII, indicating that they may require signals from the environments to retain neural identity, since neural identity is confirmed before grafting (Figure 3.13).

Differentiation of grafted cells towards a motor neuron identity was determined by staining for Islet1. A higher proportion of grafts negative for Islet1 (n= 38 negative grafts out of 44) were found in comparison to those stained for TubIII (n=16 negative grafts out of 44). This observation was the same regardless of the type of graft. Before grafting, anterior and cervical cells were negative for Islet1, while posterior cells were positive, as shown in Figure 3.13. This indicates that 24h may not be enough time for cells to differentiate or retains motor neuron expression in an endogenous environment

5.1.2. Grafted cells retain original hox identity regardless of location.

In figure 3.13 I confirmed the axial identity of NPCs at the time they are transplanted into the host. To determine whether cells grafted retain their original axial identity or change to match the host environment, I stained sections for cervical marker Hoxb4 and posterior marker Hoxc9. Results show that all grafts retain their original hox identity regardless of the grafted site.

Interestingly, the total number of grafts of anterior cells recovered was less than that for cervical and posterior cells. This suggests that anterior cells integrate less efficiently than cervical or posterior cells. Grafts of posterior cells are the only cell type showing coexpression for Hoxb4 and Hoxc9 (Table 5.4). This is only observed when posterior grafts are found in a region where the adjacent tissue is positive for Hoxb4 (shown in appendix 4 and 5). This could suggest that posterior cells have a greater degree of plasticity capable of adapting to the hosts environment.

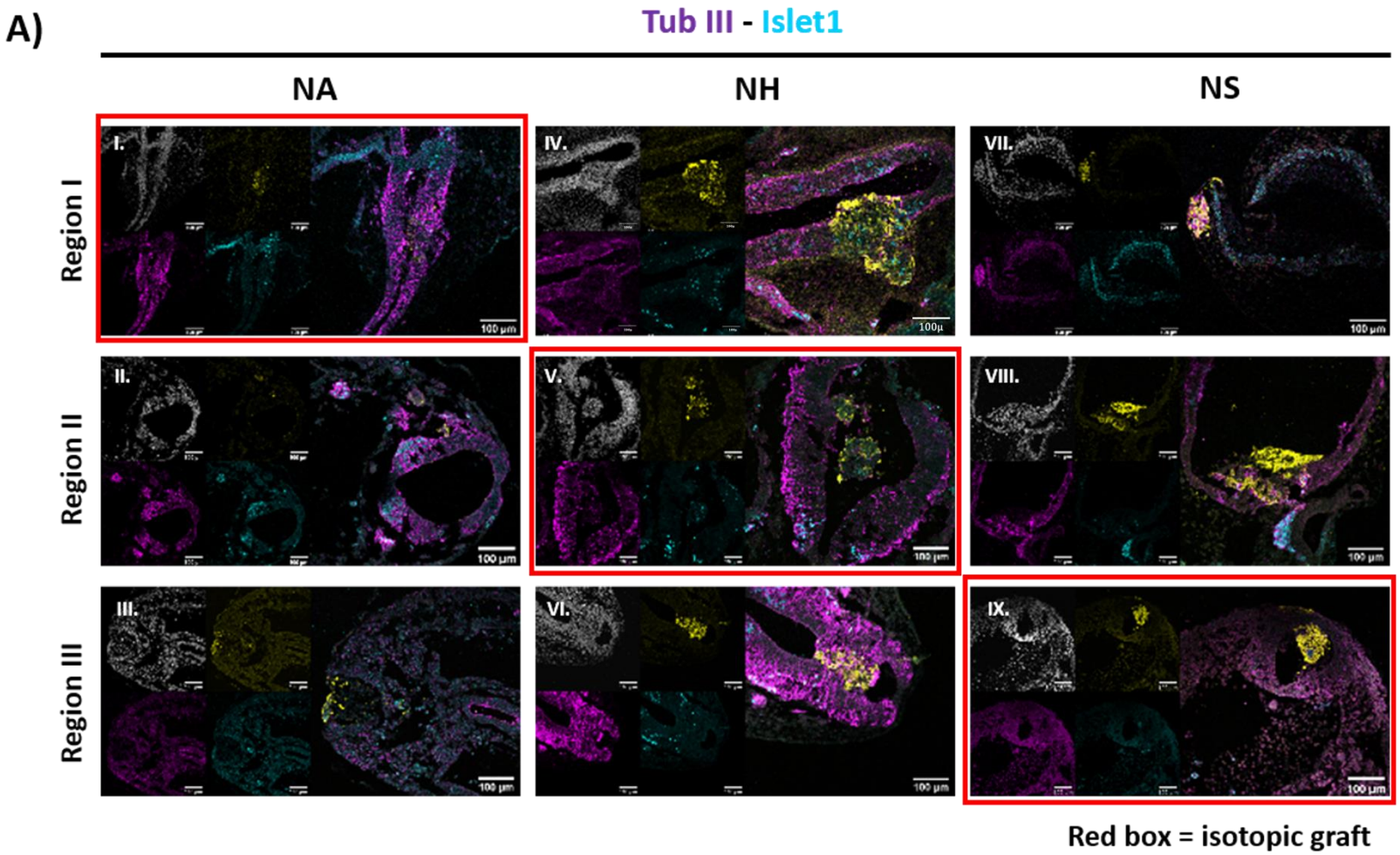

Figure 5.3. Determining neural identity in "Whole-embryo culture grafts".

Panel of representative embryo sections with successful grafts at different homotopic and heterotopic locations stained for GFP (yellow), TubIII (purple) and Islet1 (cyan) by ICC. Region I (anterior site), Region II (cervical site), Region III (posterior site). Anterior cells grafted in region I (I.), region II (II.), Region III (III.) Region III. Cervical cells grafted in region I (IV.), region II (V.), Region III (VII.) Posterior cells grafted in region I (VII.), region II (VIII), Region III (IX.) Selected images are representative of grafted cells in the neural lumen, the NT or adjacent to this.

Table 5.1. Summary of "Whole-embryo culture grafts" scored for neural identity.

Engraftment results sorted by their grafted cell identity, graft location and overall number of recorded grafts. Summary results of grafted cells stained for neural markers TubIII and Islet1. G (Graft), H (Host environment), + (positive gene expression), - (negative gene expression). Symbol ± indicate the number of samples which could not be fully confirmed. Samples therefore were inserted into the table according to most likely to match.

Grafts in the neural tube

	TubIII				Islet1			
Grafted cell identity	G H	G H	G H	G H	G H	G H	G H	G H
	+ -	- +	+ +	- -	+ -	- +	+ +	- -
Anterior N= 5	**0**	1	4	0	0	1	0	4
Cervical N= 4	0	0	4	0	0	1	1	2
Posterior N= 10	**0**	1(2±)	3	**4**	0	(3±)	0	7

Grafts in the lumen of the neural tube

	TubIII				Islet1			
Grafted cell identity	G H	G H	G H	G H	G H	G H	G H	G H
	+ -	- +	+ +	- -	+ -	- +	+ +	- -
Anterior (N= 2)	**0**	0	1	1	0	1	0	4
Cervical (N= 5)	**0**	1	3	1	0	1	1	2
Posterior (N= 1)	0	0	0	**1**	0	0	0	**1**

Grafts in the adjacent tissue

	TubIII				Islet1			
Grafted cell identity	G H	G H	G H	G H	G H	G H	G H	G H
	+ -	- +	+ +	- -	+ -	- +	+ +	- -
Anterior (N= 2)	**0**	0	1	1	0	1	0	1
Cervical (N= 4)	**2**	0	2	0	**0**	(1±)	1	2
Posterior (N= 11)	(1±)	0	4	**6**	(1±)	**0**	(1±)	9

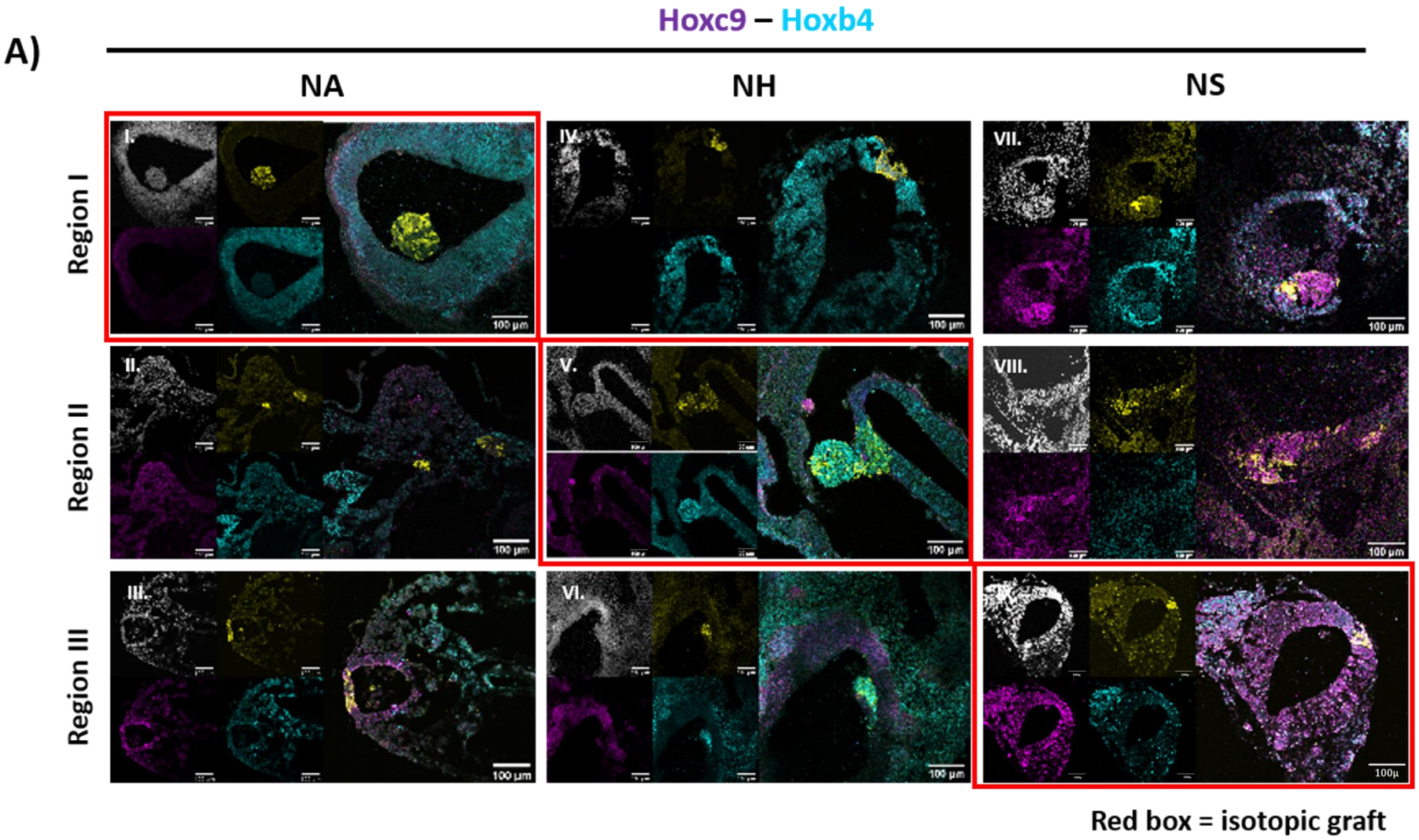

Figure 5.4. Determining axial identity in "Whole-embryo culture grafts".

Panel of representative embryo sections with successful grafts at different homotopic and heterotopic locations stained for GFP (yellow), TubIII (purple) and Islet1 (cyan) by ICC. Region I (anterior site), Region II (cervical site), Region III (posterior site). Anterior cells grafted in region I (I.), region II (II.), Region III (III.) Region III. Cervical cells grafted in region I (IV.), region II (V.), Region III (VII.) Posterior cells grafted in region I (VII.), region II (VIII), Region III (IX.) Selected images are representative of grafted cells in the neural lumen, the NT or adjacent to this.

Table 5.2. Summary of "Whole-embryo culture grafts" scored for axial identity.

Engraftment results sorted by their grafted cell identity, graft location and overall number of recorded grafts. Summary results of grafted cells stained for axial markers Hoxc9 and Hoxb4. G (Graft), H (Host environment), + (positive expression), - (negative expression). Symbol ± indicate the number of samples which could not be fully confirmed. Samples therefore were inserted into the table according to most likely to match.

Grafts in the neural tube

	Hoxb4					Hoxc9			
Grafted cell identity	**G H**	**G H**	**G H**	**G H**		**G H**	**G H**	**G H**	**G H**
	+ -	**- +**	**+ +**	**- -**		**+ -**	**- +**	**+ +**	**- -**
Anterior (N= 1)	0	0	0	1	**Anterior** (N= 1)	0	0	0	**1**
Cervical (N= 3)	**1**	0	2	0	**Cervical** (N= 3)	0	0	0	**3**
Posterior (N= 7)	**0**	1	(1±)	5	**Posterior** (N= 7)	4	0	0	3

Grafts in the lumen of the neural tube

	Hoxb4					Hoxc9			
Grafted cell identity	**G H**	**G H**	**G H**	**G H**		**G H**	**G H**	**G H**	**G H**
	+ -	**- +**	**+ +**	**- -**		**+ -**	**- +**	**+ +**	**- -**
Anterior (N= 0)	--	--	--	--	**Anterior** (N= 0)	--	--	--	--
Cervical (N= 6)	(1±)	1	2 (1±)	1	**Cervical** (N= 6)	0	0	0	6
Posterior (N= 1)	0	0	0	1	**Posterior** (N= 1)	0	0	0	1

Grafts in adjacent tissue

	Hoxb4					Hoxc9			
Grafted cell identity	**G H**	**G H**	**G H**	**G H**		**G H**	**G H**	**G H**	**G H**
	+ -	**- +**	**+ +**	**- -**		**+ -**	**- +**	**+ +**	**- -**
Anterior (N= 1)	**0**	0	1	0	**Anterior** (N= 1)	0	0	0	**1**
Cervical (N= 3)	**1**	0	(2±)	**0**	**Cervical** (N= 3)	0	0	0	**3**
Posterior (N= 5)	0	0	1 (1±)	3	**Posterior** (N= 5)	3	0	(1±)	1

5.1.3. Tail cells can retain neural identity but lose expression of Hoxc13 after grafting to regions I-III.

In chapter 4, I describe the conditions to generate NPCs of posterior spinal cord identity. These cells were grafted into an E10.5 embryo and analysed following the same principles as previously discussed. Representative images were compiled and shown in figure 5.5, while results were summarised and tabulated in tables 5.3 and 5.4. Results show that tail grafts found to be positive for TubIII would match the host environment when also positive for TubIII. However, the total number of grafts positive for TubIII is lower in comparison to any other cell type described. When stained for Islet1, few grafts were positive for islet1 and only when the adjacent tissue was also positive. I then examined any changes in axial identity by staining for Hoxc9 and Hoxc13. Grafted cells only showed expression for Hoxc9, the expression for Hoxc13 was never found after grafting. This indicates that Hoxc13 identity is not fixed in tail cells at the of grafting and may require additional signals within the embryo to retain tail identity.

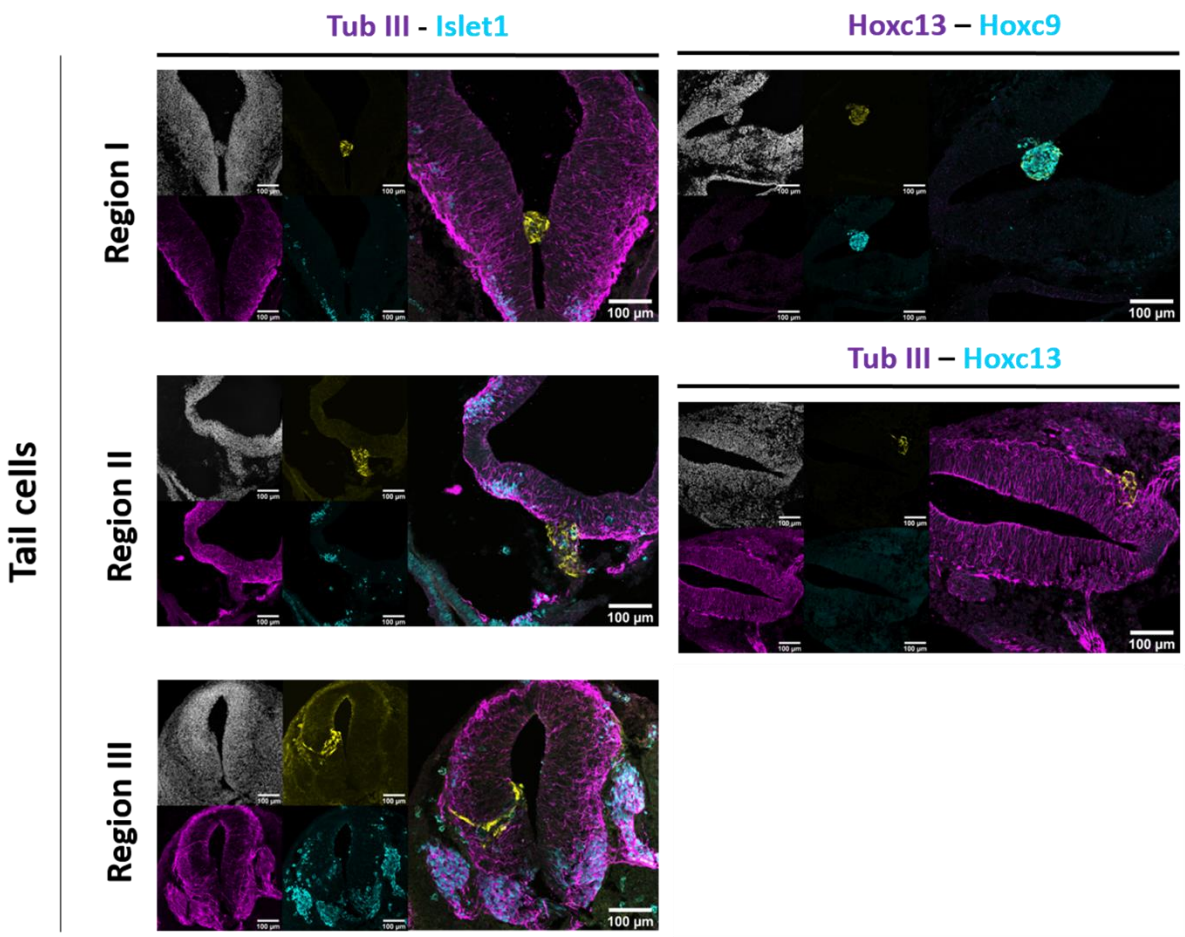

Figure 5.5. Determining neural and axial identity of NS-P cells in "Whole-embryo culture grafts".

Panel of representative embryo sections with successful grafts at different homotopic and heterotopic locations stained for selected markers in different combinations as shown by ICC. Region I (anterior site), Region II (cervical site), Region III (posterior site). Selected images are representative of grafted cells in the neural lumen, the NT or adjacent to this.

Table 5.3. Summary of NS-P cells in "Whole-embryo culture grafts".

Engraftment results sorted by their grafted cell identity, graft location and overall number of recorded grafts. Summary results of grafted cells stained for neural markers TubIII and Islet1. G (Graft), H (Host environment), + (positive expression), - (negative expression). Symbol ± indicate the number of samples which could not be fully confirmed. Samples therefore were inserted into the table according to most likely to match.

Grafts in the neural tube

	TubIII					Islet1			
Grafted cell identity	**G H**	**G H**	**G H**	**G H**		**G H**	**G H**	**G H**	**G H**
	+ -	**- +**	**+ +**	**- -**		**+ -**	**- +**	**+ +**	**- -**
Spinal cord posterior (NS-P) N= 7	0	1	1(2±)	3	**Spinal cord posterior (NS-P)** N= 7	(2±)	0	(2±)	3

Grafts in the lumen of the neural tube

	TubIII					Islet1			
Grafted cell identity	**G H**	**G H**	**G H**	**G H**		**G H**	**G H**	**G H**	**G H**
	+ -	**- +**	**+ +**	**- -**		**+ -**	**- +**	**+ +**	**- -**
Spinal cord posterior (NS-P) N= 7	0	5	1	1	**Spinal cord posterior (NS-P)** N= 7	1	(2±)	1(1±)	2

Grafts in adjacent tissue

	TubIII					Islet1			
Grafted cell identity	**G H**	**G H**	**G H**	**G H**		**G H**	**G H**	**G H**	**G H**
	+ -	**- +**	**+ +**	**- -**		**+ -**	**- +**	**+ +**	**- -**
Spinal cord posterior (NS-P) N= 3	0	0	2	1	**Spinal cord posterior (NS-P)** N= 3	0	(1±)	1	0

Table 5.4. Summary of NS-P cells in "Whole-embryo culture grafts".

Engraftment results sorted by their grafted cell identity, graft location and overall number of recorded grafts. Summary results of grafted cells stained for TubIII and Hoxc13. G (Graft), H (Host environment), + (positive expression), - (negative expression). Symbol ± indicate the number of samples which could not be fully confirmed. Samples therefore were inserted into the table according to most likely to match.

Grafts in the neural tube

	TubIII					Hoxc13			
Grafted cell identity	**G H**	**G H**	**G H**	**G H**		**G H**	**G H**	**G H**	**G H**
	+ -	**- +**	**+ +**	**- -**		**+ -**	**- +**	**+ +**	**- -**
Spinal cord posterior (NS-P) N= 4	0	0	3(1±)	0	**Spinal cord posterior (NS-P)** N= 4	0	0	0	4

Grafts in the lumen of the neural tube

	TubIII					Hoxc13			
Grafted cell identity	**G H**	**G H**	**G H**	**G H**		**G H**	**G H**	**G H**	**G H**
	+ -	**- +**	**+ +**	**- -**		**+ -**	**- +**	**+ +**	**- -**
Spinal cord posterior (NS-P) N= 6	0	0	1	5	**Spinal cord posterior (NS-P)** N= 6	0	0	0	6

Grafts in adjacent tissue

	TubIII					Hoxc13			
Grafted cell identity	**G H**	**G H**	**G H**	**G H**		**G H**	**G H**	**G H**	**G H**
	+ -	**- +**	**+ +**	**- -**		**+ -**	**- +**	**+ +**	**- -**
Spinal cord posterior (NS-P) N= 3	1	0	(1±)	1	**Spinal cord posterior (NS-P)** N= 3	0	0	0	3

5.2. Pilot study to test the feasibility of assessing NPC identity in explanted tissue slice culture.

The experimental design previously shown has provided important insights into how grafted cells integrate and survive when grafted in vivo. However, this approach presents a series of drawbacks. One of the major objectives of this project is to assess the rate of integration and survival. However, this is challenging to do through cryosections as three-dimensional information is lost. I will assess the extent of each graft, as well as whether the grafts form clumps or proliferate/spread throughout the tissue explant as a mean to determine success of engraftment. Furthermore carrying out engraftment in vivo is limiting as it only allows us to observe how cells integrate, proliferate, differentiate and adapt to the surrounding environment within a timeframe of 24 hours, during which little axonal outgrowth occurs. Therefore we developed an approach to maintain grafted cells in culture for a prolonged length of time. NPCs grafted into rat brain slices can be maintained in culture over prolonged periods of time (Marques-Torrejon, Gangoso and Pollard., 2018). Using a similar approach we manually cut sections along the antero-posterior axis of E10-11 mouse embryos into three regions (Region I, region II, region III) at the same location as previously mentioned, and grafted cells of different axial identity into each of these regions. Grafted spinal cord slices were then placed on cell culture inserts and submerged in defined neural media for 5 days (Figure 5.6). After 5 days, tissue begins to lose integrity, compromising the sample. Therefore samples were fixed and analysed at 5 days. I will refer to these grafts as “slice culture grafts”. To determine neural identity samples were stained for TubIII and to assess changes in axial identity, samples were stained for Hoxb4 or Hoxc9.

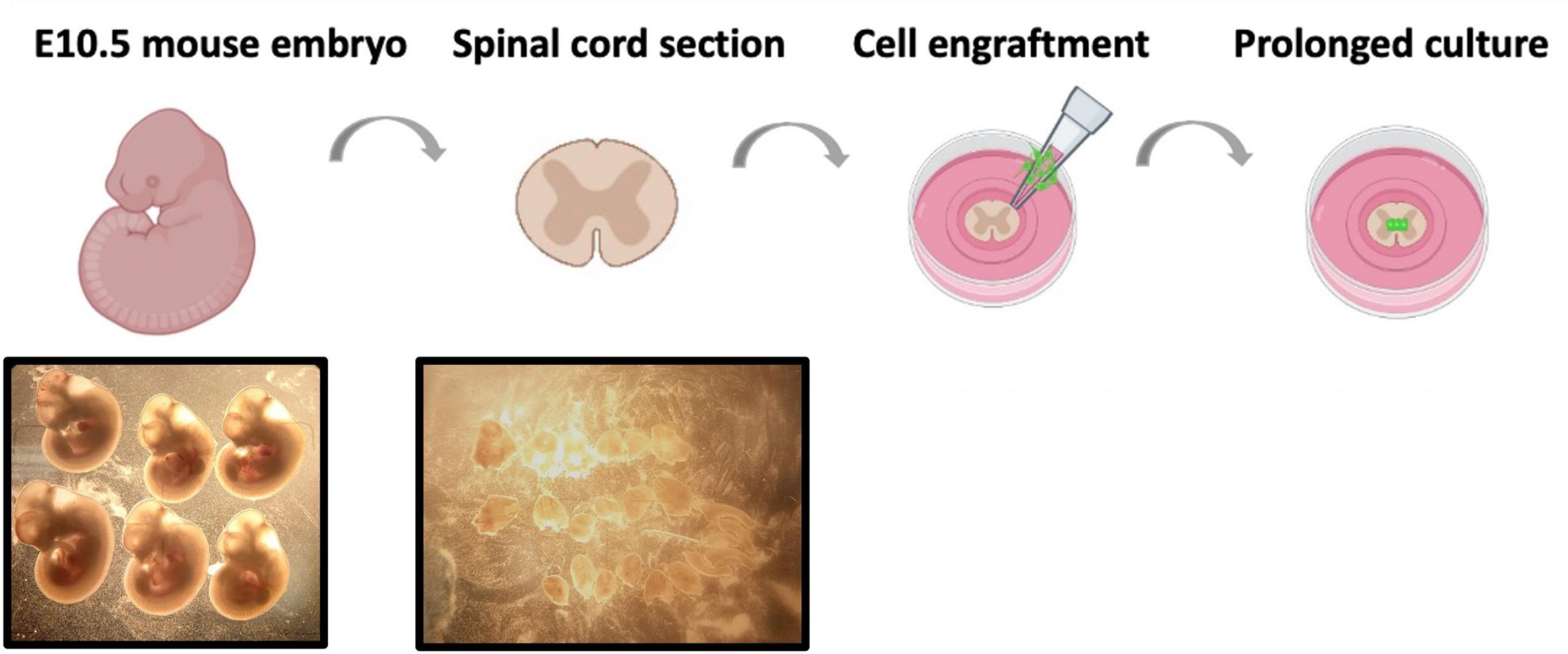

Figure 5.6. Diagram of cell engraftment in "slice culture graft".

Schematic representation of grafting protocol employed to engraft cells of specific axial identity into spinal cord slices of different axial levels. Region I (anterior site), Region II (cervical site), Region III (posterior site). Tissue slices were placed on cell culture inserts and submerged in N2B27 media for 5 days.

5.3. Grafted cells at homotopic locations show a higher degree of integration and distribution.

As previously mentioned, to assess the rate of integration, I determined how much the graft penetrates into the tissue. To do this, I found the graft in the cleared tissue explant and carrie out confocal imaging to generate a z-stack image of the region of interest. This was done for each tissue explant (Figure 5.7). The image was then rendered and visualised in 3D. Scoring of all grafts are tabulated in table 5.5 and 5.6. I found that grafts containing cells of cervical and posterior axial identity are positive for TubIII for all regions except for region I. Grafted cell match the host environment also positive for TubIII. However, I found posterior grafts in region II containing cells positive for TubIII at a region where tissue was not neural. This suggests that grafted cells can retain neural identity when grafted in non-neural sites. Once more, the total number of grafts of anterior cells recovered was less than that for cervical and posterior cells. Overall, grafts matching their homotopic locations showed grafted cells expressing TubIII and matching its surrounding tissue. Furthermore, TubIII+ve cells in homotopic regions had longer axons. This suggests that homotopic engraftment may promote neural differentiation.

To track any changes in Hox gene expression grafts were stained for Hoxb4 and Hoxc9. Anterior grafts were Hoxb4 positive in region III and Hoxc9+ve in region II. Cervical grafts were Hoxb4+ve in regions I and II, and Hoxc9+ve in regions II and III. Finally, posterior cells were Hoxc9+ve in region II and III, but uncertain for Hoxb4. However, the grafts found in the different regions show different levels of distribution throughout the explant (Figure 5.7). The extent of distribution of GFP+ve across the tissue explant was quantified (Figure 5.11) showing to be higher at homotopic sites. While grafts found at heterotopic sites organised as clumps. This suggests grafts at homotopic sites present higher probabilities of integration into the host while continuing to proliferate across the tissue.

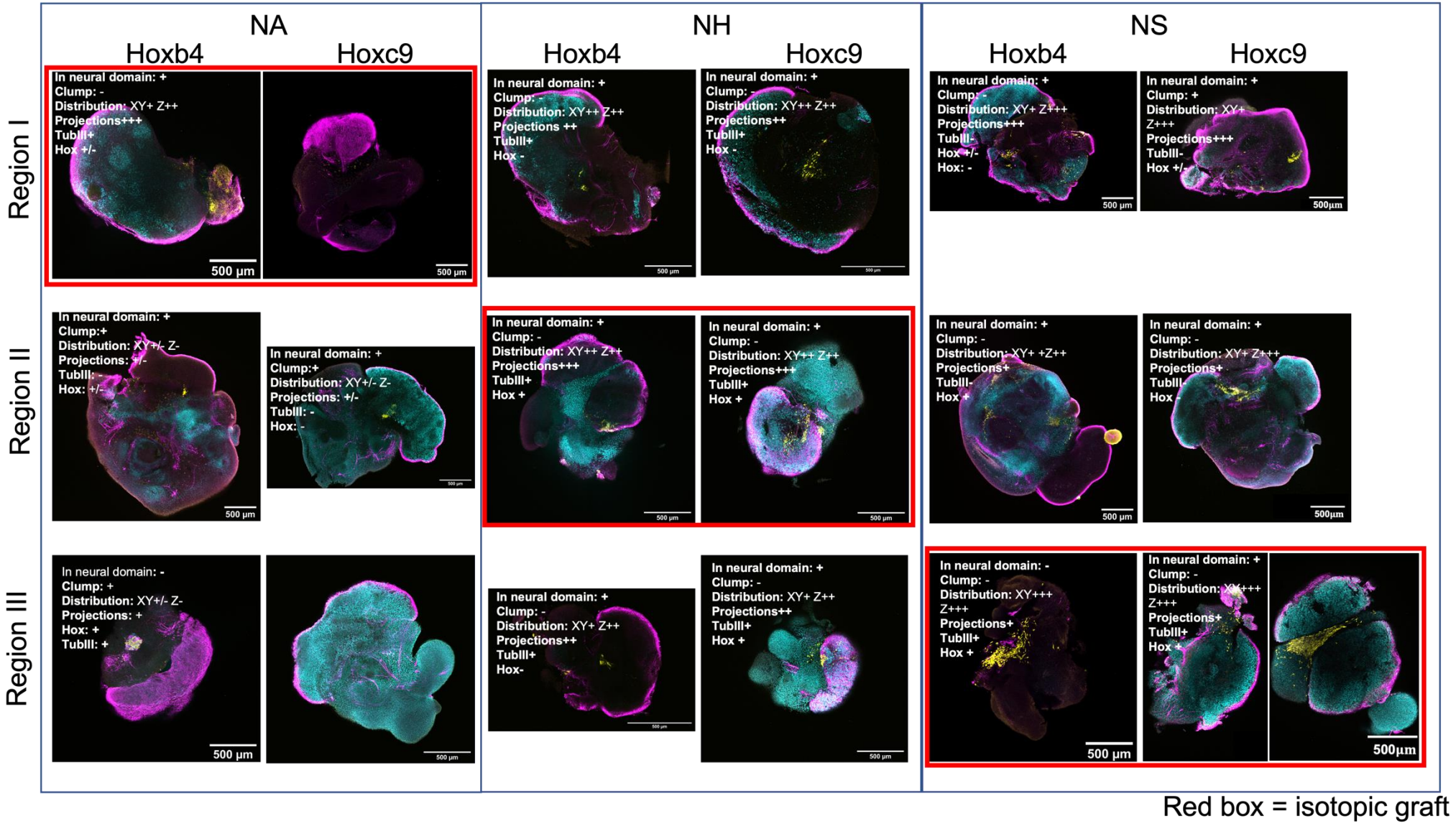

Figure 5.7. Determining phenotypical differences between grafts of different axial identity at different anteroposterior levels.

Panel of spinal cord slices at D5 post-engraftment at different homotopic and heterotopic locations stained for ICC with (yellow), TubIII (purple) and Hoxb4 or Hoxc9 (cyan) (as indicated). Region I (anterior site), Region II (cervical site), Region III (posterior site). + (positive gene expression) – (negative gene expression) XY (distribution of cells across the surface) z (distribution of cells along the z-stack = into the tissue) projections (length of axon-like structures).

Table 5.5. Summary of grafts in "In-slice cultures" for neural identity.

Engraftment results sorted by their grafted cell identity, graft location and overall number of recorded grafts. Summary results of grafted cells stained for neural marker TubIII. G (Graft), H (Host environment), + (positive gene expression), - (negative gene expression). Symbol ± indicate the number of samples which could not be fully confirmed. Samples therefore were inserted into the table according to most likely to match.

Region I

TubIII

Grafted cell identity	G H	G H	G H	G H
	+ -	- +	+ +	- -
Anterior (N= 1)	0	0	1	0
Cervical (N= 2)	0	0	(2±)*	0
Posterior (N= 2)	0	2	0	0

Region II

TubIII

Grafted cell identity	G H	G H	G H	G H
	+ -	- +	+ +	- -
Anterior (N= 1)	0	0	(1±)	1
Cervical (N= 2)	0	0	2	0
Posterior (N= 2)	2	0	0	0

Region III

TubIII

Grafted cell identity	G H	G H	G H	G H
	+ -	- +	+ +	- -
Anterior (N= 1)	0	0	1	0
Cervical (N= 2)	0	0	2	0
Posterior (N= 2)	0	0	2	0

Table 5.6. Summary of grafts in "In-slice cultures" for axial identity.

Engraftment results sorted by their grafted cell identity, graft location and overall number of recorded grafts. Summary results of grafted cells stained for axial markers Hoxb4 and Hoxc9. G (Graft), H (Host environment), + (positive gene expression), - (negative gene expression). Symbol ± indicate the number of samples which could not be fully confirmed. Samples therefore were inserted into the table according to most likely to match.

Region I

	Hoxb4					Hoxc9			
Grafted cell identity	**G H**	**G H**	**G H**	**G H**		**G H**	**G H**	**G H**	**G H**
	+ -	**- +**	**+ +**	**- -**		**+ -**	**- +**	**+ +**	**- -**
Anterior (N= 1)	0	1	0	0	**Anterior** (N= 0)	--	--	--	--
Cervical (N= 1)	0	0	1	0	**Cervical** (N= 1)	0	1	0	0
Posterior (N= 1)	0	0	(1±)	0	**Posterior** (N= 1)	0	(1±)	0	0

Region II

	Hoxb4					Hoxc9			
Grafted cell identity	**G H**	**G H**	**G H**	**G H**		**G H**	**G H**	**G H**	**G H**
	+ -	**- +**	**+ +**	**- -**		**+ -**	**- +**	**+ +**	**- -**
Anterior (N= 1)	0	1	0	0	**Anterior** (N= 1)	0	0	(1±)*	0
Cervical (N= 1)	0	0	1	0	**Cervical** (N= 1)	0	0	1	0
Posterior (N= 1)	0	0	(1±)	0	**Posterior** (N= 1)	0	0	1	0

Region III

	Hoxb4					Hoxc9			
Grafted cell identity	**G H**	**G H**	**G H**	**G H**		**G H**	**G H**	**G H**	**G H**
	+ -	**- +**	**+ +**	**- -**		**+ -**	**- +**	**+ +**	**- -**
Anterior (N= 1)	0	0	1	0	**Anterior** N=0	--	--	--	--
Cervical (N= 1)	0	0	0	**1**	**Cervical** N=1	0	0	1	0
Posterior (N= 0)	--	--	--	--	**Posterior** N=2	0	0	2	0

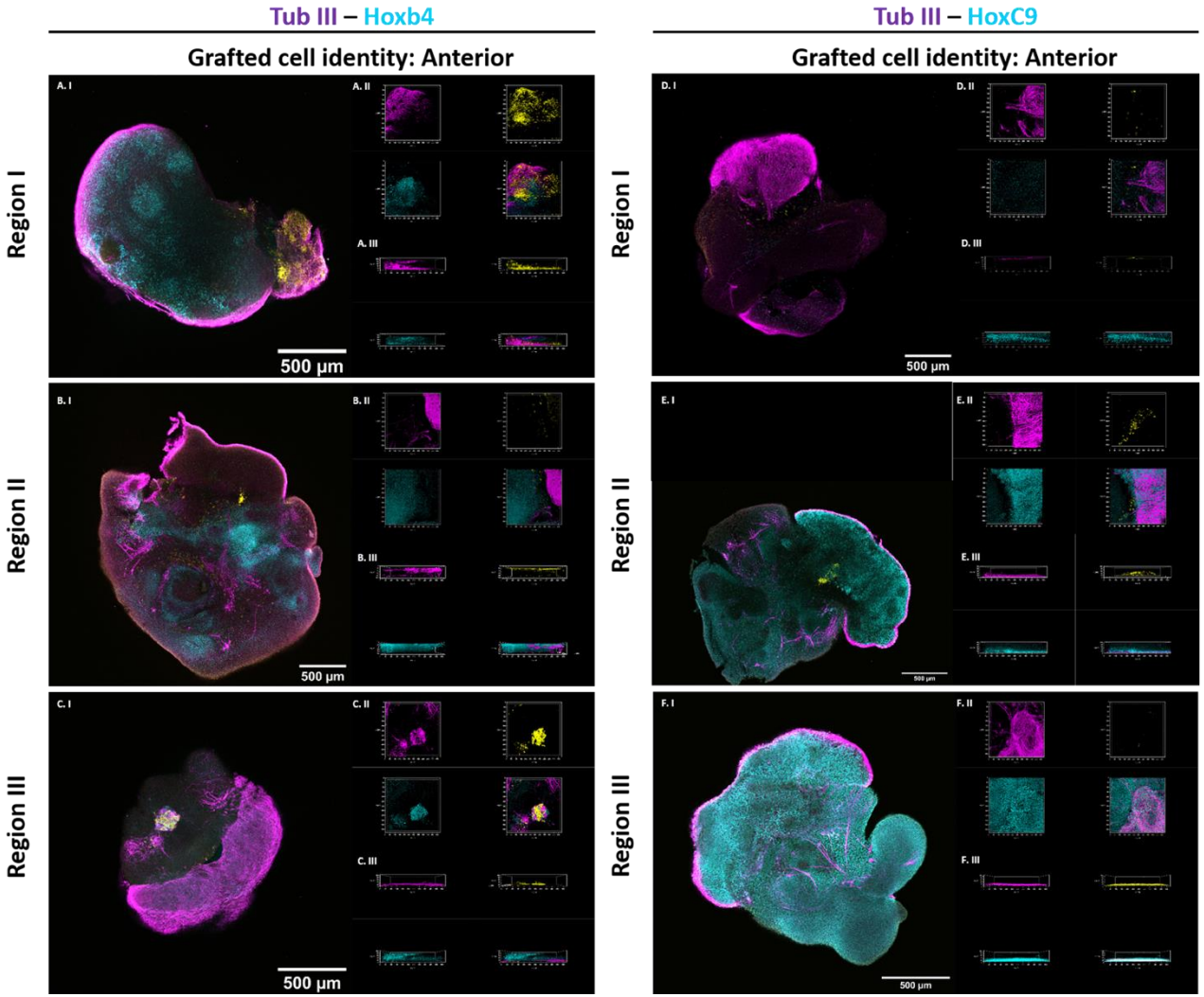

Figure 5.8. Determining phenotypical differences of anterior grafts in "Whole-embryo culture grafts".

Panel of spinal cord slices at D5 post-engraftment at different homotopic and heterotopic locations stained for ICC with GFP (yellow), ßIII tubulin (purple) and Hoxb4 or Hoxc9 (cyan) (as indicated). Region I (anterior site), Region II (cervical site), Region III (posterior site). A z-stack was carried out for each graft at a 20x magnification to assess differences in phenotype and extent of penetration and distribution into and throughout the tissue. This panel is an overview of cells of an anterior identity grafted into anterior, cervical and posterior spinal cord slices. I. Tissue slice, II. XY view of the region of interest, III. Z-stack view.

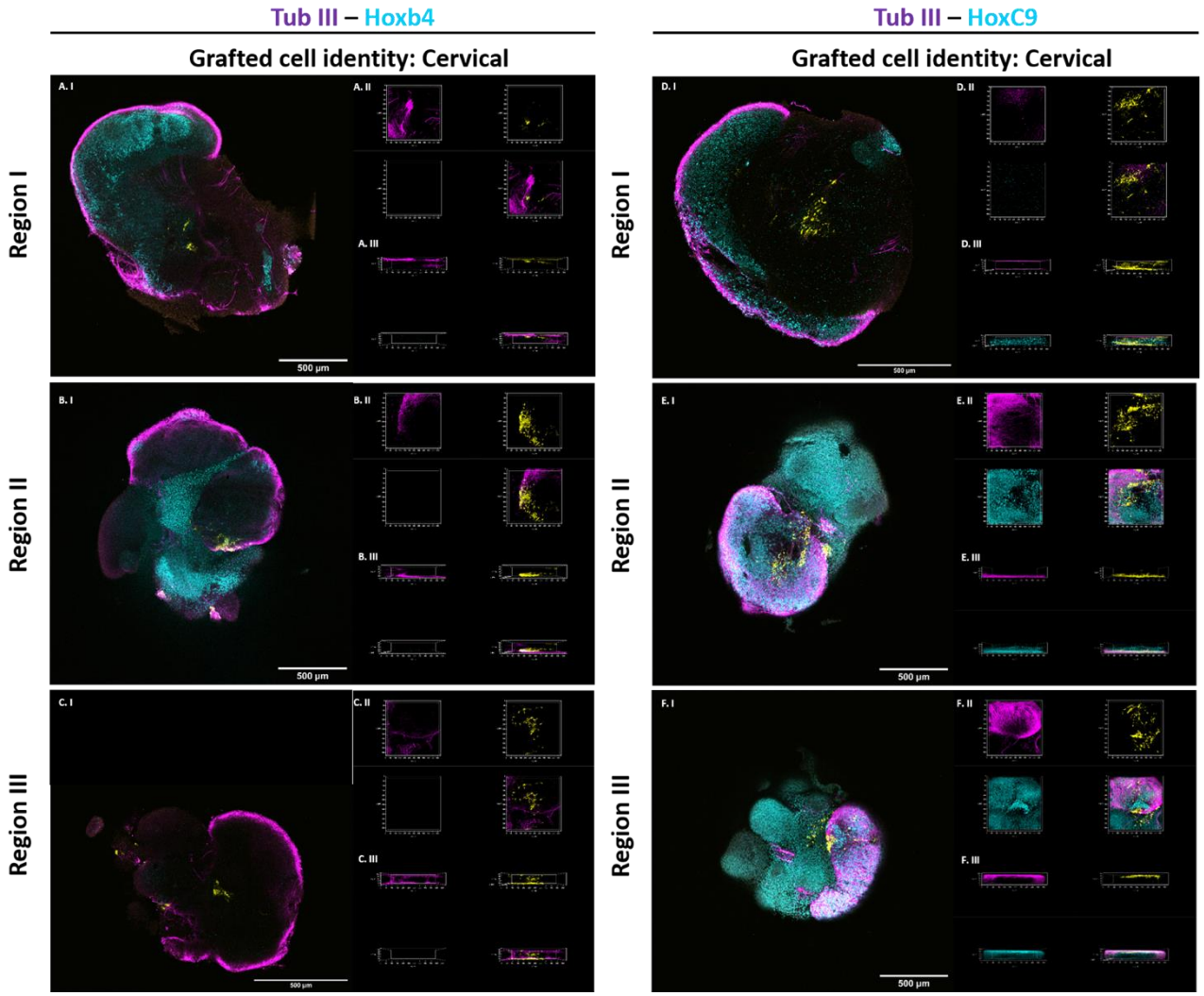

Figure 5.9. Determining phenotypical differences of cervical grafts in "Whole-embryo culture grafts".

Panel of spinal cord slices at D5 post-engraftment at different homotopic and heterotopic locations stained for ICC with GFP (yellow), ßIII tubulin (purple) and Hoxb4 or Hoxc9 (cyan) (as indicated). Region I (anterior site), Region II (cervical site), Region III (posterior site). A z-stack was carried out for each graft at a 20x magnification to assess differences in phenotype and extent of penetration and distribution into and throughout the tissue. This panel is an overview of cells of a cervical identity grafted into anterior, cervical and posterior spinal cord slices. I. Tissue slice, II. XY view of the region of interest, III. Z-stack view.

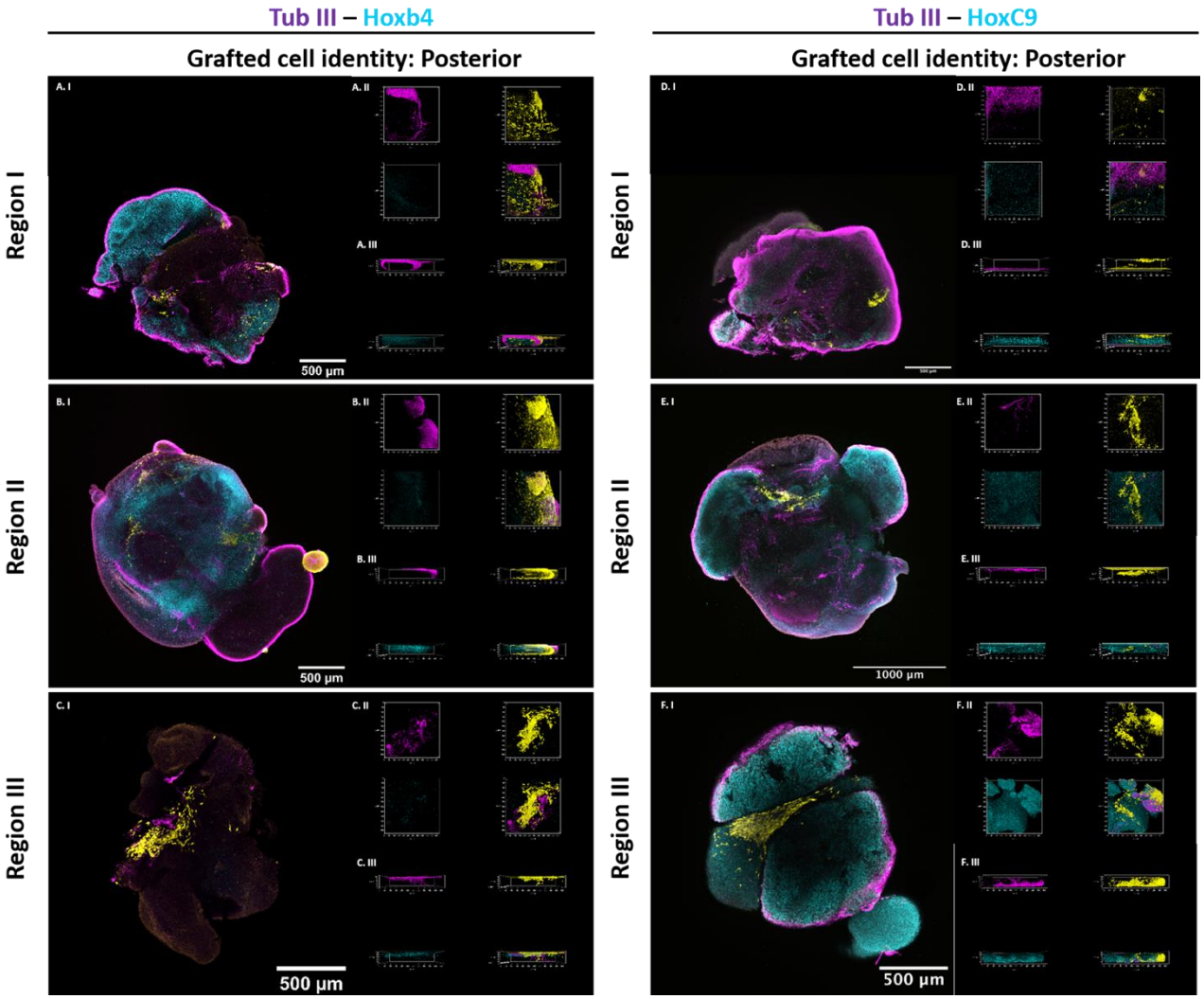

Figure 5.10. Determining phenotypical differences of posterior grafts in "Whole-embryo culture grafts".

Panel of spinal cord slices at D5 post-engraftment at different homotopic and heterotopic locations stained for ICC with GFP (yellow), ßIII tubulin (purple) and Hoxb4 or Hoxc9 (cyan) (as indicated). Region I (anterior site), Region II (cervical site), Region III (posterior site). A z-stack was carried out for each graft at a 20x magnification to assess differences in phenotype and extent of penetration and distribution into and throughout the tissue. This panel is an overview of cells of posterior identity grafted into anterior, cervical and posterior spinal cord slices. I. Tissue slice, II. XY view of the region of interest, III. Z-stack view.

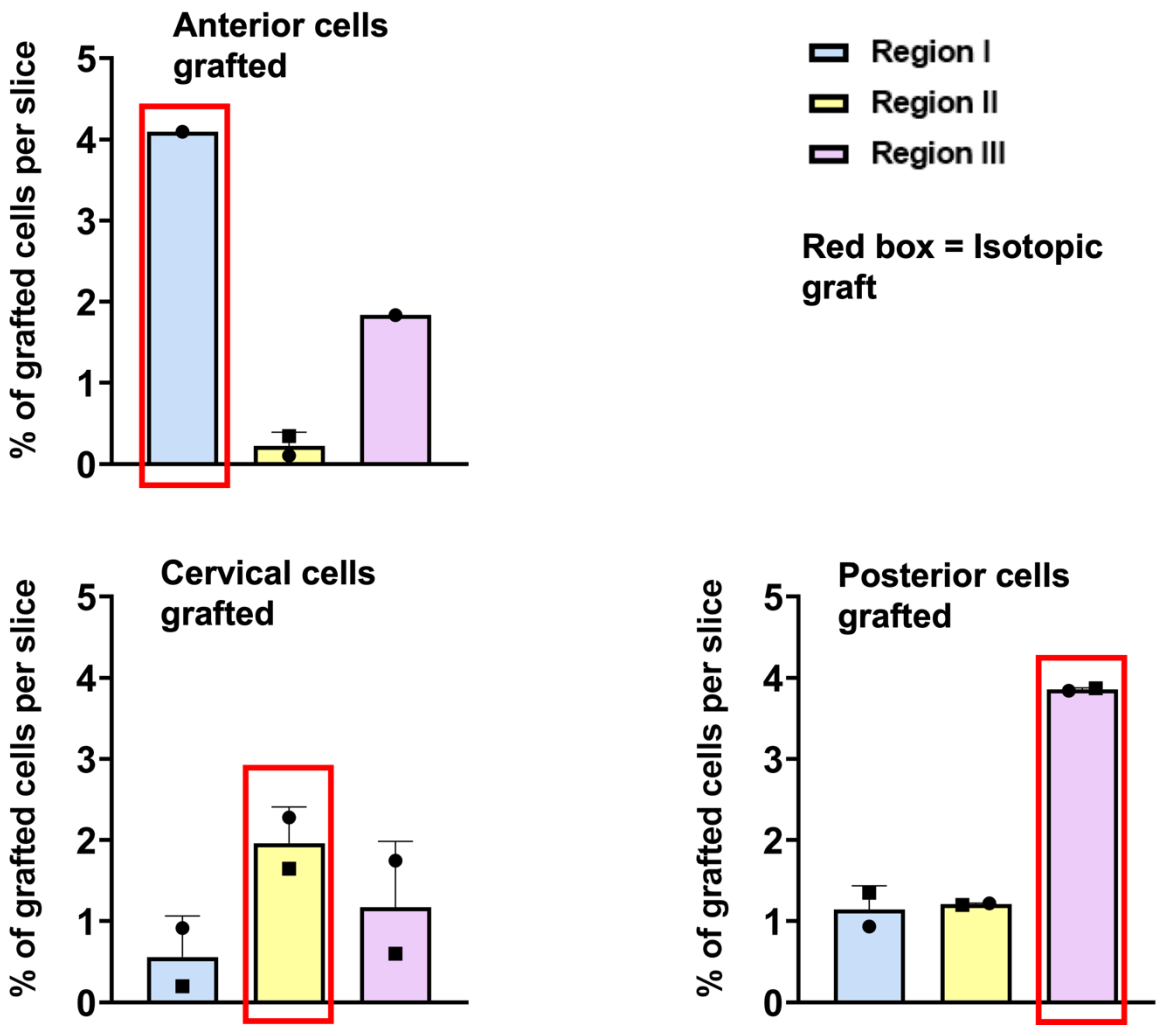

Figure 5.11. Quantification of grafted cells in spinal cord tissue slices.

Bar plots representing the percentage of grafted GFP+ve cells recorded for each slice at different regions. Error bars represent the standard deviation for 2 biological replicates with 2 loading replicates each. Except for grafted cells of anterior identity at regions I and III, where only one 1 replicate was recovered.

5. Discussion of chapter 5

In chapter 5, I have demonstrated that NPCs of different axial identity generated from EpiSCs can survive and, under certain conditions, integrate well when grafted in E10.5 embryos and spinal cord slices. This allows us to determine graft plasticity and neural differentiation in different environments. Cells were grafted into embryos as “whole-embryo culture grafts” or into spinal cord slices as "slice culture grafts". Most grafts stained positive for TubIII when the grafted site was also positive for TubIII. This suggests that grafted cells may benefit from paracrine effects from the neural populations at the grafted site (Table 1, .3, .4 and .5). Cells may benefit from neural niche, which contributes to the development and proliferation of neural cells (Riquelme, Drapeau and Doetsch., 2008). This suggests that grafted cells experience paracrine effects released from the endogenous neural populations in the neural tube. This allows cells to survive, retain neural identity and integrate within the graft site. The absence of paracrine effects in TubIII negative regions in the host may lead grafted cells to lose neural identity. Moreover, I found that some cells within the graft become positive for islet1 when grafted in an environment expressing islet1. This further supports the idea that grafts are benefiting from an existing microenvironment that surrounds the CNS. In addition, most grafts were Islet1 negative. This observation was the same regardless of the type of graft. Before grafting, anterior and cervical cells were negative for Islet1, while posterior cells were positive. This indicates that 24h may not be enough time for cells to differentiate or retains motor neuron expression in an endogenous environment

Cells transplanted in whole embryo culture provided insight on how grafted cells integrate, respond, and adapt in an environment in vivo. To further explore the effects of a neural niche on grafted cells, prolonging the culture of NPCs in slice cultures allowed an assessment of NPC differentiation.

Past studies have used micro-dissected regions of postnatal brain or spinal cord slices in the presence of serum for long-term viability (Ulrich et al., 2011, Sypecka et al., 2015). Our system can maintain spinal cord slice cultures for up to 5 days in serum free, defined media. This indicating the possibility of adding factors without any confounding effects of unknown factors present in serum. During this period, slices survived well and TubIII positive axons were visible by 5 days. This allowed the

assessment of grafted cell integration with the host and its effects on Hox gene expression.

In the pilot experiments of “slice culture grafts”, a high proportion of grafts integrate within the spinal cord slices; however, how much the graft extended across the tissue varies depending on the site of the graft. Isotopic grafts show a higher number of GFP+ve cells per unit area in comparison to heterotopic grafts (Figure 5.10). Grafts located at heterotopic sites form cluster which could indicates poor integration. The data shown supports previous observations from cell engraftments studies carried out in the anterior CNS, as reported by Kris et al., 2011; Ma et al., 2012 and at anterior sites of the posterior CNS, as described by Kadoya et al., 2016, where cells grafted at different CNS locations have higher integration rates if the graft matches the corresponding axial level. To determine any changes in morphology in grafted NPCs at different axial levels I scored for axonal length. Axonal length is a principal measure of neuron morphology and a proxy for neural function, as it correlates with the number of synapses formed by the axon in its target regions (Rubio-Teves et al., 2021) I found that NPCs in isotopic sites showed longer axons while NPCs at heterotopic sites were shorter. In addition, isotopic grafts were embedded in tubulin-rich populations suggesting higher degree of integration, while NPCs in heterotopic grafts appeared to be at different focal planes.

Transplantation experiments carried out by Trainor and Krumlauf suggest that neural crest cell axial identity can adapt to that of the surrounding environment, perhaps because these cells intermingle extensively with the host. However, these observations are primarily from posterior cells grafted into anterior sites and not vice-versa. Results shown in Table 5.2 and 5.6 and figures 5.3 and 5.6 show that whether they are being grafted in vivo or ex vivo, grafted cells retain their corresponding axial identity regardless of grafting location. In contrast to the observations made for neural identity, axial identity of grafted cells does not appear to be influenced by the axial identity of adjacent cells. However, as shown in appendix 6 and table 5.2 posterior grafted cells appear to be able to coexpress posterior and cervical markers when grafted in a cervical site (Region II). This suggests that posterior cells may partially revert to an anterior axial identity to adapt better to the surrounding environment.

Itasaki et al., 1996 findings suggest the existence of a posterior dominance. Krumlauf suggests that anterior segments would express low-inducing signals, while more posterior segments would be exposed to increasing levels of signals, causing them to adopt more posterior identities. Anterior tissues grafted in posterior regions would become exposed to higher signals and switch fate, while posterior tissue grafted to the anterior would move tissues from a high signal area to a lower one resulting in no changes regarding their axial identity. This can result in cells retaining the signals they were exposed to, resulting in a posterior dominance. Therefore, plasticity is revealed only in A-P rhombomere transplantation, suggesting a ratchet-like mechanism where changes in cell fate can occur only on one direction (posteriorly). My results suggest that this model does not hold for the CNS posterior to the hindbrain. Posterior cells are the only grafts recovered which appear to be able to change fate when grafted to a cervical site with grafts showing signs of coexpression for Hoxb4 and Hoxc9. This is interesting because before grafting, NS cultures produced cells expressing Hoxc9 and Hoxb4. However, expression of Hoxb4 was found in a minority of cells and expression was mutually exclusive in NS cultures dictating that cells in this condition had already adopted either a cervical or posterior identity (appendix 5).

As discussed in chapter 1 (sections 1.4 and 1.5), the regulatory networks that operate in the anterior and posterior CNS are different. In addition, the anterior CNS is more differentiated than the posterior CNS at any one time during axis elongation, because the more posterior parts of the CNS have been produced more recently. Either or both of these factors could lead to a higher degree of plasticity in cells in the posterior CNS (spinal cord) than those found more anteriorly (head and neck).

Finally, I decided to study the functional properties of the in vitro-differentiated NPS of posterior spinal cord cells (NS-P) described in chapter 4. I found that grafts lost expression of Hoxc13 but retained expression of Hoxc9 (figure 5.5). This would support our previous finding suggesting that posterior cells have a higher degree of plasticity. However, this was only observed in one graft and further staining must be done prior to reaching any conclusion. In situ data in mice does not show strong expression of Hoxc13 in tissue until stages E11.5-12.5 of development. In addition, tail cells were grafted at a thoracic site and not in a region matching their axial identity. The lack of supportive environment could have led to the loss observed in sacral

identity and instead showing expression for Hoxc9 which would match the grafted site. Heterochronic transplantation studies by McGrew et al., 2008 of cells from the tail tip to the earlier primitive streak showed that the anteroposterior identity of cells can be reset, therefore indicating that cells can change their transcriptome upon grafting. Together this suggests that extrinsic signals may play a big role in defining the temporal NMP transcriptional state.

Furthermore, I also observed that NS and NS-P grafts can retain neural identity after transplantation. However, the number of recovered grafts positive for TubIII was very low in comparison to NA and NH grafts. This was also observed in NS grafts, where the number of recovered grafts positive for TubIII was lower in comparison to grafts from NA and NH cells. A possible explanation could be that at E10.5, neuralising signals are much more predominant at anterior sites, and this allows cells to retain neural identity better.

6. Conclusion and future work.

The discovery of how to generate neuromesodermal progenitors in vitro from pluripotent stem cells (Gouti et al., 2014) led to several new studies aimed at optimising protocols to generate Sox2+ Tbra+ ve cultures from human (hPSC) (Frith et al., 2018) and mouse PSCs (ESCs and EpiSCs). These cells are able to express caudal markers up to PG9, differentiate into neural and mesodermal cells types in vitro and contribute to neural tube and paraxial mesoderm after engraftment (Tsakiridis et al., 2014). These cells offer an attractive approach to advance a broad range of discoveries in both basic and translational medicine by providing a deeper understanding of the events that occur during the development of the anteroposterior axis.

Subsequent studies further described protocols using NMPs to generate a broad range of cell types: NPCs, neural crest cells (NCCs), paraxial mesoderm and lateral plate/intermediate mesoderm. This provided the opportunity to study a broad range of abnormalities such as limb defects, muscular dystrophies, neural crest defects (neurocristopathies), neurodegenerative and neuromuscular conditions and spinal cord injury (reviewed in Cooper and Tsakiridis et al., 2022). However, despite the thorough work published it is still not possible to generate tissue of all axial level. The starting points of my thesis was to overcome these limitations and contribute towards the use of NMPs as viable tools to study events that occur late in the axis or to fully understand the clinical importance of axial identity across all anteroposterior levels. In this thesis, I aim to address some of these limitations. In chapter 3, I report the generation of reproducible and homogenous NPCs of different axial identity in EpiSCs and ESCs which allowed to compare my results with those already published. In addition, I showed that I can generate cells with similar levels of axial marker expression to those found in E10.5 embryos. In chapter 4, I describe in detail the effects of GDF11 on NMP cultures, showing protocols to generate neural and endoderm progenitors. This further shows the potential of NMPs to generate derivatives of posterior cell types. Furthermore, for the first time, I show expression of Hoxc13 in neural progenitor cells derived from EpiSCs. In chapter 3, I tested the effects of different matrices and prolonged culture to generate lumbar/sacral identity in 2D. However, cells only showed thoracic identity. Unpublished work in the lab showed that

by culturing NMPs in a 3D matrigel suspension, it is possible to induce PG13. Therefore, It would be interesting to test different mechanical stimuli on NMP cultures that recapitulates an NMP niche environment and test whether this causes changes in axial expression. Overall, this is exciting as it provides important insights into how to generate tissue expressing sacral identity which can be used in disease modelling for defects in the late axis.

In this thesis, I also explored the importance of axial identity in cell survival, integration, and differentiation in an attempt to further understand the therapeutic potential of NMPs.

In chapter 5, I described direct stem cell transplantation of NPCs of different axial identity into whole embryos and spinal cord slices. This approach has allowed me to follow the fate of transplanted cells, their ability to differentiate and their potential to migrate across the tissue and form connections. Overall, I show that grafting cells to isotopic regions results in higher levels of distribution throughout the tissue. However, the spinal cord slice experiments were a pilot experiment and therefore, it is important to increase the number of replicates before making any conclusions from the data here shown. To determine functional differences, further studies could include direct stem cell transplantation in spinal cord organotypic slice cultures. This would allow us to understand long fibre trajectories and the formation of new connections by further staining and electrophysiology tests to determine synaptic activity. The use of a spinal cord injury model would also allow us to understand the formation of new connections, and neurorepair processes occurring after the spinal cord injury. It would also be possible to observe local inflammatory responses to the grafts caused by macrophages/microglia activation in respects of the type of cell grafted.

In conclusion, I envisage that the efficient generation of NPCs of posterior axial identity described in these protocols will allow for a direct functional comparison to anterior counterparts, allowing us to determine whether any changes observed in vivo from EpiSC-derived spinal cord cells are a result of the differences in axial identity or due

to extrinsic factors. Overall, I hope that the in vivo work here described and reported positive effects from isotopic grafting contributes to further understand the importance of axial identity as a crucial factor in cell replacement therapies for spinal cord injury, and, therefore their use in regenerative medicine.

Appendix

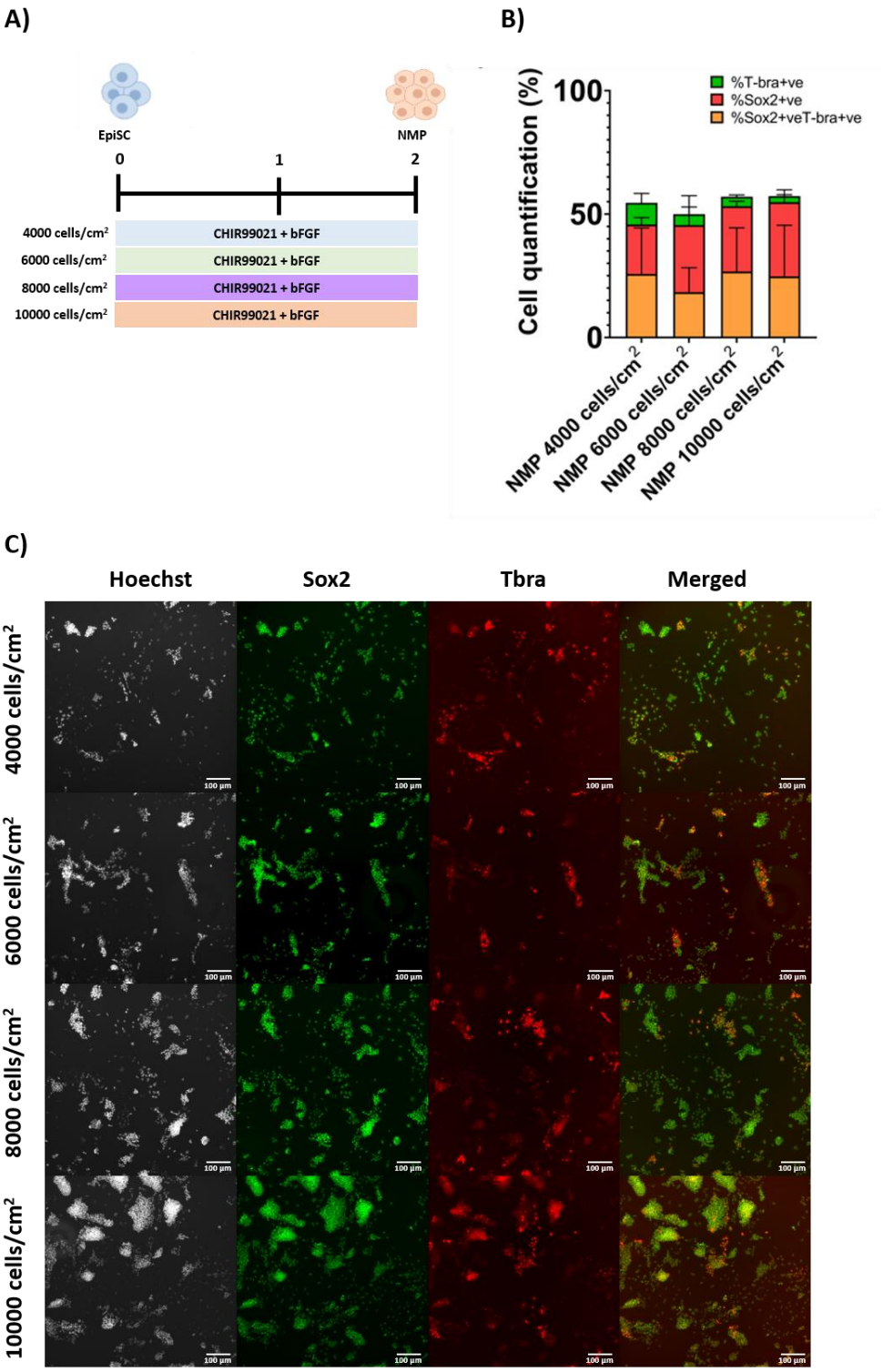

Appendix 1. Generation of NMPs at different cell densities from EpiSC.

(A) Scheme describing the culture conditions employed for NMP differentiation of EpiSCs plated at different cell densities treated for 48h with FGF/Chiron. (B) Brachyury/Sox2 immunocytochemistry in EpiSC cells plated at different densities treated with FGF/Chiron. (C) Quantification of $Sox2^{+}$, T-$brachyury^{+}$ and $Sox2^{+}$T-$brachyury^{+}$ cells. DAPI was used as a nuclear counterstain. Error bars represent the standard deviation for 3 biological replicates.

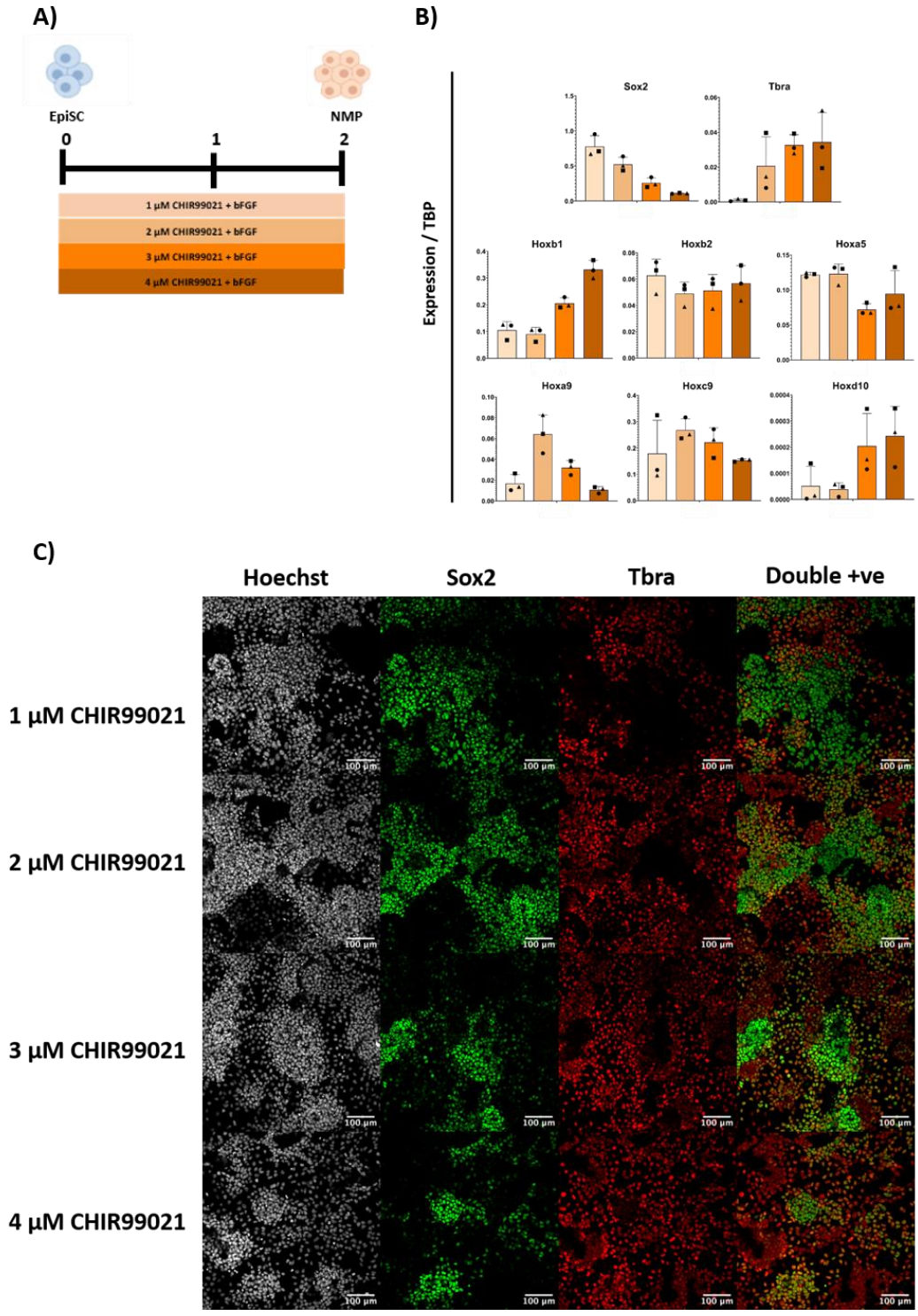

Appendix 2. Chiron titration in NMPs.

A) Scheme describing the culture conditions employed for NMP differentiation of EpiSCs plated for 48h with FGF/Chiron. Chiron concentration used were 1uM, 2uM, 3uM and 4uM. (B) qPCR analysis for indicated markers in mouse cells treated with bFGF + Chiron at different concentrations. Results are represented as values relative to housekeeping gene TBP (One-way ANOVA). Error bars represent the standard deviation for 3 biological replicates with 3 loading replicates each. (C) Brachyury/Sox2 immunohistochemistry in EpiSC cells treated with FGF and Chiron at different concentrations.

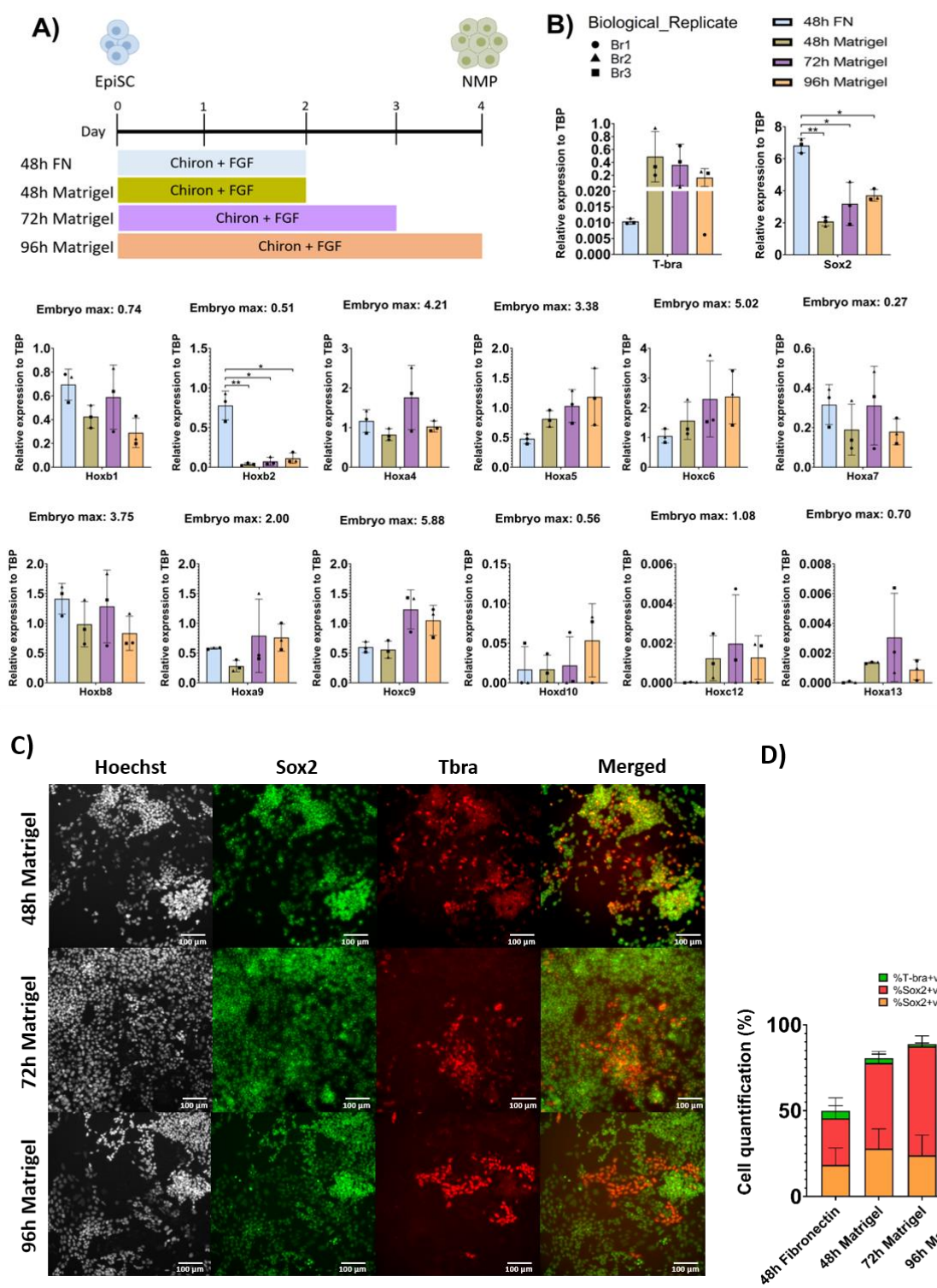

Appendix 3. Charatcterisation of NMPs in prolonged culture.

(A) Scheme describing the culture conditions employed for NMP differentiation of EpiSCs treated for 48h, 72h and 96h. (B) qPCR analysis for indicated markers in mouse cells treated with bFGF + Chir. Results are represented as values relative to housekeeping gene TBP (*p≤0.05, **p≤0.01) (One-way ANOVA). Error bars represent the standard deviation for 3 biological replicates with 3 loading replicates each. (C) T-Brachyury/Sox2 immunohistochemistry in EpiSC cells treated with FGF/Chiron for 48h, 72h and 96h on matrigel (D) Quantification of showed Sox2+ and T-brachyury+ and Sox2+T-brachyury+ across treatments. DAPI was used as a nuclear counterstain. Error bars represent the standard deviation for 3 biological replicates. Maximum expression levels detected in vivo for each Hox gene are shown above each qPCR plot respectivel

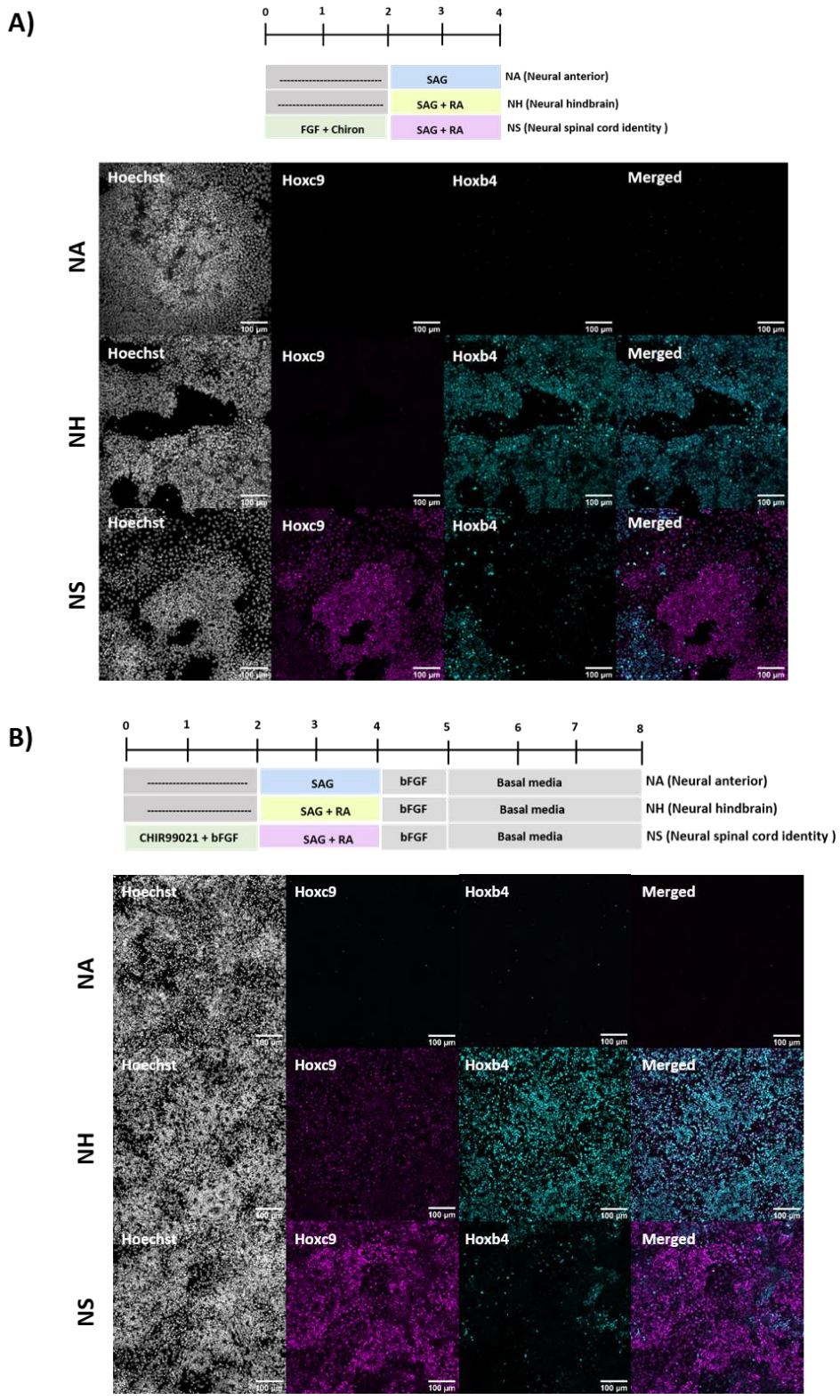

Appendix 4. Identifying axial identity in NPC cultures at D4 and D5 of differentiation.

ICC staining for Hoxc9 and Hoxb4 in NPCs of Anterior (NA), Hindbrain (NH) and spinal cord (NP) identities at A) Day 4 and B) Day 8 of differentiation.

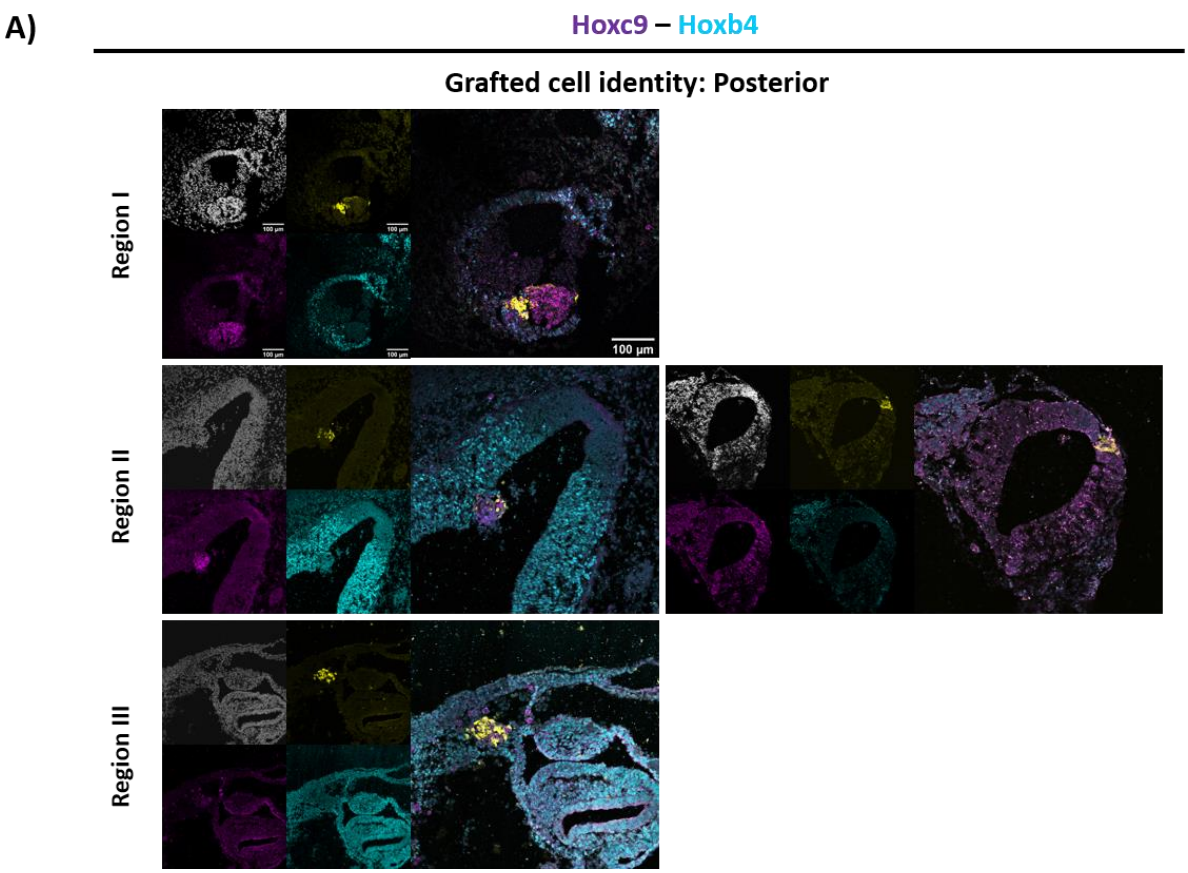

Appendix 5. Assessing axial plasticity of posterior grafted cells.

A) Panel of representative embryo sections with successful grafts at different homotopic and heterotopic locations stained for GFP (yellow), Hoxc9 (purple) and Hoxc4 (cyan) by ICC. Region I (anterior site), Region II (cervical site), Region III (posterior site). Selected images are representative of grafted cells at the neural tube or adjacent unless stated otherwise

References.

Aaku-saraste, E., Hellwig, A. and Huttner, W. B. (1996). Loss of Occludin and Functional Tight Junctions, but not ZO-1, during Neural Tube Closure — Remodeling of the Neuroepithelium Prior to Neurogenesis. Dev. Biol. 679, 664–679.

Abu-Abed, S., Dolle, P., Metzger, D., Beckett, B., Chambon, P., Petkovich, M., (2001). The retinoic acid-metabolizing enzyme, CYP26A1, is essential for normal hindbrain patterning, vertebral identity, and development of posterior structures. Genes Dev. 15, 226–240.

Agarwala, S., Sanders, T. A. and Ragsdale, C. W. (2001). Sonic hedgehog control of size and shape in midbrain pattern formation. Science 291,2147-2150.

Aiba K., Sharov A.A., Carter M.G., Foroni C., Vescovi A.L., Ko M.S.H. (2006). Defining a developmental path to neural fate by global gene expression profiling of mouse embryonic stem cells and adult neural stem progenitor cells. Stem Cells 24:889-895.

Aires, R., de Lemos, L., Novoa, A., Jurberg, A. D., Mascrez, B., Duboule, D. and Mallo, M. (2019). Tail bud progenitor activity relies on a network comprising Gdf11, Lin28, and Hox13 genes. Dev. Cell 48, 383-395.e8.

Amin, S., Neijts, R., Simmini, S., van Rooijen, C., Tan, S. C., Kester, L., van Oudenaarden, A., Creyghton, M. P. and Deschamps, J. (2016). Cdx and T Brachyury co-activate growth signaling in the embryonic axial progenitor niche. Cell Rep 17, 3165-3177.

Amoroso, M. W., Croft, G. F., Williams, D. J., O'Keeffe, S., Carrasco, M. A., Davis, A. R., Roybon, L., Oakley, D. H., Maniatis, T., Henderson, C. E. *et al*. (2013). Accelerated high-yield generation of limb-innervating motor neurons from human stem cells. J. Neurosci. 33, 574-586.

Anderson, M. J., Naiche, L. A., Wilson, C. P., Elder, C., Swing, D. A. and Lewandoski, M. (2013). TCreERT2, a transgenic mouse line for temporal control of Cre-mediated

recombination in lineages emerging from the primitive streak or tail bud. PLoS ONE 8, e62479.

Andersson O, Reissmann E, Ibáñez CF (2006) Growth differentiation factor 11 signals through the transforming growth factor-beta receptor ALK5 to regionalize the anterior-posterior axis. *EMBO Rep*. 7: 831–837

Andersson O, Reissmann E, Ibáñez CF. (2006). Growth differentiation factor 11 signals through the transforming growth factor-beta receptor ALK5 to regionalize the anterior-posterior axis. EMBO Rep. Aug;7(8):831-7.

Arkell, R.M., and Tam, P.P.L. (2012). Initiating head development in mouse embryos: integrating signalling and transcriptional activity. Open Biol. *2*, 120030–120030.

Avagliano L, Massa V, George TM, Qureshy S, Bulfamante GP, Finnell RH (2019). Overview on neural tube defects: From development to physical characteristics. Birth Defects Res. Nov 15;111(19):1455-1467.

Bachiller, D., Klingensmith, J., Kemp, C., Belo, J.A., Anderson, R.M., May, S.R., McMahon, J.A., McMahon, A.P., Harland, R.M., Rossant, J., et al. (2000). The organizer factors Chordin and Noggin are required for mouse forebrain development. Nature *403*, 658–661.

Bain, G., Kitchens, D., Yao, M., Huettner, J.E., and Gottlieb, D.I. (1995). Embryonic Stem Cells Express Neuronal Properties in Vitro. Dev. Biol. *168*, 342–357.

Beccari, L., Moris, N., Girgin, M., Turner, D. A., Baillie-Johnson, P., Cossy, A. C., Lutolf, M. P., Duboule, D. and Arias, A. M. (2018). Multi-axial self-organization properties of mouse embryonic stem cells into gastruloids. Nature 562, 272-276

Beddington R.S.P., Robertson E.J. (1999). Axis development and early asymmetry in mammals. Cell 96:195-209.

Beddington, B. R. S. P. (1981). An autoradiographic analysis of the potency of embryonic ectoderm in the 8th day postimplantation mouse embryo. J. Embryol. Exp. Morphol. 64, 87–104.

Beddington, B. R. S. P. (1982). An autoradio graphic analysis of tissue potency in different regions of the embryonic ectoderm during gastrulation in the mouse. J. Embryol. Exp. Morphol. 69, 265–285.

Beddington, R.S. (1994). Induction of a second neural axis by the mouse node. Development 120, 613–620.

Bernemann, C., Greber, B., Ko, K., Sterneckert, J., Han, D.W., Araúzo-Bravo, M.J., and Schöler, H.R. (2011). Distinct developmental ground states of epiblast stem cell lines determine different pluripotency features. Stem Cells *29*, 1496–1503.

Bialecka, M., Wilson, V. and Deschamps, J. (2010). Cdx mutant axial progenitor cells are rescued by grafting to a wild type environment. Dev. Biol. 347, 228-234.

Boulet, A.M., and Capecchi, M.R. (2012). Signaling by FGF4 and FGF8 is required for axial elongation of the mouse embryo. Dev. Biol. *371*, 235–245.

Bradley A., Evans M., Kaufman M.H., Robertson E. (1984). Formation of germ-line chimaeras from embryo-derived teratocarcinoma cell lines. Nature 309:255-256.

Brons I.G.M., Smithers L.E., Trotter M.W.B., Rugg-Gunn P., Sun B., Chuva de Sousa Lopes S.M., Howlett S.K., Clarkson A., Ahrlund-Richter L., Pedersen R.A., Vallier L. (2007). Derivation of pluripotent epiblast stem cells from mammalian embryos. Nature 448:191-195.

Cambray, N., and Wilson, V. (2002). Axial progenitors with extensive potency are localised to the mouse chordoneural hinge. Development *129*, 4855–4866.

Cambray, N., and Wilson, V. (2007). Two distinct sources for a population of maturing axial progenitors. Development *134*, 2829–2840.

Carpenter AE, Jones TR, Lamprecht MR, Clarke C, Kang IH, Friman O, Guertin DA, Chang JH, Lindquist RA, Moffat J, Golland P, Sabatini DM (2006) CellProfiler: image analysis software for identifying and quantifying cell phenotypes. Genome Biology 7:R100.

Chalamalasetty, R. B., Garriock, R. J., Dunty, W. C., Jr, Kennedy, M. W., Jailwala, P., Si, H. and Yamaguchi, T. P. (2014). Mesogenin 1 is a master regulator of paraxial presomitic mesoderm differentiation. Development 141, 4285-4297

Chambers S.M., Fasano C.A., Papapetrou E.P., Tomishima M., Sadelain M., Studer L. (2009). Highly efficient neural conversion of human ES and iPS cells by dual inhibition of SMAD signaling. Nature Biotechnology 27:275-280.

Chiang, C., Litingtung, Y., Lee, E. *et al.* (1996) Cyclopia and defective axial patterning in mice lacking *Sonic hedgehog* gene function. *Nature* 383, 407–413.

Clevers, H. (2006). Wnt/B-Catenin Signaling in Development and Disease. *Cell* 127, 469–480.

Cooper, F., Gentsch, G. E., Mitter, E., Bouissou, C., Healy, L., Hernandez-Rodriguez, A., Smith, J. C. and Bernardo, A. S. (2020). Rostrocaudal patterning and neural crest differentiation of human pre-neural spinal cord progenitors in vitro. bioRxiv Curr. Opin. Cell Biol., 73 pp. 133-140

Couly G, Grapin-Botton A, Coltey P, Ruhin B, Le Douarin NM. (1998). Determination of the identity of the derivatives of the cephalic neural crest: incompatibility between Hox gene expression and lower jaw development. *Development* ;125:3445–3459.

De Santa Barbara P, Roberts DJ. Tail gut endoderm and gut/genitourinary/tail development: a new tissue-specific role for Hoxa13. Development. 2002 Feb;129(3):551-61.

Di-Gregorio A., Sancho M., Stuckey D.W., Crompton L.A., Godwin J., Mishina Y., Rodriguez T.A. (2007). BMP signalling inhibits premature neural differentiation in the mouse embryo. Development 134:3359-3369.

Diaz-Cuadros, M., Wagner, D. E., Budjan, C., Hubaud, A., Tarazona, O. A., Donelly, S., Michaut, A., Al Tanoury, Z., Yoshioka-Kobayashi, K., Niino, Y. et al. (2020). In vitro characterization of the human segmentation clock. Nature 580, 113-118.

Edri, S., Hayward, P., Baillie-Johnson, P., Steventon, B. J. and Martinez Arias, A. (2019a). An epiblast stem cell-derived multipotent progenitor population for axial extension. Development 146, dev168187.

Edri, S., Hayward, P., Jawaid, W. and Martinez Arias, A. (2019b). Neuro-mesodermal progenitors (NMPs): a comparative study between pluripotent stem cells and embryo-derived populations. Development 146, dev180190.

Evans M.J., Kaufman M.H. (1981). Establishment in culture of pluripotential cells from mouse embryos. Nature 292:154-156.

F.J. Wymeersch, V. Wilson, A. Tsakiridis. (2021).Understanding axial progenitor biology in vivo and in vitro. Development, 148

Faunes F., Hayward P., Muñoz Descalzo S., Chatterjee S.S., Balayo T., Trott J., Christoforou A., Ferrer-Vaquer A., Hadjantonakis A.K., Dasgupta R., Martinez Arias A. (2013). A membrane-associated β-catenin/Oct4 complex correlates with ground-state pluripotency in mouse embryonic stem cells. Development 140:1171-1183.

Forlani, S., Lawson, K. a, and Deschamps, J. (2003). Acquisition of Hox codes during gastrulation and axial elongation in the mouse embryo. Development *130*, 3807–3819.

Frith, T. J., Granata, I., Wind, M., Stout, E., Thompson, O., Neumann, K., Stavish, D., Heath, P. R., Ortmann, D., Hackland, J. O. et al. (2018). Human axial progenitors generate trunk neural crest cells in vitro. Elife 7, e35786.

Frith, T. J., Granata, I., Wind, M., Stout, E., Thompson, O., Neumann, K., Stavish, D., Heath, P. R., Ortmann, D., Hackland, J. O. et al. (2018). Human axial progenitors generate trunk neural crest cells in vitro. Elife 7, e35786

Galvin K.E., Travis E.D., Yee D., Magnuson T., Vivian J.L. (2010). Nodal signaling regulates the bone morphogenic protein pluripotency pathway in mouse embryonic stem cells. The Journal of Biological Chemistry 285:19747-19756.

Garriock RJ, Chalamalasetty RB, Kennedy MW, Canizales LC, Lewandoski M, Yamaguchi TP (2015). Lineage tracing of neuromesodermal progenitors reveals novel

Wnt-dependent roles in trunk progenitor cell maintenance and differentiation. *Development.* 2015;142:1628–1638.

Gaunt, S J., Coletta, P L., Pravtcheva, D and Sharpe, P T (1990) Mouse Hox-3.4 homeobox sequence and embryonic expression patterns compared with other members of the Hox gene network. *Development* 109, 329–337

Goetz, R., and Mohammadi, M. (2013). Exploring mechanisms of FGF signalling through the lens of structural biology. *Nat. Rev. Mol. Cell Biol*. 14, 166–180.

Gould A, Itasaki N, Krumlauf R. 1998. Initiation of rhombomeric *Hoxb4* expression requires induction by somites and a retinoid pathway. *Neuron* 21: 39–51.

Gouti, M., Delile, J., Stamataki, D., Wymeersch, F. J., Huang, Y., Kleinjung, J., Wilson, V. and Briscoe, J. (2017). A Gene Regulatory Network Balances Neural and Mesoderm Specification during Vertebrate Trunk Development. *Dev. Cell* 41, 243–261.e7.

Gouti, M., Metzis, V. and Briscoe, J. (2015). The route to spinal cord cell types: A tale of signals and switches. *Trends Genet.* 31, 282–289.

Gouti, M., Tsakiridis, A., Wymeersch, F.J., Huang, Y., Kleinjung, J., Wilson, V., and Briscoe, J. (2014). In vitro generation of neuromesodermal progenitors reveals distinct roles for wnt signalling in the specification of spinal cord and paraxial mesoderm identity. PLoS Biol. *12*.

Graham, A., Maden, M., Krumlauf, R., (1991). The murine Hox-2 genes display dynamic dorsoventral patterns of expression during central nervous system development. Development 112, 255–264.

Grandel, H., Lun, K., Rauch, G. J., Rhinn, M., Piotrowski, T., Houart, C., Sordino, P., Küchler, A. M., Schulte-Merker, S., Geisler, R., et al. (2002). Retinoic acid signalling in the zebrafish embryo is necessary during pre-segmentation stages to pattern the anterior-posterior axis of the CNS and to induce a pectoral fin bud. Development 129, 2851-2865.

Greber B., Wu G., Bernemann C., Joo J.Y., Han D.W., Ko K., Tapia N., Sabour D., Sterneckert J., Tesar P., Schöler H. (2010). Conserved and divergent roles of FGF signaling in mouse epiblast stem cells and human embryonic stem cells. Cell Stem Cell 6:215-226.

Guo G., Yang J., Nichols J., Hall J.S., Eyres I., Mansfield W., Smith A. (2009). Klf4 reverts developmentally programmed restriction of ground state pluripotency. Development 136:1063-1069.

Gurdon, J. B., Mitchell, A. and Mahony, D.(1995). Direct and continuous assessment by cells of their position in a morphogen gradient. Nature 376,520-521.

Hackland, J. O. S., Shelar, P. B., Sandhu, N., Prasad, M. S., Charney, R. M., Gomez, G. A., Frith, T. J. R. and Garcia-Castro, M. I. (2019). FGF modulates the axial identity of trunk hPSC-derived neural crest but not the cranial-trunk decision. Stem Cell Reports 12, 920-933.

Han D.W., Tapia N., Joo J.Y., Greber B., Araúzo-Bravo M.J., Bernemann C., Ko K., Wu G., Stehling M., Do J.T., Schöler H.R. (2010). Epiblast stem cell subpopulations represent mouse embryos of distinct pregastrulation stages. Cell 143:617-627.

Han DW, Tapia N, Joo JY, Greber B, Araúzo-Bravo MJ, Bernemann C, Ko K, Wu G, Stehling M, Do JT, et al. (2010). Epiblast stem cell subpopulations represent mouse embryos of distinct pregastrulation stages. *Cell* 143: 617–627.

Henrique, D., Abranches, E., Verrier, L., and Storey, K.G. (2015). Neuromesodermal progenitors and the making of the spinal cord. Development *142*, 2864–2875.

Huang Y., Osorno R., Tsakiridis A., Wilson V. (2012). In vivo differentiation potential of epiblast stem cells revealed by chimeric embryo formation. Cell Reports 2:1571-1578.

Hunt, P., Clarke, J. D. W., Buxton, P., Ferretti, P. & Thorogood, P. (1998). Stability and plasticity of neural crest patterning and branchial arch *Hox* code after extensive cephalic crest rotation. *Dev. Biol*. 198, 82–104.

Hynes M, Porter JA, Chiang C, Chang D, Tessier-Lavigne M, Beachy PA, Rosenthal A (1995b) Induction of midbrain dopaminergic neurons by Sonic hedgehog. Neuron 15:35–44.

Itasaki N, Sharpe J, Morrison A, Krumlauf R. (1996). Reprogramming Hox expression in the vertebrate hindbrain: influence of paraxial mesoderm and rhombomere transposition. Neuron. Mar;16(3):487-500.

J.S. Dasen, J.P. Liu, T.M. Jessell. (2003). Motor neuron columnar fate imposed by sequential phases of Hox-c activity. Nature, 425 pp. 926-933,

Jaeger, I., Arber, C., Risner-Janiczek, J. R., Kuechler, J., Pritzsche, D., Chen, I., Naveenan, T., Ungless, M. A. and Li, M. (2011). Temporally controlled modulation of FGF/ERK signaling directs midbrain dopaminergic neural progenitor fate in mouse and human pluripotent stem cells. *Development* 138, 4363–4374.

Jessell, T. (2000). Neuronal specification in the spinal cord: inductive signals and transcriptional codes. *Nat Rev Genet* 1, 20–29

Joo JY, Choi HW, Kim MJ, Zaehres H, Tapia N, Stehling M, Jung KS, Do JT, Schöler HR (2014). Establishment of a primed pluripotent epiblast stem cell in FGF4-based conditions. Sci Rep. 17;4:7477.

Jurberg, A. D., Aires, R., Novoa, A., Rowland, J. E. and Mallo, M. (2014). Compartment-dependent activities of Wnt3a/beta-catenin signaling during vertebrate axial extension. Dev. Biol. 394, 253-263.

K. Niederreither, J. Vermot, B. Schuhbaur, P. Chambon, P. Dolle. (2000) Retinoic acid synthesis and hindbrain patterning in the mouse embryo. *Development* 1 January; 127 (1): 75–85.

Kadoya, K., Lu, P., Nguyen, Kenny., Lee-Kubli, C., Kumamaru, H., Yao, L., Knacker, J., Poplawski, G., Dulin, J N., *et al*., (2016). Spinal cord reconstitution with homologous neural grafts enables robust corticospinal regeneration. Nature medicine 22, 479–487.

Kalkan, T. and Smith, A. (2014). Mapping the route from naive pluripotency to lineage specification. *Philos. Trans. R. Soc. Lond. B. Biol. Sci.* 369, 20130540-.

Katsimpardi L, Litterman NK, Schein PA, Miller CM, Loffredo FS, Wojtkiewicz GR, Chen JW, Lee RT, Wagers AJ, Rubin LL (2014). Vascular and neurogenic rejuvenation of the aging mouse brain by young systemic factors. Science. ;344:630–634.

Kawakami A.Nojima Y.Toyoda A.Takahoko M.Satoh M.Tanaka H.Wada H.Masai I.Terasaki H.Sakaki Y.et al. (2005). The zebrafish-secreted matrix protein you/scube2 is implicated in long-range regulation of hedgehog signaling. *Curr. Biol.* 15: 480-488

Kawakami Y, et al. (2006) Wnt/beta-catenin signaling regulates vertebrate limb regeneration. Genes Dev. ;20:3232–3237.

Kawasaki H., Mizuseki K., Nishikawa S., Kaneko S., Kuwana Y., Nakanishi S., Nishikawa S.I., Sasai Y. (2000). Induction of midbrain dopaminergic neurons from ES cells by stromal cell-derived inducing activity. Neuron 28:31-40.

Kin Ting Kam, R., Deng, Y., Chen, Y. *et al.* (2012) Retinoic acid synthesis and functions in early embryonic development. *Cell Biosci* 2, 11

Kinder, S.J., Tsang, T.E., Wakamiya, M., Sasaki, H., Behringer, R.R., Nagy, a, and Tam, P.P. (2001). The organizer of the mouse gastrula is composed of a dynamic population of progenitor cells for the axial mesoderm. Development *128*, 3623–3634.

Kleinsmith L.J., Pierce G.B. (1964). Multipotentiality of single embryonal carcinoma cells. Cancer Research 24:1544-1551.

Klingensmith, J., Ang, S.-L., Bachiller, D., and Rossant, J. (1999). Neural Induction and Patterning in the Mouse in the Absence of the Node and Its Derivatives. Dev. Biol. *216*, 535–549.

Kohtz J. D., Baker D. P., Corte G. and Fishell G. (1998). Regionalization within the mammalian telencephalon is mediated by changes in responsiveness to Sonic Hedgehog. *Development* 125, 5079-5089.

Kojima, Y., Kaufman-Francis, K., Studdert, J. B., Steiner, K. A., Power, M. D., Loebel, D. A. F., Jones, V., Hor, A., De Alencastro, G., Logan, G. J., et al. (2014). The transcriptional and functional properties of mouse epiblast stem cells resemble the anterior primitive streak. *Cell Stem Cell* 14, 107–120.

Kojima, Y., Kaufman-Francis, K., Studdert, J.B., Steiner, K.A., Power, M.D., Loebel, D.A.F., Jones, V., Hor, A., De Alencastro, G., Logan, G.J., et al. (2014a). The transcriptional and functional properties of mouse epiblast stem cells resemble the anterior primitive streak. Cell Stem Cell *14*, 107–120.

Kojima, Y., Tam, O.H., and Tam, P.P.L. (2014b). Timing of developmental events in the early mouse embryo. Semin. Cell Dev. Biol. *34*, 65–75.

Kretzchmar M., Liu F., Hata A., Doody J., Massagué J. (1997). The TGF-β family mediator Smad1 is phosphorylated directly and activated functionally by the BMP receptor kinase. Genes & Development 11:984-995.

Kunath, T., Saba-El-Leil, M. K., Almousailleakh, M., Wray, J., Meloche, S. and Smith, A. (2007). FGF stimulation of the Erk1/2 signalling cascade triggers transition of pluripotent embryonic stem cells from self-renewal to lineage commitment. *Development* 136, 1063–9.

Kunath, T., Saba-El-Leil, M.K., Almousailleakh, M., Wray, J., Meloche, S., and Smith, A. (2007). FGF stimulation of the Erk1/2 signalling cascade triggers transition of pluripotent embryonic stem cells from self-renewal to lineage commitment. Development *134*, 2895–2902.

Kuratani S.C., Eichele G (1993). Rhombomere transplantation repatterns the segmental organization of cranial nerves and reveals cell-autonomous expression of a homeodomain protein. *Development* ;117:105–117.

Kvon K. V. V. A. (2016). Progressive loss of function in a limb enhancer during snake evolution. Cell 633–642.

Lagna G., Hata A., Hemmati-Brivanlou A., Massagué J. (1996). Partnership between DPC4 and SMAD proteins in TGF-β signalling pathways. Nature 383:832-836.

Lawson, K. A. and Wilson, V. (2016). *3 – A Revised Staging of Mouse Development Before Organogenesis*. Elsevier Inc.

Lawson, K.A., Meneses, J.J., and Pedersen, R.A. (1991). Clonal analysis of epiblast fate during germ layer formation in the mouse embryo. Development *113*, 891–911.

Levine, A.J., and Brivanlou, A.H. (2007). Proposal of a model of mammalian neural induction. Dev. Biol. *308*, 247–256.

Lewis EB. (1978). A gene complex controlling segmentation in *Drosophila*. *Nature.* 1978;276:565–570.

Li L., Liu C., Biechele S., Zhu Q., Song L., Lanner F., Jing N., Rossant J. (2013). Location of transient ectodermal progenitor potential in mouse development. Development 140:4533-4543.

Li X, Xiao J, Fröhlich H, Tu X, Li L, Xu Y, Cao H, Qu J, Rappold GA, Chen JG. (2015). Foxp1 regulates cortical radial migration and neuronal morphogenesis in developing cerebral cortex. PLoS One. May 26;10(5):e0127671.

Li, M., Pevny, L., Lovell-Badge, R., and Smith, A.G. (1998). Generation of purified neural precursors from embryonic stem cells by lineage selection. Current Biology *8*, 971–S972.

Lin Y.-L., Lin Y.-W., Nhieu J., Zhang X., Wei L.-N. (2020). Sonic Hedgehog-Gli1 Signaling and Cellular Retinoic Acid Binding Protein 1 Gene Regulation in Motor Neuron Differentiation and Diseases. Ijms 21 (11), 4125.

Lippmann, E. S., Williams, C. E., Ruhl, D. A., Estevez-Silva, M. C., Chapman, E. R., Coon, J. J. and Ashton, R. S. (2015). Deterministic HOX patterning in human pluripotent stem cell-derived neuroectoderm. Stem Cell Reports 4, 632-644.

Liu JP, Laufer E, and Jessell TM (2001). Assigning the positional identity of spinal motor neurons: rostrocaudal patterning of Hox-c expression by FGFs, Gdf11, and retinoids. Neuron 32, 997–1012.

Mahony, S., Mazzoni, E.O., McCuine, S. *et al.* (2011).Ligand-dependent dynamics of retinoic acid receptor binding during early neurogenesis. *Genome Biol* 12, R2

Maria Angeles Marques-Torrejon, Ester Gangoso, Steven M. Pollard (2018). Modelling glioblastoma tumour-host cell interactions using adult brain organotypic slice co-culture. *Dis Model Mech* 11 (2): dmm031435.

Marti E, Bumcrot DA, Takada R, McMahon AP, Ritsuko T and McMahon AP (1995). Requirement of 19K form of Sonic hedgehog for induction of distinct ventral cell types in CNS explants. *Nature* 375, 322–325.

Martin G.R. (1981). Isolation of a pluripotent cell line from early mouse embryos cultured in medium conditioned by teratocarcinoma stem cells. Proceedings of the National Academy of Sciences of the United States of America 78:7634-7638.

Martin G.R., Evans M.J. (1975). Differentiation of clonal lines of teratocarcinoma cells: formation of embryoid bodies in vitro. Proceedings of the National Academy of Sciences of the United States of America 72:1441-1445.

Martinez Arias, A., and Steventon, B. (2018). On the nature and function of organizers. Development *145*, dev159525.

Mathis, L., Kulesa, P. M. and Fraser, S. E. (2001). FGF receptor signalling is required to maintain neural progenitors during Hensen's node progression. *Nat. Cell Biol.* 3, 559– 66.

Mazzoni, E. O., Mahony, S., Peljto, M., Patel, T., Thornton, S. R., McCuine, S., Reeder, C., Boyer, L. A., Young, R. A., Gifford, D. K. et al. (2013). Saltatory remodeling of Hox chromatin in response to rostrocaudal patterning signals. Nat. Neurosci. 16, 1191-1198.

McGrew, M.J., Sherman, A., Lillico, S.G., Ellard, F.M., Radcliffe, P.A., Gilhooley, H.J., Mitrophanous, K.A., Cambray, N., Wilson, V., and Sang, H. (2008). Localised axial progenitor cell populations in the avian tail bud are not committed to a posterior Hox identity. Development 135, 2289–2299.

McPherron AC, Lawler AM, Lee SJ. (1999). Regulation of anterior/posterior patterning of the axial skeleton by growth/differentiation factor 11. Nat Genet. Jul;22(3):260-4.

Metzis V, Steinhauser S, Pakanavicius E, Gouti M, Stamataki D, Ivanovitch K, Watson T, Rayon T, Mousavy Gharavy SN, Lovell-Badge R, Luscombe NM, Briscoe J (2018). Nervous System Regionalization Entails Axial Allocation before Neural Differentiation. Cell. Nov 1;175(4):1105-1118.e17.

Morgani, S., Nichols, J., and Hadjantonakis, A.-K. (2017). The many faces of Pluripotency: in vitro adaptations of a continuum of in vivo states. BMC Dev. Biol. *17*, 7.

Mugele, D., Moulding, D. A., Savery, D., Mole, M. A., Greene, N. D. A., Martinez-Barbera, J. P. and Copp, A. J. (2018). Genetic approaches in mice demonstrate that neuro-mesodermal progenitors express T/Brachyury but not Sox2. bioRxiv.

Muñoz-Sanjuán I., Brivanlou A.H. (2002). Neural induction, the default model and embryonic stem cells. Nature Reviews Neuroscience 3:271-280.

Naiche, L. a, Holder, N., and Lewandoski, M. (2011). FGF4 and FGF8 comprise the wavefront activity that controls somitogenesis. Proc. Natl. Acad. Sci. *108*, 4018–4023.

Nakao A., Imamura T., Souchelnytskyi S., Kawabata M., Ishisaki A., Oeda E., Tamaki K., Hanai J., Heldin C.H., Miyazono K., ten Dijke P. (1997). TGF-β receptor-mediated signalling through Smad2, Smad4 and Smad4. The EMBO Journal 16:5353-5362.

Nakashima K, Yanagisawa M, Arakawa H, Kimura N, Hisatsune T, Kawabata M, Miyazono K, Taga T. (1999). Synergistic signaling in fetal brain by STAT3-Smad1 complex bridged by p300. Science. Apr 16;284(5413):479-82.

Nichols J, Smith A. (2009). Naive and primed pluripotent states. Cell Stem Cell; 4(6):487–92.

Niederreither K., Subbarayan V., Dolle P., Chambon P. (1999) Embryonic retinoic acid synthesis is essential for early mouse post-implantation development. Nature Genet 21, 444–448

Nieuwkoop PD, Nigtevecht GV (1954) *J Embryol Exp Morph* 2: 175–193

Nieuwkoop, P. D. and Nigtevecht, G. V. (1954). Neural activation and transformation in explants of competent ectoderm under the influence of fragments of anterior notochord in urodeles. J. Embryol. Exp. Morph. 2, 175-193.

Ohgushi, M., Matsumura, M., Eiraku, M., Murakami, K., Aramaki, T., Nishiyama, A., Muguruma, K., Nakano, T., Suga, H., Ueno, M., et al. (2010). Molecular pathway and cell state responsible for dissociation-induced apoptosis in human pluripotent stem cells. *Cell Stem Cell* 7, 225–239.

Olivera-Martinez I., Harada H., Halley P. A. and Storey K. G. (2012). Loss of FGF-dependent mesoderm identity and rise of endogenous retinoid signalling determine cessation of body axis elongation. *PLoS Biol.* 10, e1001415 10.1371/journal.pbio.1001415

Osorno R., Tsakiridis A., Wong F., Cambray N., Economou C., Wilkie R., Blin G., Scotting P.J., Chambers I., Wilson V. (2012). The developmental dismantling of pluripotency is reversed by ectopic Oct4 expression. Development 139:2288-2298.

P. Dolle, E. Ruberte, P. Leroy, G. Morriss-Kay, P. Chambon (1990). Retinoic acid receptors and cellular retinoid binding proteins. I. A systematic study of their differential pattern of transcription during mouse organogenesis. *Development* 1; 110 (4): 1133–1151.

Papaioannou, V.E., GARDNER, R.L., McBurney, M.W., Babinet, C., and Evans, M.J. (1978). Participation of cultured teratocarcinoma cells in mouse embryogenesis. Development 44, 93–104.

Papaioannou, V.E., McBurney, M.W., Evans, M.J., and GARDNER, R.L. (1975). Fate of teratocarcinoma cells injected into early mouse embryos. Nature 258, 70–73.

Patani, R., Hollins, A. J., Wishart, T. M., Puddifoot, C. A., Alvarez, S., de Lera, A. R., Wyllie, D. J., Compston, D. A., Pedersen, R. A., Gillingwater, T. H. *et al*. (2011). Retinoid-independent motor neurogenesis from human embryonic stem cells reveals a medial columnar ground state. Nat. Commun. 2, 214.

Perantoni, A. O., Timofeeva, O., Naillat, F., Richman, C., Pajni-Underwood, S., Wilson, C., Vainio, S., Dove, L. F. and Lewandoski, M. (2005). Inactivation of FGF8 in early mesoderm reveals an essential role in kidney development. Development 132, 3859-3871

Perrier, A.L., Tabar, V., Barberi, T., Rubio, M.E., Bruses, J., Topf, N., Harrison, N.L., and Studer, L. (2004). Derivation of midbrain dopamine neurons from human embryonic stem cells. Proceedings of the National Academy of Sciences *101*, 12543–12548.

Philippidou, P. and Dasen, J. S. (2013). Hox genes: choreographers in neural development, architects of circuit organization. *Neuron* 80, 12-34.

Pollard S.M., Benchoua A., Lowell S. (2006). Neural stem cells, neurons and glia. Methods in Enzymology 418:151-169.

Prince, V. and Lumsden, A. (1994). Hoxa-2 expression in normal and transposed rhombomeres: independent regulation in the neural tube and neural crest. *Development* 120, 911–923.

Qin Z, Chen Z, Weng J, Li S, Rong Z, Zhou C (2019). Elevated *HOXA13* expression promotes the proliferation and metastasis of gastric cancer partly via activating Erk1/2. Onco Targets Ther. Mar 4;12:1803-1813.

Ribes V, Briscoe J. (2009). Establishing and interpreting graded Sonic Hedgehog signaling during vertebrate neural tube patterning: the role of negative feedback. Cold Spring Harb Perspect Biol. Aug;1(2):a002014.

Rodrigo Albors AHalley PAStorey KG (2018) Lineage tracing of axial progenitors using Nkx1-2CreERT2 mice defines their trunk and tail contributions *Development* 145:dev164319.

Roelink H, Porter JA, Chiang C, Tanabe Y, Chang DT, Beachy PA, Jessell TM. (1995). Floor plate and motor neuron induction by different concentrations of the amino-terminal cleavage product of sonic hedgehog autoproteolysis. Cell. May 5;81(3):445-55.

Ruiz i Altaba A, Nguyên V, Palma V. (2003). The emergent design of the neural tube: prepattern, SHH morphogen and GLI code. Curr Opin Genet Dev. Oct;13(5):513-21.

S. Bel-Vialar, N. Itasaki, R. Krumlauf. (2002). Initiating Hox gene expression: in the early chick neural tube differential sensitivity to FGF and RA signaling subdivides the HoxB genes in two distinct groups. Development, 129 pp. 5103-5115,

Saiz, N., and Plusa, B. (2013). Early cell fate decisions in the mouse embryo. Reproduction *145*, R65-80.

Saldivar JR, Krull CE, Krumlauf R, Ariza-McNaughton L, Bronner-Fraser M. (1996). Rhombomere of origin determines autonomous versus environmentally regulated expression of Hoxa-3 in the avian embryo. *Development.*;122:895–904

Selleck, M.A.J., and Stern, C.D. (1991). Fate mapping and cell lineage analysis of Hensen's node in the chick embryo. Development *112*, 615–626.

Shi Y, Liu JP (2011). Gdf11 facilitates temporal progression of neurogenesis in the developing spinal cord. J Neurosci. Jan 19;31(3):883-93.

Smith A.G., Heath J.K., Donaldson D.D., Wong G.G., Moreau J., Stahl M., Rogers D. (1988). Inhibition of pluripotential embryonic stem cell differentiation by purified polypeptides. Nature 336:688-690.

Smith A.G., Hooper M.L. (1987). Buffalo rat liver cells produce a diffusible activity which inhibits the differentiation of murine embryonal carcinoma and embryonic stem cells. Developmental Biology 121:1-9.

Smith, A. (2017). Formative pluripotency: the executive phase in a developmental continuum. *Development* In Press, 365–373.

Smukler SR, Runciman SB, Xu S, van der Kooy D. (2006). Embryonic stem cells assume a primitive neural stem cell fate in the absence of extrinsic influences. J Cell Biol. Jan 2;172(1):79-90.

Stavridis M.P., Lunn J.S., Collins B.J., Storey K.G. (2007). A discrete period of FGF-induced Erk1/2 signalling is required for vertebrate neural specification. Development 134:2889-2894.

Stern C.D. (2005). Neural induction: Old problem, new findings, yet more questions. Development. 132:2007–2021. doi: 10.1242/dev.01794.

Stern C.D. (2006). Neural induction: 10 years on since the 'default model'. Current Opinion in Cell Biology 18:692-697.

Sterneckert J., Stehling M., Bernemann C., Araúzo-Bravo M.J., Greber B., Gentile L., Ortmeier C., Sinn M., Wu G., Ruau D., Zenke M., Brintrup R., Klein D.C., Ko K., Schöler H.R. (2010). Neural induction intermediates exhibit distinct roles of Fgf signalling. Stem Cells 28:1772-1781.

Stevens L.C., Little C.C. (1954). Spontaneous testicular teratomas in an inbred strain of mice. Proceedings of the National Academy of Sciences of the United States of America 40:1080-1087.

Stoykova A, Gruss P (1994). Roles of Pax-genes in developing and adult brain as suggested by expression patterns. J Neurosci. Mar;14(3 Pt 2):1395-412.

Streit A., Berliner A.J., Papanayotou C., Sirufnik A., Stern C.D. (2000). Initiation of neural induction by FGF signalling before gastrulation. Nature 406:74-78.

Streit A., Lee K.J., Woo I., Roberts C., Jessell T.M., Stern C.D. (1998). Chordin regulates primitive streak development and the stability of induced neural cells, but is not sufficient for neural induction in the chick embryo. Development 125:507-519.

Berg S, Kutra D, Kroeger T, Straehle CN, Kausler BX, Haubold C, et al. (2019). ilastik: interactive machine learning for (bio)image analysis. *Nat Methods*. Dec;16(12):1226–32.

Takada, S., Stark, K. L., Shea, M. J., Vassileva, G., McMahon, J. A. and McMahon, A. P. (1994). Wnt-3a regulates somite and tailbud formation in the mouse embryo. Genes Dev. 8, 174-189.

Takemoto, T., Uchikawa, M., Kamachi, Y. and Kondoh, H. (2006). Convergence of Wnt and FGF signals in the genesis of posterior neural plate through activation of the Sox2 enhancer N-1. Development 133, 297-306.

Takemoto, T., Uchikawa, M., Yoshida, M., Bell, D. M., Lovell-Badge, R., Papaioannou, V. E. and Kondoh, H. (2011). Tbx6-dependent Sox2 regulation determines neural or mesodermal fate in axial stem cells. Nature 470, 394-398.

Tam P.P.L., Loebel D.A.F. (2007). Gene function in mouse embryogenesis: get set for gastrulation. Nature Reviews Genetics 8:368-381.

Tam, P. P. (1989). Regionalisation of the mouse embryonic ectoderm: allocation of prospective ectodermal tissues during gastrulation. *Development* 107, 55–67.

Tam, P. P. L. and Quinlan, G. A. (1996). Mapping vertebrate embryos. *Curr. Biol.* 6, 104–106.

Tarkowski A.K., Wróblewska J. (1967). Development of blastomeres of mouse eggs isolated at the 4- and 8-cell stage. Journal of Embryology and Experimental Morphology 18:155-180.

Tesar P.J., Chenoweth J.G., Brook F.A., Davies T.J., Evans E.P., Mack D.L., Gardner R.L., McKay R.D.G. (2007). New cell lines from mouse epiblast share defining features with human embryonic stem cells. Nature 448:196-199.

Thisse B., Thisse C. (2005). Functions and regulations of fibroblast growth factor signaling during embryonic development. Developmental Biology 287:390-402.

Tsakiridis A, Huang Y, Blin G, Skylaki S, Wymeersch F, et al. (2014) Distinct Wnt-driven primitive streak-like populations reflect in vivo lineage precursors. *Development* 141: 1209–1221.

Tsakiridis, A., and Wilson, V. (2015). Assessing the bipotency of in vitro-derived neuromesodermal progenitors. F1000Research *4*, 100.

Tsakiridis, A., Huang, Y., Blin, G., Skylaki, S., Wymeersch, F., Osorno, R.R., Economou, C., Karagianni, E., Zhao, S., Lowell, S., et al. (2014). Distinct Wnt-driven

primitive streak- like populations reflect in vivo lineage precursors. Development *141*, 1209–1221.

Turco, M.Y., Furia, L., Dietze, A., Diaz, L.F., Ronzoni, S., Sciullo, A., Simeone, A., Constam, D., Faretta, M., and Lanfrancone, L. (2012). Cellular heterogeneity during embryonic stem cell differentiation to epiblast stem cells is revealed by the ShcD/RaLP adaptor protein. Stem Cells *30*, 2423–2436.

Turner, D. a, Hayward, P.C., Baillie-Johnson, P., Rué, P., Broome, R., Faunes, F., and Martinez Arias, A. (2014). Wnt/β-catenin and FGF signalling direct the specification and maintenance of a neuromesodermal axial progenitor in ensembles of mouse embryonic stem cells. Development *141*, 4243–4253.

Tzouanacou, E., Wegener, A., Wymeersch, F.J., Wilson, V., and Nicolas, J.F. (2009). Redefining the Progression of Lineage Segregations during Mammalian Embryogenesis by Clonal Analysis. Dev. Cell *17*, 365–376.

Uehara M, Yashiro K, Takaoka K, Yamamoto M, Hamada H. (2009). Removal of maternal retinoic acid by embryonic CYP26 is required for correct nodal expression during early embryonic patterning. Genes Dev. ;23(14):1689–1698.

van den Brink, S. C., Alemany, A., van Batenburg, V., Moris, N., Blotenburg, M., Vivie, J., Baillie-Johnson, P., Nichols, J., Sonnen, K. F., Martinez Arias, A. et al. (2020). Single-cell and spatial transcriptomics reveal somitogenesis in gastruloids. Nature 582, 405-409.

Veenvliet, J. S., Bolondi, A., Kretzmer, H., Haut, L., Scholze-Wittler, M., Schifferl, D., Koch, F., Guignard, L., Kumar, A. S., Pustet, M. et al. . (2020). Mouse embryonic stem cells self-organize into trunk-like structures with neural tube and somites. Science 370, eaba4937.

Vermot J, Gallego Llamas J, Fraulob V, Niederreither K, Chambon P, Dolle P. (2005). Retinoic acid controls the bilateral symmetry of somite formation in the mouse embryo. *Science* 308: 563– 566.

Vermot J, Pourquie O. (2005). Retinoic acid coordinates somitogenesis and left-right patterning in vertebrate embryos. *Nature* 435: 215– 220.

Verrier, L., Davidson, L., Gierlinski, M., Dady, A. and Storey, K. G. (2018). Neural differentiation, selection and transcriptomic profiling of human neuromesodermal progenitor-like cells in vitro. Development 145, dev166215

Villegas S.N., Canham M., Brickman J.M. (2010). FGF signalling as a mediator of lineage transitions – Evidence from embryonic stem cell differentiation. Journal of Cellular Biochemistry 110:10-20.

Wichterle H, Lieberam I, Porter JA, Jessell TM. (2002). Directed differentiation of embryonic stem cells into motor neurons. Cell.;110:385–397. doi: 10.1016/S0092-8674(02)00835-8.

Williams R.L., Hilton D.J., Pease S., Willson T.A., Stewart C.L., Gearing D.P., Wagner E.F., Metcalf D., Nicola N.A., Gough N.M. (1988). Myeloid leukaemia inhibitory factor maintains the developmental potential of embryonic stem cells. Nature 336:684-688.

Wilson P.A., Hemmati-Brivanlou A. (1995). Induction of epidermis and inhibition of neural fate by Bmp-4. Nature 376:331-333.

Wilson, V., and Beddington, R.S.P. (1996). Cell fate and morphogenetic movement in the late mouse primitive streak. Mech. Dev. *55*, 79–89.

Wilson, V., Olivera-Martinez, I., and Storey, K.G. (2009). Stem cells, signals and vertebrate body axis extension. Development *136*, 2133–2133.

Wind, M., Gogolou, A., Manipur, I., Granata, G., Butler, L., Andrews, P. W., Barbaric, I., Ning, K., Guarracino, G. M., Placzek, M. et al. (2020). Defining the signalling determinants of a posterior ventral spinal cord identity in human neuromesodermal progenitor derivatives. bioRxiv.

Wu R.Y., Zhang Y., Feng X.H., Derynck R. (1997). Heteromeric and homomeric interactions correlate with signaling activity and functional cooperativity of Smad3 and Smad4/DPC4. Molecular and Cellular Biology 17:2521.

Wymeersch, F. J., Skylaki, S., Huang, Y., Watson, J. A., Economou, C., Marek-Johnston, C., Tomlinson, S. R. and Wilson, V. (2019). Transcriptionally dynamic progenitor populations organised around a stable niche drive axial patterning. Development 146, dev168161.

Wymeersch, F.J., Huang, Y., Blin, G., Cambray, N., Wilkie, R., Wong, F.C.K., and Wilson, V. (2016). Position-dependent plasticity of distinct progenitor types in the primitive streak. Elife *5*, 1–28.

Yaguchi Y., Yu T., Ahmed M. U., Berry M., Mason I., Basson M. A. (2009). Fibroblast growth factor (FGF) gene expression in the developing cerebellum suggests multiple roles for FGF signaling during cerebellar morphogenesis and development. Dev. Dyn. 238, 2058–2072. 10.1002/dvdy.22013

Yamaguchi, T. P., Takada, S., Yoshikawa, Y., Wu, N. and McMahon, A. P. (1999). T (Brachyury) is a direct target of Wnt3a during paraxial mesoderm specification. Genes Dev. 13, 3185-3190.

Ying Q.L., Nichols J., Chambers I., Smith A. (2003a). BMP induction of Id proteins suppresses differentiation and sustains embryonic stem cell self-renewal in collaboration with STAT3. Cell 115:281-292.

Ying Q.L., Stavridis M., Griffiths D., Li M., Smith A. (2003b). Conversion of embryonic stem cells into neuroectodermal precursors in adherent monoculture. Nature Biotechnology 21:183-186.

Ying, Q.L., and Smith, A.G. (2003). Defined Conditions for Neural Commitment and Differentiation. Methods Enzymol. *365*, 327–341.

Yoshikawa, Y., Fujimori, T., McMahon, A. P. and Takada, S. (1997). Evidence that absence of Wnt-3a signaling promotes neuralization instead of paraxial mesoderm development in the mouse. Dev. Biol. 183, 234-242.

Young T, Rowland JE, van de Ven C, Bialecka M, Novoa A, Carapuco M, van Nes J, de Graaff W, Duluc I, Freund JN, Beck F, Mallo M, Deschamps J. (2009) Cdx and Hox

genes differentially regulate posterior axial growth in mammalian embryos. *Dev Cell.* ;17:516–26.

Zhang Y, Wei Y, Liu D, Liu F, Li X, Pan L, Pang Y, Chen D. (2017) Role of growth differentiation factor 11 in development, physiology and disease. Oncotarget. Aug 14;8(46):81604-81616.

Zhao F, Wu T, Lau A, Jiang T, Huang Z, Wang XJ, Chen W, Wong PK, Zhang DD (2009). Nrf2 promotes neuronal cell differentiation. Free Radic Biol Med.15;47(6):867-79.

Zhu, Q., Song, L., Peng, G., Sun, N., Chen, J., Zhang, T., Sheng, N., Tang, W., Qian, C., Qiao, Y., et al. (2014). The transcription factor Pou3f1 promotes neural fate commitment via activation of neural lineage genes and inhibition of external signaling pathways. *Elife* 2014, 1–21.